WESTINGHOUSE NON-PROPRIETARY CLASS 3

Westinghouse Energy Systems

WESTINGHOUSE NON-PROPRIETARY CLASS 3

Westinghouse Energy Systems

Westinghouse Non-Proprietary Class 3

WCAP14274

SG 95-02-004

TECHNICAL SUPPORT FOR ALTERNATE PLUGGING CRITERIA WITH TUBE EXPANSION AT TUBE SUPPORT PLATE INTERSECTIONS FOR BRAIDWOOD-1 AND BYRON-1 MODEL D4 STEAM GENERATORS

FEBRUARY 1995

WESTINGHOUSE ELECTRIC CORPORATION
NUCLEAR SERVICES DIVISION
P.O. BOX 158
MADISON, PENNSYLVANIA 15663-0158

Technical Support for Alternate Plugging Criteria with Tube Expansion at TSP Intersections for Braidwood-1 and Byron-1 Model D4 Steam Generators

TABLE OF CONTENTS

TABLE OF CONTENTS (Continued)

TABLE OF CONTENTS (Continued)

TABLE OF CONTENTS (Continued)

LIST OF FIGURES

LIST OF FIGURES (Continued)

LIST OF FIGURES (Continued)

LIST OF FIGURES (Continued)

LIST OF FIGURES (Continued)

LIST OF FIGURES (Continued)

LIST OF FIGURES (Continued)

LIST OF FIGURES (Continued)

LIST OF FIGURES (Continued)

LIST OF FIGURES (Continued)

LIST OF FIGURES (Continued)

LIST OF FIGURES (Continued)

LIST OF FIGURES (Continued)

LIST OF TABLES

LIST OF TABLES (Continued)

LIST OF TABLES (Continued)

LIST OF TABLES (Continued)

1.0 INTRODUCTION

This report provides technical support for implementing alternate plugging criteria (APC) with tube expansion at tube support plate (TSP) intersections for Westinghouse Model D4 steam generators (S/Gs). The supporting technical data and analyses are generic to Model D4 S/Gs although the recommended tube repair limits are specific to the Braidwood-1 and Byron-1 S/Gs.

With tube expansion, TSP displacements in a steam line break (SLB) event are limited to negligible levels and the axial tube burst probability is thereby also reduced to negligible levels. For very large bobbin voltage indications with a cellular corrosion morphology, it is possible for the axial pressure loads on the tube to cause axial tensile tearing of the indications. This condition establishes the structural limit for voltage repair limits and, based on current data, this limit is developed in this report and shown to be much higher than any indications reasonably expected at Braidwood-1 and Byron-1 for the repair limits recommended in this report. Thus repair limits with tube expansion are primarily limited by the requirement to limit accident condition leakage to acceptable levels. For conservatism, deterministic repair limits are proposed for Braidwood-1 and Byron-1.

The evaluations of this report include hydraulic SLB analyses to obtain the time dependent pressure drop loads on the TSPs (Sections 4 to 6), structural analyses that apply the hydraulic loads to determine the tube locations requiring expansion to limit TSP displacements to acceptable levels (Sections 7 and 8), a description of the analysis methods for evaluating SLB leak rates and tube burst probabilities (Section 9), a description of the tube expansion process and test results (Section 10), a development of the TSP displacement requirements (Section 11) and the integration of these results to develop the tube repair criteria (Section 12). The methods and results for the hydraulic loads and the methods for structural analyses are essentially the same as previously reported in WCAP-14222 (Reference 13.1). However, minor extensions of load sensitivity analyses were performed and full documentation of analysis methods and results are given in this report. For conservatism in the tube expansion design and supporting analyses, a factor of two increase in the TRANFLO code loads is applied to envelope the results of load sensitivity studies and comparisons with loads obtained with the MULTIFLEX code.

The analysis methods for SLB leak rate and tube burst probability assessments given in Section 9 are essentially the same as the EPRI methodology and are consistent with the requirements of the NRC draft generic letter (Reference 13.2). An extension of the leak rate methodology is required for potentially overpressurized indications within the confines of the TSP and the methodology for this analysis is also given in Section 9. This section also includes development of the voltage structural limit for axial tensile tearing as the applicable structural limit with tube expansion.

Section 10 provides the tube expansion process requirements, description and supporting test and analysis results. A hydraulic expansion process with a sleeve stabilizer is applied to implement the required expansions at TSP intersections. Also included is an assessment of the potential for circumferential cracking in the expanded tubes in their plugged tube condition and considerations of TSP integrity for application of the expansion process.

The requirements on limiting TSP displacements to obtain negligible tube burst probabilities are developed in Section 11. Section 12 integrates the results of the prior report sections to develop the alternate plugging criteria with tube expansion for Braidwood-1 and Byron-1. Inspection and SLB analysis requirements are also given in Section 12. Overall conclusions and a summary of this report are given in Section 2.

2.0 SUMMARY AND CONCLUSIONS

This report documents the technical support for APC with tube expansion at TSP intersections for Model D4 S/Gs. The development of the matrix of tube locations and TSP elevations for tube expansion is a generic matrix for Model D4 S/Gs. The generic matrix identifies groups of adjacent tubes for each tube location requiring expansion. On a plant specific basis, candidates for tube expansion can be selected from each acceptable group, thereby providing flexibility in finalizing the plant specific tubes for expansion. The report is plant specific for Braidwood-1 and Byron-1 primarily in regard to the voltage repair limits for which a 3.0 volt IPC repair limit is proposed for hot leg TSP intersections with expanded tubes and a 1.0 volt IPC repair limit is proposed for the FDB and cold leg TSP intersections which do not have expanded tubes. The technical assessment of this report supports full APC repair limits in the 10 to 15 volt range or higher for hot leg intersections with tube expansion.

Overall conclusions and a summary of the report are provided in this section.

2.1 Overall Conclusions

Although TSP displacements up to 0.31 inch are adequate to reduce axial tube burst probabilities to a negligible 10^{-5}, the tube expansion S/G modification has been designed to obtain maximum TSP displacements of ≤ 0.1 inch with associated tube burst probabilities of $\leq 10^{-10}$. These bounding tube burst probabilities have been obtained by the unrealistically conservative assumption that all hot leg TSP intersections have throughwall cracks exposed by the TSP displacements. The negligible TSP displacements with tube expansion are achieved by hydraulically expanding 21 tubes at 72 TSP intersections. Tubes are expanded at the hot leg TSP intersections and the FDB and cold leg TSP intersections are not expanded. A sleeve stabilizer is expanded with the parent tube and functions to increase the stiffness of the expansion against TSP motion and to capture a severed tube end under the assumption that a circumferential crack at the parent tube expansion caused the tube to sever.

Since axial tube burst probabilities are negligibly small with tube expansion, repair limits to preclude burst are not required and tube repair requirements would be primarily based on limiting accident condition leakage to acceptable levels. At very high voltage levels and crack morphologies including cellular corrosion, it is possible that the axial pressure loads on the tube could cause tensile tearing of an indication. This limit represents the structural limit applicable with tube expansion and, based on available data, is estimated to exceed 35 volts at the lower 95% confidence level on the data at the $3\Delta P_{NO}$ structural margin guideline of Regulatory Guide 1.121.

Although voltage repair limits as high as 15 volts are justifiable with tube expansion, a 3.0 volt repair limit is proposed for the hot leg TSP intersections at Braidwood-1 and Byron-1. For FDB and cold leg TSP intersections without tube expansion, the previously approved IPC voltage repair limit of 1.0 volt is recommended. Inspection requirements with tube expansion are essentially the same as required for IPC inspections without tube expansion although supplemental inspections at the time of tube expansion and for periodic monitoring of the expanded tubes are required as described in Section 2.2 below.

2.2 Summary

Overall Approach to Tube Expansion APC

The approach applied to develop the tube expansion APC basis is to: define acceptable TSP displacements to achieve a negligible (very small compared to NRC reporting guideline of 10^{-2}) tube burst probability, utilize conservative SLB hydraulic loads on the TSPs by applying a factor of two margin on the expected loads obtained with the TRANFLO code, determine the number and locations for tube expansion by structural analyses with additional redundant expanded tubes as margin for the low likelihood of circumferential cracking at the expansions and demonstrate that the TSP displacements with tube expansion are significantly smaller than the acceptable TSP displacements.

An acceptable TSP displacement requirement of ≤ 0.31 inch was very conservatively developed assuming that all TSPs are uniformly displaced and by the bounding assumption that the displacements exposed throughwall cracks at all hot leg TSP intersections (32,046 throughwall indications). With tube expansion, the resulting maximum TSP displacements are < 0.1 inch for all tube locations at all hot leg TSPs. This 0.1 inch TSP displacement goal, with a resulting tube burst probability of < 10^{-10} for the bounding hot leg indication assumption, was established to permit a longer term option for in situ leak testing. Braidwood-1 and Byron-1 will conservatively apply the EPRI free span leak rate methodology consistent with the requirements of the NRC draft generic letter for ODSCC at TSPs.

Tube Locations and TSP Elevations Requiring Tube Expansion

The required tube expansion matrix includes 21 tube locations with a total of 72 expansions. The reference expansion to limit TSP displacements to 0.1 inch requires 16 expanded tubes. In addition, 3 tubes are expanded for redundant expansions at critical locations for TSP displacements and 2 tubes are expanded for structural reasons to limit plate stresses at the top TSP. An example generic tube expansion matrix is given in Table 2-1. This matrix identifies specific tubes for expansion. However, plant specific tubes can be selected from the nearby locations shown as darkened tube locations in Figure 2-1.

Performance of Tube Expansion for Limiting TSP Displacements

The TSP displacement goal of 0.1 inch and resulting tube burst probability of

$< 10^{-10}$ is satisfied with or without the redundant and structural expansions functional (i.e., with or without postulated severing of these expansions). The tube expansion design provides large margins against postulated severed expansions and hydraulic loads. For example, the maximum TSP displacement is < 0.2 inch, as compared to the 0.31 inch design requirement, for any of the following very conservative postulates: hydraulic loads increased from the conservative design basis factor of 2 on TRANFLO hydraulic loads to a factor of 4 on the loads; assuming all but the 2 redundant expanded tubes (all but 4 of 18 TSP expansions) of the 8 tubes expanded at the lower 3 TSPs (above the FDB) are severed; all but 5 of the 17 tubes expanded (all but 10 of 54 TSP expansions) at the top 4 TSPs are severed; or only 7 of the 21 tubes expanded (all but 14 of 72 TSP expansions) are functional. The expansion design is fail safe against severed expansions for the bottom 3 TSPs which have downward (toward tubesheet) hydraulic loads and at which most of the indications at TSPs occur. This results as the expansion design includes a sleeve stabilizer which prevents significant lateral motion for a severed tube such that the severed expansion continues to resist downward motion of the TSPs.

Tube Expansion Process

The tube expansion at the TSPs is performed by a hydraulic expansion process that expands the parent tube and the sleeve stabilizer at the same time. Expansions are performed below and above each TSP intersection that requires expansion. The design requirements on the tube expansion process, as developed to restrain TSP displacement, are a minimum expanded [

]^{a,c,e}. The sleeve stabilizer expanded with the parent tube increases the expansion stiffness at a given diametral expansion and prevents lateral motion or adjacent tube damage for a postulated severed expansion. Testing of expanded tube sections has shown that all design requirements are satisfied. Following the field expansions, bobbin coil profilometry is used to confirm that acceptable expanded tube diameters have been achieved and that the expansions are properly located relative to the TSP.

Hydraulic Load Analyses

Hydraulic loads on the TSPs for application to the TSP displacement analyses were obtained using the TRANFLO code. The analyses show that the TSP loads are higher for a SLB event at hot standby operating conditions than for full power conditions and the hot standby loads are used for the tube expansion design even though only a small fraction of the operating cycle is spent at hot standby conditions. A TRANFLO sensitivity analysis to input variables was performed to assess the dependence of the TSP loads to potential uncertainties in the input variables such as TSP pressure drop loss coefficients and water level. When the potential uncertainties that increase the TSP hydraulic loads compared to the reference or expected parameters are simultaneously combined, the TSP loads can be bounded by a factor of two increase over the reference loads. This factor of two increase on the reference hot standby loads was applied to obtain the design basis loads for tube expansion. Analyses of TSP loads were also performed with the MULTIFLEX code. The primary objective of the MULTIFLEX analyses was to assess the potential for acoustic wave effects influencing the TSP loads. The results of these analyses demonstrate that acoustic wave effects have no significant influence on the TSP loads. In addition, the TRANFLO design loads bound the TSP loads obtained with the MULTIFLEX code. Overall, it is concluded that the TRANFLO code provides acceptable thermal-hydraulic analyses to determine the SLB loads on the TSPs and that the factor of two margin applied to the reference or expected loads bounds the uncertainties in obtaining the loads.

Tube Repair Limits

By essentially eliminating tube burst as a credible event with tube expansion at the TSPs, the Regulatory Guide 1.121 guidelines for structural margins are inherently satisfied by the TSP constraint at both normal operating and accident conditions including a postulated SLB event. Consequently, tube repair limits are not required to satisfy tube burst margins and tube repair would be required only as necessary to satisfy allowable leakage limits. At very high bobbin voltages corresponding to relatively large ODSCC indications compared to those obtained with domestic tube repair limits, a structural limit based on axial tensile tearing of indications with cellular or IGA (not significant at TSP intersections) corrosion becomes applicable for the axial pressure differentials across the tube. Available pulled tube and laboratory specimen data on axial tensile tests and measured undegraded tube cross sectional area were used to estimate the tensile tearing structural limit. Based on a regression analysis of the residual tube cross sectional area to bobbin voltage, the tensile structural limit at the lower 95% confidence bound on the data, as adjusted for lower tolerance limit material properties at operating temperatures, is greater than 35 volts. With a conservative factor of two allowance for crack growth and NDE uncertainties (current data indicates that typically a 1.7 factor is required), a full APC repair limit for tube expansion would be about 15 volts. For Braidwood-1 and Byron-1, the full APC repair limit, above which tube repair is required independent of RPC confirmation of indications at TSPs, is conservatively set at 10 volts.

For Braidwood-1 and Byron-1, a tube repair limit of > 3.0 volts is recommended for the hot leg TSPs with tube expansion. Bobbin voltage indications ≤ 3.0 volts can be left in service independent of RPC confirmation as a flaw indication. Bobbin indications > 3.0 volts and ≤ 10 volts are repaired if confirmed as flaw indications by RPC inspection and bobbin indications > 10 volts are repaired independent of RPC confirmation. For indications at FDB and cold leg TSP intersections for which tube expansion is not applied, the NRC approved repair limits of the Generic Letter for ODSCC at TSPs are to be applied. Currently, the draft generic letter establishes tube repair limits of 1.0 volt for 3/4 inch diameter tubing. Based on this tube repair limit, Braidwood-1 and Byron-1 bobbin indications at FDB and cold leg TSP intersections > 1.0 volt would be repaired if confirmed as flaw indications by RPC inspection. Bobbin indications > 1.0 volt and less than or equal to the full APC repair limit without tube expansion are to be repaired if confirmed as flaw indications by RPC inspection. Bobbin indications greater than the full APC repair limit are to be repaired independent of RPC confirmation. The full APC repair limit is based on the structural limit reduced by allowances for growth and NDE uncertainties. The structural limit is dependent on the latest database applied to develop the burst pressure versus bobbin voltage correlation and is to be updated on a periodic basis. The full APC repair limit will be updated to the latest database and plant specific growth rate data at each inspection outage at which the alternate plugging criteria of this report are applied. For FDB intersections which have large tube to plate clearances, the structural limit is based on a $3\Delta P_{NO}$ structural margin. At cold leg TSP intersections for which the small clearances provide constraint against tube burst, the structural limit is based on a $1.43\Delta P_{SLB}$ structural margin. Based on the latest 3/4 inch diameter database and the prior cycle Braidwood-1 growth rates, the full APC repair limits developed in this report are 1.9 volt for indications at the FDB and 2.7 volt for indications at cold leg TSPs.

Inspection Requirements

Inspection requirements for applying the tube repair limits of this report are essentially the same as those required by the NRC draft letter with adjustment of the RPC inspection requirements for hot leg TSP intersections to reflect the higher tube repair limits with tube expansion. All hot leg FDB and TSP intersections and cold leg TSP intersections down to the lowest TSP at which ODSCC indications are found are to have 100% bobbin inspection. For cold leg TSP and hot leg FDB intersections, all bobbin indications above the IPC repair limit of 1.0 volt are to be RPC inspected. For hot leg TSP intersections, all bobbin indications above the 3.0 volt repair limit and a minimum of 100 intersections below the 3.0 volt repair limit are to be RPC inspected. All TSP intersections with dent (mechanically induced dings at Braidwood-1 and Byron-1) voltages > 5 volts and residual bobbin signals that could mask a flaw at the voltage repair limit are to be RPC inspected and RPC flaw indications at these intersections are to be repaired. The RPC inspection results are to be evaluated for responses typical of that found for dominantly axial ODSCC and to confirm that flaw indications are within the confines of the TSPs. RPC indications at dented TSP intersections are to be evaluated for potential PWSCC indications. If the RPC inspections identify indications outside the confines of the TSP, circumferential crack indications or PWSCC at dents, these results are to be reported to the NRC prior to restart.

Additional inspections are required for implementation and monitoring of expanded tubes. TSP intersections selected for tube expansion and all surrounding TSP intersections shall be confirmed to be free of corrosion induced denting by bobbin inspection. For Braidwood-1 and Byron-1, no corrosion induced denting has been identified. At the time of tube expansion, the expanded TSP intersections are to be bobbin inspected following implementation of the expansions. By applying bobbin profilometry, the inspection must confirm that adequate expanded tube diameters have been achieved and that the expansions are properly located relative to the TSP. At every third scheduled inspection following tube expansion, hot leg plugs in three expanded tubes shall be removed and the expanded TSP intersections inspected for circumferential cracking at the expansions. A probe capable of inspecting for circumferential cracks in the parent tube shall be used for this inspection.

SLB Analyses

SLB leak rate and tube burst probability analyses are required for the actual voltage distribution found by inspection at each outage and for the projected next EOC distribution. Methods of analysis are consistent with the NRC draft generic letter. With tube expansion, tube burst probability analyses are required only for FDB and cold leg TSP indications and the resulting burst probabilities are to be compared to the NRC reporting guideline of 10^{-2}. For the FDB and cold leg TSP indications, which are assumed to be free span indications in a SLB event due to postulated large TSP displacements, the SLB leak rate can be calculated by the EPRI methodology as included in the draft generic letter. For conservatism, Braidwood-1 and Byron-1 will also apply the EPRI methodology to the hot leg TSP intersections. However, with tube expansion, the hot leg SLB leak rate must include an additional term that accounts for indications within the TSP that become potentially overpressurized with crack openings larger than included in the free span leakage estimate.

The probability of an overpressurized condition is essentially the probability of a free span burst. With overpressurization, the flanks of the crack face can open until contact is made with the inside surface of the tube hole. For this condition, bounding analyses can be made for the leak rates associated with the overpressurized indications. The bounding leak rates are given in this report and related to bobbin voltage to obtain the overpressurized leak rate as a function of voltage. The SLB leak rate for the overpressurized indications is then obtained as the probability of free span burst (probability of leakage with an overpressurized indication) times the bounding leak rate for an overpressurized indication. It is roughly estimated that the overpressurized indications will add a few gpm of leakage to that calculated for the hot leg TSP indications by free span analysis methods. For applications of the alternate repair limits of this report, Monte Carlo analyses will be used for all SLB leak rate and tube burst probability analyses.

Table 2-1

Example of Generic Tube Expansion Matrix

a,c

a,c

Figure 2-1. Map of Tube Expansion Locations

3.0 MODEL D4 S/G DESIGN DESCRIPTION

3.1 Overall Design

The Byron Unit 1 and Braidwood Unit 1 steam generators are of the Westinghouse Model D4 preheat steam generator design. Each steam generator (S/G) contains 4578 mill-annealed Alloy 600 U-tubes, 0.75 inch OD x 0.043 inch wall, which provide 48,300 sq. ft. of heat transfer area per S/G. Figure 3-1 shows the steam generator layout; a detailed layout of the preheater region is shown in Figure 3-2. Primary coolant enters the hot leg channelhead and passes through the U-tubes, which transfer heat from the primary side to water on the secondary side, which is converted to steam. On the secondary side, about 10% of the feedwater flow at full power is bypassed to an auxiliary nozzle to enter the upper plenum in the region of the primary moisture separators. Most (about 90%) of the feedwater enters the S/G through the preheater inlet nozzle into the preheater region (see Figure 3-2). The feedwater flow entering the preheater nozzle is directed to the bottom of the preheater by a waterbox at the nozzle, from where it circulates upward through a series of preheater baffle plates which discharge the flow upward into the tube bundle. As the secondary fluid passes through the tube bundle, it is converted to a water/steam mixture which passes upward through the transition cone region of the S/G shell, into the primary and secondary moisture separators in the upper shell region. Water is separated from the steam before the dry steam exits the S/G via the steam outlet nozzle. Water removed by the moisture separators flows down the annulus between the shell and the wrapper surrounding the tube bundle region. Upon reaching the tubesheet, the water is once again directed upward through the flow distribution baffle into the tube bundle. A partition plate between plates B and L (see Figure 3-2) separates the preheater and hot leg sides of the S/G. Below plate B and above plate L, secondary flow can cross between the hot and cold leg sides of the S/G.

The S/G tubes pass through tube support plates (TSPs) which provide lateral support to the tubes and contain circulation holes through which the water/steam passes upward through the tube bundle. On the cold leg side in the preheater region, these support plates contain no circulation holes, and act to direct the flow across the tubes; therefore, these plates are also referred to as baffle plates. The flow distribution baffle, at an elevation of 6.0 inches above the top of the tubesheet, distributes flow across the tubesheet and upward through a cutout in the plate on the hot leg side.

During normal operation, a slight pressure drop exists across each TSP or baffle plate. This pressure drop causes small displacement of the TSPs relative to the tubes during normal operating conditions. At hot standby conditions, there is no secondary flow or pressure drop across the TSPs. However, during postulated accident conditions such as steam line break (SLB), pressure differentials across individual TSPs can act to displace unsupported regions of the TSPs in such a manner as to uncover degradation within the TSP crevice. The following sections provide specific design information concerning the Model D4 baffle and support plates.

3.2 Tube Support Plate Design

The Model D4 steam generators at Byron 1 and Braidwood 1 utilize 0.75 inch thick carbon steel support plates with drilled (round) tube holes set on a square pitch of 1.0625 inches. With the exception of the flow distribution baffle and preheater baffle plates (described below), the tube support plates also include flow circulation holes measuring 0.50 inch in diameter, set on a square pitch of 1.0625 inches within the tube hole array.

The tube support plates of the Byron 1 and Braidwood 1 S/Gs may be classified as one of three types: the flow distribution baffle, preheater baffle plates, and tube support plates. The flow distribution baffle (FDB), located 6.0 inches above the top of the tubesheet, is comprised of two halves, with the cold leg side containing no circulation holes or cutouts; a moon-shaped cutout on the hot leg side permits the secondary fluid to pass upward through the tube bundle. On the cold leg side of the FDB, the drilled tube holes measure 0.900" in diameter, compared to the 0.750" OD of the tube. Therefore, the FDB provides no lateral support for the tubes. On the hot leg side, the drilled tube holes inside a radius of 32" from center of the S/G measure 0.875" in diameter, and the tube holes measure 0.833" in diameter outside a 32" radius from the center of the S/G. Hence, the enlarged FDB holes allow some secondary fluid to pass upward through the tube/FDB crevices, but no lateral support is provided for the tubes at the FDB level due to the large tube to FDB clearances.

The preheater baffle plates, shown in Figure 3-3, contain 0.766" diameter drilled tube holes and no circulation holes. Their function is to provide lateral support to the tubes and direct the flow back and forth across the tubes as the feedwater passes upward through the preheater. Letter designations are used by Westinghouse for the baffle plates at various elevations, with "A" representing the FDB and "B", "D", "E", "G", and "H" representing preheater baffle plates with no circulation holes.

On the hot leg side, two semi-circular plates ("C" and "F") with 0.766" diameter tube holes as well as 0.50" diameter circulation holes are located at the elevations of the "D" and "G" preheater baffle plates. These plates permit flow upward through the tube bundle and provide lateral support for the tubes. Plates "J" and "K", on the hot and cold leg side of the S/G at the top of the preheater, similarly contain 0.766" diameter tube holes and 0.50" diameter circulation holes. The remainder of the tube support plates, "L", "M", "N" and "P" are full size circular plates with similar tube and circulation holes. In addition, the "L" through "P" plates contain central flow slots along the tube lane to enhance flow upward through the bundle.

At Braidwood 1 and Byron 1, number designations are used for the plates, counting upward from the FDB through the preheater to the top TSP. The correspondence with the Westinghouse letter designations are: 1 = A, 2 = B, 3 = C, 4 = E, 5 = F and G, 6 = H, 7 = J and K, 8 = L, 9 = M, 10 = N and 11 = P.

3.3 Tube Support Plate Supports

The FDB, TSPs and preheater baffle plates are supported vertically using several support mechanisms, including five tierods/spacers in each half of the tube bundle. Preheater baffle plates C (3H), F (5H), and J (7H) are supported at their center by a vertical bar welded to the partition plate, while all of the TSPs above the preheater are supported at their center by a central tierod and spacer. Each of the baffle plates and TSPs are supported at the edges by vertical bars welded to the wrapper and/or partition plate immediately above the plates. In-plane supports are provided by wedges located around the circumference of each plate. The wedges are welded to the wrapper; their tapered design provides additional resistance to upward movement, in addition to in-plane support, due to the sloped face of the wedge.

Section 7.3 provides a detailed description of the Model D4 S/G TSP support system. Figure 7-1 shows a schematic of the tube bundle region, and support locations for each of the plates are shown in Figures 7-2 to 7-10. Detailed descriptions of the support components, including the tierods, spacer bars, and wedges groups, are provided in Section 7.3.

3.4 Secondary System Considerations

The steam generator secondary side consists of a natural circulation loop with feedwater inlets and a steam outlet. The steam generator water level at Braidwood Unit 1 is maintained at 66% of the narrow range taps, which is 487" above the top of the tubesheet. Byron Unit 1 has been at 61 to 63% of the narrow range taps, but will be going up to 66%. The current study considers a normal water level of 487" for the reference analysis applicable to both the Braidwood and Byron Units.

Most (~90%) of the feedwater enters the preheater of the generator through the main feedwater nozzle. The feedwater then flows through four crossflow passes; it moves upward and leaves the preheater to join the flow from the hot leg side, after passing upward through the tube support plate L. A fraction of the feedwater flow comes down through the bottom baffle to meet with the flow from the downcomer. The resulting flow then moves into the hot leg side via the tube lane.

A small fraction (~10%) of the feedwater enters the steam generator through an auxiliary feedwater nozzle in the upper shell. The feedwater from the auxiliary nozzle mixes with the separated water from the moisture separators. This takes place in the upper water reservoir. The mixed water flows down the downcomer annulus, which is separated from the tube bundle by the wrapper. The downcomer flow enters the tube bundle through the wrapper opening above the tubesheet. As the fluid approaches the first tube support plate in the hot leg side, axial flow becomes dominant. Boiling takes place and the flow moves upward along the hot leg side.

The hot and cold leg tube bundle flow meet above TSP L. The combined flow moves upward while boiling continues, leaving the tube bundle and entering the primary separators. A large portion of the water is separated by the primary separators and returned to the water reservoir. The steam with the remaining entrained moisture then enters the secondary separators. This entrained moisture is trapped by a system of hook and pocket vanes and returned to the water reservoir. The steam then leaves the steam generator through the steam outlet nozzle.

The Model D4 S/Gs utilize a venturi type flow limiter in the steam outlet nozzle. The venturi flow area at the throat is about 1.4 ft^2, while the steam line flow area is about 4.7 ft^2; therefore, the critical discharge flow is controlled by the flow limiter throat area of 1.4 ft^2 when a guillotine steam line break is postulated.

a

Figure 3-1. Model D4 Steam Generator Layout

a

Figure 3-2. Model D4 Steam Generator Preheater Region

a

Figure 3-3. Flow Distribution and Preheater Baffle Plates

4.0 THERMAL HYDRAULIC MODELING

A postulated steam line break (SLB) event results in blowdown of steam and water. The fluid blowdown leads to depressurization of the secondary side. Pressure drops develop and exert hydraulic loads on the tube support plates (TSPs) or baffle plates. These hydraulic loads were determined for the Model D4 steam generator using the TRANFLO computer code.

4.1 TRANFLO Code Description

The TRANFLO code uses an elemental control volume approach to calculate the thermal and hydraulic characteristics of a steam and water system undergoing rapid changes. Fluid conditions may be subcooled, two-phase or superheated. The code considers fluid flow as one-dimensional. It predicts the mass flow rate, pressure, pressure drop, fluid temperature, steam quality and void fraction.

Control volumes simulate the geometrical model, and flow connectors allow mass and energy exchange between control volumes. Each nodal volume has mass and energy that are uniform throughout the volume. Flow connectors account for flow and pressure drops. The system model allows for flow entering or leaving any control volume. This then allows that feedwater flows into the steam generator and steam flows out of it. The system models also permit a heat source, which then can simulate the tube bundle with hot water flow.

TRANFLO solves for system conditions by satisfying mass, momentum and energy equations for all control volumes. It models the effects of two-phase flows on pressure losses. The code allows a variety of heat transfer correlations for the tube bundle. It covers all regimes from forced convection to subcooled liquid through boiling and forced convection to steam.

4.2 Model D4 TRANFLO Models

The TRANFLO computer model for Model D4 steam generator is composed of a network of nodes and connectors that represent the secondary side fluid, tube metal heat transfer and primary coolant. Figures 4-1 and 4-2 show the nodal layout of the secondary side of the Model D4 steam generator. Figures 4-3 and 4-4 present the nodal network of the secondary fluid, primary fluid and tube metal. The computational model consists of the following elements:

1. 31 nodes (i.e., No's. 22 through 52) for secondary fluid.
2. 44 fluid connectors (i.e., No's. 23 through 66) for secondary fluid.
3. 21 nodes (i.e., No's. 1 through 21) for primary coolant.
4. 22 fluid connectors (i.e., No's. 1 through 22) for primary coolant.
5. 21 heat transfer nodes (i.e., No's. 1 through 21) for tubes.
6. 42 heat transfer connectors (i.e., No's. 1 through 42) from primary to secondary fluid.

For a postulated SLB event, the above model considers a break just outside the steam outlet nozzle. However, the break may be further downstream, outside the containment building. Figure 4-5 illustrates such a model; it has three additional nodes and three more flow connectors to simulate the steamline from the steam nozzle to the containment. For the Braidwood-1 and Byron-1 plants, this length is about 120 feet with about three elbow turns.

The TRANFLO modeling reported in WCAP-14046, Rev. 1 involved a coding error in flow connectors. Flow connector No. 22 is in the primary coolant side; its upstream node is No. 21 and its downstream node is No. 0 (an outside node, see Figure 4-3). Instead of using outside node No. 0, node No. 22 was coded in the input. Note that node No. 22 is a secondary side node (see Figure 4-4). This error is corrected in this report. Results for the hot standby case are similar between this report and WCAP-14046, Rev.1. However, there are significant differences between this report and WCAP-14046, Rev. 1 for the full power case. The error in the prior full power analyses leads to an overestimate of the TSP loads in WCAP-14046. The correction results in proper simulation of full power behavior. The results show that hot standby yields higher loads than full power, as expected since the water flashing due to depressurization is greater for hot standby than full power conditions.

4.3 Calculation of TSP Pressure Drop from Dynamic Analysis

In the tube bundle area, the space between support plates or baffles forms a fluid node, and a flow connector links the adjacent nodes (see Figures 4-1 and 4-2). Pressure drops through support plates or baffles are calculated by the code for each flow connector, which includes a plate or baffle. The whole length of the flow connector is very long compared to the thin plate of less than an inch. For example, flow connector 39 links node 30 to node 29. Tube support plate P is the boundary between node 33 and node 32. Node 29 is the U-bend and the space below the inlet of riser barrels. The pressure drop through TSP P is calculated along flow connector 39.

For example, the pressure difference between the centroids of nodes 30 and 29 acts to accelerate the flow for the whole connector 39, including the inertia of all the fluid in the flow path. It would be highly unrealistic to apply the overall pressure difference between nodes or along the whole connector to the thin plate. Note that connector 39 has a length of 66.6 inches and that TSP P is only 0.75 inch thick. A correct approach is to apply only the form pressure drop to TSP P, since the fluid itself absorbs most of the unsteady pressure drop through inertia, and the momentum flux and friction terms are distributed through the fluid.

It can be shown that the force on an orifice plate (or a TSP) resulting from the transient, blowdown-type flow of a compressible fluid in a pipe can be calculated from a form loss. The orifice pressure drop is equal to a loss coefficient times the fluid dynamic head. The TRANFLO code is a proven code for dynamic analysis of two-phase blowdown flow resulting from a SLB event. The hydraulic loads on the

TSPs as calculated by the TRANFLO code or any other alternate code are based on the form loss of pressure through the TSP.

4.4 Model D4 S/G Operating Conditions

Both Braidwood Unit 1 and Byron Unit 1 are plants with Model D4 steam generators; hence, they have identical designs for the tube bundle and tube support plates.

Design operating conditions at full power for the Braidwood Unit 1 S/Gs are as follows:

Thermal Power	=	856.25 Megawatts
Thermal Design Flow	=	94,400 gpm
Primary Inlet Temperature	=	618.4°F
Primary Operating Pressure	=	2250 psia
Feedwater Temperature	=	440°F
Steam Pressure	=	997 psia
Circulation Ratio	=	2.35

Byron Unit 1 has similar operating conditions to those above, with the exception of the primary side temperature and secondary steam pressure. The plant is licensed to operate at a reduced primary temperature, as low as 600°F, which results in a lower steam pressure (824 psia).

In addition, both plants have identical hot standby conditions. The steam temperature at hot standby is 557°F. Both plants operate at the same water level. The steam piping layouts are similar between the two plants.

In summary, both plants have essentially the same geometrical and thermal-hydraulic conditions. The TRANFLO model developed for the Braidwood Unit 1 S/Gs can also be used for Byron Unit 1. The TRANFLO calculations were made at the Braidwood-1 inlet temperature of 618.48°F. Differences in the dynamic transient due to a SLB event are considered insignificant between an initiation of 618.48°F or 600°F.

4.5 TSP Pressure Drop Data

Laboratory tests were made to correlate the loss coefficient through a tube support plate (see Figure 5-2 in Section 5.2.4). As discussed in more detail in Section 5.2.4, Figure 5-2 shows the test data and correlation of the loss coefficient for determining the pressure drop through a TSP. The correlation constant ranges from 0.8 to 1.4, and its best estimate is 1.1. This correlation has been incorporated in the GEN code, a steam generator performance code.

The circulation ratio depends on pressure drops through the circulation loop. The circulation loop consists of the downcomer, tube bundle and primary separator.

The downcomer has a small pressure drop. The major pressure drops come from various TSPs and swirlvanes of the primary separator.

4.6 Acoustic Pressure Wave Considerations

Acoustic pressure can affect the fluid flow through the tube bundle and thus the pressure drop through the TSP if it is significant inside the steam generator, in particular, in the tube bundle. The steamline break can generate a depressurization wave into the steam generator. Because of hardware elements inside the steam generator, this decompression wave will reflect and not be transmitted into the tube bundle. The nature of tortuous paths from the steam nozzle to the tube bundle (see Figure 4-1) weakens the penetration of the wave into the tube bundle. In addition, since the secondary side is two-phase, there is ample compressibility of the mixture and the speed of sound is significantly reduced. The secondary side will respond to the depressurization by flashing of the two-phase mixture to a higher void fraction. The pressure drops that will occur will be due to mainly the two-phase flow acceleration, friction and form loss of hydraulic motion.

If the steam generator is in a hot standby condition when the break occurs, the vapor space above the water level would provide compressibility for the flow. Also, as the secondary side begins to depressurize, vapor forms within the hot liquid due to flashing, which will also provide additional compressibility to the mixture.

The TRANFLO code uses the complete transient mass, momentum and energy conservation equations; the acoustic propagation of pressure waves through steam or water occurs naturally within the solution obtained from these equations. Results obtained from the TRANFLO code have been tested against analytical results of acoustic phenomena. Their comparison has demonstrated that the TRANFLO code has the capability to simulate the acoustic effect. Its simulation for a steamline break depressurization would be able to calculate the effect of a depressurization wave initiated at the steam nozzle, if not negligible. A smaller time increment would be appropriate to properly simulate the acoustic effect.

However, a finer nodalization than that shown in Figures 4-1 and 4-2 may be needed to adequately analyze the acoustic effect by the TRANFLO code. The MULTIFLEX code retains the same conservation equations and it uses the method of characteristics with an explicit numerical solution scheme. The method and numerical scheme thus minimize numerical diffusion. The effect of numerical diffusion is to stretch the wave out spatially. For relatively thin structures like the tube support plate, the effect of numerical diffusion can be significant because the pressure difference across the plate due to an acoustic wave is underestimated. Therefore, MULTIFLEX provides the most accurate spatial representation of acoustic waves. In terms of two-phase flow modeling, the TRANFLO code uses the drift-flux model to consider the effect of flow slip between water and steam phases. The MULTIFLEX code uses a homogeneous model without flow slip between phases.

MULTIFLEX has been used (Section 5) to simulate the SLB event with equivalent modeling to the TRANFLO model. Results are compared with those of the TRANFLO model, and the effect of acoustic waves are assessed. As noted in Section 5, the effects of acoustic waves are shown to be negligible, as expected, based on the above discussion.

4.7 Balance of Plant Modeling

A postulated steam line break could take place in any operating mode of the plant; it could occur at any location along the steam line, and the size of the break could be double ended (i.e., guillotine) or limited. These variables all lead to different blowdown flow rates and two-phase motion inside the steam generator. Therefore, they all result in different hydraulic loads on the tube support plates. For example, a dynamic transient initiated from full power operation is different from that initiated from hot standby. A guillotine break will have higher blowdown flow than a limited break.

A complete assessment of these variables requires a parametric study. This assessment is given in Section 6; it covers reference cases, best estimates and a sensitivity study for the above variables in plant conditions, as well as for the TSP pressure drop.

a

Figure 4-1. Secondary Side Nodes and Tube Support Plates - Identification for Model D4 S/G (See Figure 4-2 for Preheater Detail)

a

Figure 4-2. Preheater Nodes and Baffle Identification for Model D4 S/G

a

Figure 4-3. Primary Fluid Nodes and Flow Connectors, Metal Heat Nodes and Heat Transfer Connectors, and Secondary Fluid Nodes Within Tube Bundle (Model D4 S/G)

a

Figure 4-4. Secondary Side Fluid Nodes and Flow Connectors for Model D4 S/G - Model for SLB Just Outside Steam Outlet Nozzle

a

Figure 4-5. Secondary Side Fluid Nodes and Flow Connectors for Model D4 S/G - Model for SLB Just Outside Containment Building

5.0 QUALIFICATION OF TRANFLO CODE

In the early 1970's, there was a need to accurately predict the steam generator behavior under transient conditions, such as a steam line break (SLB) event; a transient can develop thermal hydraulic loads on the internal components and shell of the steam generator. Structural analyses are required to analyze the adequacy of the individual components and the whole steam generator under various thermal and hydraulic loads. With the assistance of MPR Associates, Westinghouse developed and verified the TRANFLO computer code to conservatively model the thermal and hydraulic conditions within the steam generator under transient conditions.

Qualification of the TRANFLO code has been a continuing process in demonstrating the code's capability to accurately predict the hydraulic loads on internal components of the steam generator.

5.1 Qualification Plan

For application to Braidwood Unit 1 and Byron Unit 1, the qualification effort consists of two parts. Part 1 (Section 5.2) describes the historical verification effort. Part 2 (Sections 5.3 to 5.6) documents a specific effort for both units; this includes an evaluation of the acoustic effect on hydraulic loads on tube support plates. For Part 2, a verified computer program called MULTIFLEX has been applied as described below, together with analysis results and comparisons with TRANFLO code results.

5.2 Previously Reported Efforts

The secondary side of the steam generator involves water boiling under high pressure during normal operating conditions. During a transient such as a SLB event, it may be subject to vapor generation due to rapid depressurization. Therefore, analysis methods have to recognize this characteristic of two-phase fluid behavior. In the early stage of the computer code development and technology of two-phase flow, a homogeneous model was used. For current analyses, a more accurate slip flow model is used which takes into consideration the relative velocity between the liquid and vapor phases. Development of the TRANFLO code reflects this general trend of the two-phase flow modeling. The first version of TRANFLO was a homogeneous model, and it was later updated to a drift flux model to simulate the effect of two-phase slip. Since the original issue of the code, Westinghouse has made several enhancements to the code and has performed the appropriate verification and validation of these changes.

5.2.1 Acceptability of Application of TRANFLO

The original version of the TRANFLO code (Reference 13.10) was reviewed and approved by the NRC in Reference 13.11. TRANFLO was used as part of the Westinghouse mass and energy release/containment analysis methodology.

Specifically, the code was used to predict steam generator secondary side behavior following a spectrum of steam line breaks. Its output was the prediction of the quality of the steam at the break as a function of time. The quality is calculated as a function of power level, as well as break size. In order to assure that the TRANFLO code evaluates a conservatively high exit quality, Reference 13.11 states that the calculational sequences were reviewed for the determination of conditions prior to entering into the separation stages. The calculated rate, quality and energy content of the two-phase mixture entering the separation stages must be evaluated conservatively. This review was completed and found to be acceptable, as the NRC staff concludes in Reference 13.11 that the TRANFLO code is an acceptable code for calculating mass and energy release data following a postulated SLB. Therefore, it is concluded that the TRANFLO model is appropriate for predicting S/G behavior (including tube bundle region) under the range of SLB conditions. In particular, the NRC review concluded that the flow rate and quality entering the separation stages is adequately conservative. Therefore, if further review is required, the review would focus on the flow distribution within the tube bundle. The distribution within the tube bundle is principally influenced by the TSP loss coefficients, which are based on experimental data for Westinghouse manufactured S/Gs (see Section 5.2.3). To further address the flow distribution within the tube bundle, additional sensitivity analyses in TRANFLO pressure drop dependence on the TSP loss coefficients have been performed as described in Section 6.

For the current application, TRANFLO is used in conjunction with a structural analysis code to predict TSP movement following the same SLB event. The key data transferred between the transient code and the structural code is the pressure drop across the TSP as a function of time. This pressure drop calculation depends on the fluid conditions in the steam generator and on the adequacy of the loss coefficients along the flow paths. The conditions in the tube bundle as calculated by TRANFLO have been previously reviewed. Further justification of the adequacy of the pressure drop calculation is discussed in Section 5.2.3.

5.2.2 Different Versions of TRANFLO

The original version of the TRANFLO code has been reviewed and approved by the NRC. Westinghouse has continued to update the code with new models that more accurately predict steam generator behavior. Four versions of the TRANFLO have been used in calculations. The following are descriptions of each of them.

The Original Version (April 1974)

This is the original homogeneous model, which MPR Associates developed in April 1974. The code predicts mass flow rate, pressure, pressure drop, fluid temperature, steam quality and void fraction. The code document includes results of TRANFLO calculations for a 51 Series steam generator subject to water and steam blowdown due to a SLB event. The document also presents code verification using blowdown test data from pressurized vessels.

Westinghouse documented this version in detail in September 1976, including code verification using vessel blowdown data (Reference 13.10). Sensitivity analyses were also performed and documented to show that the modelling was conservative.

The TRANFLO code uses an elemental control volume approach to calculate the thermal-hydraulics of a steam and water system undergoing rapid changes. Fluid conditions may be subcooled, two-phase or superheated. The code considers fluid flow being one-dimensional.

Control volumes simulate the geometrical model, and flow connectors allow mass and energy exchange between control volumes. Each nodal volume has mass and energy that are homogeneous throughout the volume. Flow connectors account for flow and pressure drops. The system model allows flow entering or leaving any control volume. This then allows that feedwater flows into a steam generator and steam flows out of it. The system models also permit a heat source, which then can simulate the tube bundle with hot water flow.

TRANFLO solves for system conditions by satisfying mass, momentum and energy equations for all control volumes. It models the effects of two-phase flows on pressure losses. The code allows a variety of heat transfer correlations for the tube bundle. It covers all regimes from forced convection to subcooled liquid through boiling and forced convection to steam.

The Drift-Flux Version (November 1980)

This version implements a drift-flux model to better simulate relative flow velocity between water and steam. For example, it allows a realistic simulation of counter-current flow of steam and water. It required modification of the mass, momentum and energy equations of the two-phase flow. A capability is provided for monitoring calculated variables for convenient examination of results.

TRANFLO Version 1.0 (November 1991)

This version accepts transient data of parameters as direct inputs, rather than supplying input subroutines, as used in the drift-flux version. It also improves printouts and plots. This version maintains the drift-flux model, and includes the addition of thermal conductivity of Alloy 690 tubing.

TRANFLO Version 2.0 (January 1993)

This version provides an option for two inlets of feedwater flow into the steam generator. It involves minor changes to a subroutine for specifying feedwater flow. This version is used for separate inlets of simultaneous feedwater flow from the main and auxiliary feedwater nozzles.

5.2.3 Verification of Loop Pressure Drop Correlations

As discussed earlier, an accurate prediction of mass and energy release from the vessel means that the TRANFLO code properly calculates local thermal-hydraulics in various nodes (i.e., elemental control volume and flow connector). It is critical to accurately simulate the pressure drop inside a steam generator that consists of various components, such as the tube bundle with tube support plates, moisture separators, and downcomer. Hydraulic loads on various components depend on accurate pressure drop calculations. Thus, it is important to verify the pressure drop calculations through the circulation loop.

The TRANFLO code uses the same pressure drop correlations as the Westinghouse GENF code, which is a performance program. The GENF code predicts one-dimensional steady state conditions, which include pressure drops along the circulation flow loop. Both laboratory tests and field data validate the accuracy of the GENF code. The GENF code is used extensively for steam generator performance analysis and has been shown to accurately predict operating steam generator conditions.

When provided with all geometrical input and operating conditions, GENF calculates the steam pressure, steam flow rate, circulation ratio, pressure drops, and other thermal-hydraulic data. The circulation ratio is a ratio of total flow through the tube bundle to feedwater flow. For a dry and saturated steam generator, there exists a hydrostatic head difference between the downcomer and the tube bundle. This head difference serves as the driving head to circulate flow between them (see Figure 5-1). The driving head is constant for given operating specifications, such as power level and water level. The total pressure drop through the circulation loop is equal to the driving head.

Pressure drops depend on loss coefficient and flow rate (i.e., velocity). Loss coefficient consists of friction loss and form loss; the majority of the loss is due to the form loss in the steam generator. Since the driving head is constant, a higher loss coefficient means a lower circulation flow rate and a lower circulation ratio. A lower loss coefficient yields a higher circulation ratio. Therefore, an accurate prediction of the circulation ratio depends on an accurate loss coefficient.

Model boiler and field tests are used in qualifying the loss coefficients in the flow loop of the steam generator. For example, the major contributors of the pressure drop are the primary separator and tube support plates. The loss coefficient of the primary separator has been verified using model boilers and field steam generators (Reference 13.12). Similarly, loss coefficients of tube support plates have been developed using test data; Figure 5-2 presents the correlation of the loss coefficient and test data.

Figure 5-3 shows a typical comparison between predicted and actual measured circulation ratios. There is good agreement in the circulation ratio between the prediction and measurement.

The TRANFLO model uses the same loss coefficient correlations as the GENF code. This provides assurance in properly calculating the pressure drops throughout the steam generator.

5.3 MULTIFLEX Code Description

The MULTIFLEX program is an engineering tool for calculation of pressure and mass flow distributions during rapid thermal-hydraulic transients caused by an imposed driving force on the system. The driving force is taken, throughout this report, to be a break of a secondary loop in a Pressurized Water Reactor (PWR) system. MULTIFLEX has been verified by comparison to test data and has been reviewed and approved by the United States Nuclear Regulatory Commission (USNRC).

The USNRC has reviewed Westinghouse WCAP-8708 (Proprietary) and WCAP-8709 (Non-proprietary). The USNRC issued an approval letter on June 17, 1977 together with a Topical Report Evaluation (Reference 13.13). It concludes that WCAP-8708 presents an acceptable computer program for use in calculations to evaluate the pressure time history of fluid within current Westinghouse reactor systems caused by subcooled decompression during a postulated loss of coolant accident. Based on this approval letter and comments in the attached Topical Report Evaluation, Westinghouse issued a revised WCAP-8708-PA-V1 (i.e., Reference 13.14), which contained the Reference 13.13 Topical Report Evaluation.

The thermal-hydraulic portion of MULTIFLEX is based on the one-dimensional homogeneous model which is expressed in a set of mass, momentum, and energy conservation equations. These equations are quasi-linear first order partial differential equations which are solved by the method of characteristics. By the method of characteristics, the partial differential equations are reduced to ordinary differential equations. The formulation of the characteristic equations results in equations which include acoustic signal transportation.

The representation and analysis of complex hydraulic systems by MULTIFLEX is accomplished using a network of hydraulic flow paths and mathematical models of various hydraulic components, such as two- and multi-pipe joints, orifices, pumps, valves, etc.

MULTIFLEX has been used extensively to analyze, among other events, loss-of-coolant transients in both the primary and secondary sides of PWRs and waterhammer transients due to valve motion.

5.4 MULTIFLEX Models

The MULTIFLEX model of the steam generator consists of a network of hydraulic flow paths, referred to as legs. Figure 5-4 shows the MULTIFLEX model in schematic form. The entire hydraulic geometry of the secondary side of the steam generator is modeled with the legs by specifying appropriate values for flow area, flow length, elevation, loss coefficient, hydraulic diameter, and boundary condition. The thermodynamic initial conditions are specified with appropriate values for pressure, enthalpy, and mass flow. The forcing function for the transient is described by a break model which simulates a double-ended, guillotine rupture of the main steamline, located at the outlet nozzle on the steam generator. The MULTIFLEX model, as depicted in Figure 5-4 and described by its associated input data, is equivalent to the TRANFLO model presented in Section 4.2.

5.5 Comparison of MULTIFLEX and TRANFLO Results

5.5.1 Hot Standby Case

In WCAP-14222 report, MULTIFLEX model did not properly enter the throat area (about 1.39 ft^2) of the venturi in the steam nozzle. This results in a use of a 5.0 ft^2 area of the steam line in calculating the break flow rate. This use of higher flow area leads to unusually high break flow, which can significantly affect flow in tube bundle and thus pressure drops through tube support plates. In present report, this is corrected; the venturi throat area is simulated.

Results of MULTIFLEX calculations for a SLB event initiated from a hot standby are shown in Figures 5-5 through 5-7. For the identical case, results of TRANFLO calculations are given in Figures 6-1 through 6-3 (see Section 6.2). From these figures, it is seen that neither MULTIFLEX nor TRANFLO results show a higher frequency oscillation in the TSP pressure drops as might be expected if acoustic wave effects were significant. Effect of the acoustic wave due to a SLB event is discussed in detail in Section 6.6.

TRANFLO predicts a flow split between TSP J and TSP L. That is, the transient flow at TSP J and below is in a downward direction, while in an upward direction at TSP L and above. MULTIFLEX gives a split between TSP L and TSP M. They differ by about one TSP span (i.e., about 43 inch tube span); this is in good agreement. It is shown in Section 8 that this shift in the flow split to above TSP L for MULTIFLEX has negligible influence on TSP displacement.

Table 5-1 presents the peak values for pressure drops over the transient for comparison. MULTIFLEX yields lower values than those of the TRANFLO.

Results presented in WCAP-14222 are reproduced here for comparison and discussion. As mentioned above, these results are obtained for a steam nozzle without the venturi flow limiter in the steam nozzle. Thus the break flow is unusually high. Figures 5-8 through 5-10 show the predicted pressure drops through tube support plates. Compared to those of Figures 5-5 through 5-7, results of the case without the flow limiter are many times higher. Peaks of these pressure drops under the conditions without the flow limiter are comparable to the TRANFLO results with the venturi flow limiter. Note that TRANFLO results show two peaks in pressure drop, and MULTIFLEX gives one peak only. This will be discussed below and in detail later.

The differences in pressure drop between TRANFLO and MULTIFLEX are considered to be due to differences in modeling and solution schemes. Since the employed numerical method of solution in MULTIFLEX is the explicit scheme, numerical diffusion is minimized, thus providing an accurate spatial representation of the acoustic waves. TRANFLO could underpredict the acoustic effect because of the use of an implicit integration technique. An implicit numerical solution scheme tends to result in greater numerical diffusion than an explicit scheme. The effect of numerical diffusion on acoustic waves is to stretch the wave out spatially. For relatively thin structures like the TSPs, the effects of numerical diffusion can be significant because the pressure difference across the plate due to acoustic waves, if present, is underestimated.

There is a difference in the physical model for two-phase flow between TRANFLO and MULTIFLEX. TRANFLO uses drift-flux modeling, which accounts the effect of flow slip between liquid and vapor phases. MULTIFLEX considers a homogeneous model without slip. A homogeneous model tends to yield a higher void fraction than a drift-flux model. A drift-flux model would have a better estimate for void fraction. However, void fraction would not totally account for the difference observed. The amount of the water flashing can influence the two-phase flow and thus the pressure drop. So can the water boiling due to heat transfer. These will be discussed in later subsections.

5.5.2 Effect of Heat Transfer on Hot Standby Case

The MULTIFLEX modeling for a SLB event was conducted without considering the heat transfer from the primary coolant under the assumption that heat transfer is not significant. This assumption greatly simplifies the MULTIFLEX modeling. This is considered to be a good assumption for a process having a short transient. In addition, the dominating thermal hydraulic process is due to break flow, subsequent depressurization and the resulting water flashing. This section presents the results of the TRANFLO calculations with and without heat transfer from the primary coolant.

Figures 6-1 through 6-3 show the TRANFLO pressure drops through tube support plates for the hot standby with heat transfer (see Section 6.2). The same TRANFLO model without heat transfer yields pressure drops given in Figures 5-11 through 5-13. These figures demonstrate that results are similar in the transient shape and magnitude. Table 5-2 lists the peak value of the pressure drop and their ratio. Their ratio is about unity, except the TSP L, which gives a ratio of 1.49. This is expected because the flow split is near the TSP L.

The good agreement between the TRANFLO calculations with and without heat transfer confirms the assumption of the dominating effect of water flashing and insignificant role of heat transfer for the extreme short transient phenomena of a SLB event.

Based on the above discussion, we show that the MULTIFLEX calculation without coupling with the primary coolant for the hot standby case is appropriate and acceptable in simulating the transient of a SLB event.

5.5.3 Effect of Heat Transfer on Full Power Case

Figures 5-14 through 5-16 show the TRANFLO pressure drops through tube support plates for the full power case without heat transfer. Figures 6-4 through 6-6 present the same TRANFLO pressure drops for the full power case with heat transfer. As can be seen, heat transfer seems to yield higher pressure drop for the upper TSPs L, M, N and P, while the no heat transfer case seems to generate higher pressure drop for the lower TSPs A, C and F. This opposite behavior could be explained below.

It may be the situation that boiling due to heat transfer and water flashing due to depressurization are mutually competitive or exclusive. For the upper tube bundle where the upper TSPs are located, the initial void fraction is high and water mass is relatively small, and the boiling dominates the thermal and hydraulic process. The boiling of the small amount of the water available in the upper tube bundle seems to be the driving mechanism to create flow motion, and thus pressure drop. If there is no heat transfer the small amount of water may not be adequate to generate enough flow motion locally. Therefore, the no heat transfer case results in much lower pressure drops for the upper TSPs.

For the lower tube bundle where void fraction is low and water body is large, the boiling may consume the water and deplete the amount of water for flashing to generate flow motion. However, if there is no heat transfer all of the water will be available for flashing to act in producing flow motion. In the lower tube bundle the flashing action dominates the thermal and hydraulic process. Any heat seems to tend to weaken the flashing effect. Therefore, the no heat transfer case leads to higher pressure drops for the lower TSPs.

In view of the above discussion, a calculation of the full power without the coupling with the primary coolant is not appropriate; it deviates drastically from the prototypical conditions. Therefore, we do not include plots of pressure drop transient from the MULTIFLEX calculation for the full power without the heat transfer. However, we will present its peak values later in table for comparison with TRANFLO calculations.

5.5.4 Effect of Water Flashing and Initial Temperature Distribution

The description of Section 5.5.3 is plausible. It implies that tube bundle two-phase flow is subject to complicate interaction of the boiling and flashing mechanism; it is a highly local phenomenon. This then points out that it is important to subscribe appropriate initial conditions, such as initial temperature of primary coolant and initial heat transfer rate. It is the most appropriate to use the prototypical conditions of full power operation as the initial conditions. Such conditions are varying along the U-tube. The full power calculation in WCAP-14222 report uses an approximation of an equivalent, averaging temperature over the total length of the U-tube. In view of the above discussion, such an approximation is not as good as a non-uniform distribution of temperature along the U-tube. Present report has changed from the average temperature approximation to actual distribution of primary coolant temperature and heat transfer rate as the initial conditions. Results shown in Figures 6-4, 6-5 and 6-6 are obtained using the prototypical, non-uniform conditions of the full power operation. Results by the present calculation show higher pressure drops than those given in WCAP-14222. For example, pressure drop through TSP P by the present calculation peaks to about 0.8 psi after time zero, and the WCAP-14222 gives a peak less than 0.2 psi for TSP P. Of course, both calculations have a same initial pressure drop of 0.56 psi.

Table 5-3 lists the relative peak value of the pressure drop for four calculations: the TRANFLO with and without heat transfer, the MULTIFLEX without heat transfer, and the TRANFLO with heat transfer reported in WCAP-14222. From the viewpoint of the relative peak of the pressure drop, both calculations of heat with uniform (i.e., average) and non-uniform initial temperature give about the same (absolute) values. Displacement calculation of the tube support plates has been made for both uniform and non-uniform temperature cases. Results indicate they are essentially the same; the non-uniform case is slightly less in displacement, except the TSP L, which is slightly higher. This trend is the same as that of the relative peak of the pressure drop (see Table 5-3). In view of this comparison, we keep the uniform temperature case as the reference and enter its results for Case 2 in Table 6-2. Note that Table 6-2 presents the results of sensitivity study for uncertainty parameters, and they are used to establish the adjustment factor of two, as discussed in Section 6.6.

The no heat transfer case leads to higher (absolute) values in the lower TSPs, and in upper TSPs M and P. The MULTIFLEX calculation without heat transfer yields lower pressure drops, except TSP M, than the TRANFLO calculation without heat transfer. It requires deeper investigation to explain such a difference between the TRANFLO and MULTIFLEX calculations. Such a difference may be due to rate of depressurization and rate of water flashing, and they may in turn depend on moisture separation and break flow calculation. These will be addressed in the next subsection.

5.5.5 Effect of Moisture Separation under Significant Water Flashing

We have made a parametric calculations of pressure drop under different water levels, ranging from 544" to 280" above the top of the tubesheet. The pressure drop through the tube support plate increases as the water level decreases; this is described in Section 6.3. We will take these calculations to examine the role of the water flashing and its impact on moisture separation, and then its influence on the break flow and the subsequent effect on pressure drop.

For a steam line break (SLB), the critical blowdown (or break) flow is limited by choking at the throat of the venturi in the steam nozzle. Use of the venturi is just for this purpose to control the break flow .. an SLB event takes place.

TRANFLO program uses the Moody critical flow model to determine mass flux (or velocity), which is a function of two-phase flow thermodynamic state upstream to the steam nozzle. The two-phase thermodynamic state is fully defined by two thermodynamic properties, such as steam quality and pressure. Once the choking mass velocity is determined from the Moody model, the break flow rate is known by multiplying the mass velocity by the flow area at the throat of the venturi.

The choking flow can change significantly with variation of the thermodynamic state upstream to the steam nozzle. This thermodynamic state changes according to flow conditions in the steam generator; a full power will behave differently from a hot standby. Even a hot standby can lead to different transient of thermodynamic state if the initial water level changes. The following is to describe this in detail.

For the hot standby at time zero, the break flow is 100% steam, and it decreases in steam content as time goes. There may be two stages. Taking the case with a water level of 487 inches for illustration (see Figure 5-17), the stage 1 has a steam quality at 99% within about 1.75 seconds after an SLB event. After 2.2 seconds, it drops down to stage 2 at a steam quality less than 4%. Between these two stages, there is a transition period with drastic change in steam quality. The lower the steam content the higher the fluid density, and thus the larger the critical mass velocity, as the Moody model gives. Figure 5-18 shows this behavior of two-stage in the break flow. Figure 5-19 depicts this two-stage phenomena in pressure immediate upstream to steam nozzle; it drops drastically during the transition period of 1.9 to 2.2 seconds. The significant flashing takes place during the transition and it leads to a temporary pressurization before it goes on a decreasing again.

During the first stage, it is essentially of single- phase steam. The steam blowdown depressurizes the steam generator, and thus triggers water flashing. The water in the upper downcomer flashes, and it entrains significant water. Thus, it results in a two-phase flow with low steam quality. Majority of the water flashing takes place outside the primary separators. Therefore, most of the resulting two-phase flow will moves directly against the secondary separator without the benefit of moisture separation by the primary separator. The secondary separator is flooded by this moisture rich flow, and can not remove it effectively. This moisture rich (i.e., low steam quality) flow continues into the steam nozzle. The Moody model then yields a much higher critical mass flux for a low steam quality in the stage 2, and thus larger break flow, as shown in Figure 5-18.

Each stage has its own acceleration and decceleration behavior of flow, and thus a peak develops, and appears in the pressure drop through TSPs. Figure 5-20 indeed shows a two-peak pressure drop through the TSP P.

Figures 5-21 through 5-23 show the similar response of break flow, pressure upstream to the steam nozzle and pressure drop through the TSP P for the case with a 544" water level. Figures 5-24 through 5-26 are the similar results for a 474" water level. The second stage appears quicker for a higher initial water level, because the available steam volume is smaller and it is depleted sooner. As shown by Figures 5-18, 5-21 and 5-24, the first stage ends at about 1.3, 2.0 and 2.3 seconds for a water level of 544", 487" and 474", respectively. The initial water level also affect the relative value of the double peak in pressure drop. Figure 5-23 shows the pressure drop through the TSP P for a 544" water level; the second peak has a higher pressure drop than the first peak. The first peak is related to the blowdown of the existing steam before the water flashing. The second peak is directly associated with the water flashing. Figure 5-20 depicts a similar two-peak pressure drop for a 487" water level, but both peaks have almost the same value. Again, Figure 5-26 gives the two-peak pressure drop for a 474" water level, the first peak is now at a higher value. This shift in relative value between the two peaks is well correlated with the amount of water flashing outside the primary separator.

The second peak of the pressure drop is dominating for a water level of 544 inches. For a water level of 487 inches, both the 1st and 2nd peak are about equal. The first peak becomes dominating at a water level of 474 inches. The second peak doesn't show for a water level of 378 inches, as indicated in Figures 5-27 through 5-29. Again, there is no second peak for a water level of 280 inches, as depicted in Figures 5-30 through 5-32. A water level of 387" is at the base of the primary separator, and thus there is no water mass in the upper internal space, except the limited water mass in the downcomer annulus. A water level of 280" results in no water mass in the upper internal space. Therefore, the only water flashing is taking place in the tube bundle; the amount of water mass is much smaller than that at a level of 474" or more. In addition, the flashing two-phase flow has the benefit of the primary separator to remove the moisture effectively. Therefore, the secondary separator is not loaded beyond its capability, and the steam quality to the steam nozzle is kept at high value. Figure 5-30 for a level of 280" thus shows a smooth decreasing trend in break flow; it does not give a rise to a second plateau like Figure 5-18 for a level of 487".

Regardless of relative magnitude between the 1st and 2nd peak, the peak value of the pressure drop increases with a decrease of the water level. This is due to significant flashing taking place across the water level. The nearer the TSP to the water level the stronger the flashing in generating fluid motion. A lower water level means a shorter distance between the TSP and water level. Therefore, a water level of 280 inches results in the highest pressure drop, as shown in Figure 6-13.

For a full power as an initial condition, the mass velocity is similar to that of the first stage of the hot standby case. The full power case does not lead to a second stage like that of the hot standby. The mass velocity of the full power goes through a deceasing transient. This is expected because the full power is still producing steam in the tube bundle by boiling, and water mass in the downcomwer continues feed into the tube bundle due to the continued flow circulation. Therefore, water flashing in the upper downcomer is limited, the primary separator effectively removes the moisture, and the secondary separator is not flooded. Thus, conditions do not exist to produce a second stage for the full power case.

TRANFLO computer program has incorporated both primary and secondary separation function, and it correctly simulates the behavior of water flashing and moisture separation, as described above. It had been reviewed by NRC, as discussed in Section 5.2.1. The NRC review concluded that flow rate and quality entering the separation stages is adequately conservative. Therefore, TRANFLO has been an appropriate computer program in simulating thermal and hydraulic process of the steam generator.

The above comparison indicates that the TRANFLO calculation yields higher pressure drops through tube support plates than the MULTIFLEX. There are still no definite answers to explain the differences in the pressure drop calculations between TRANFLO and MULTIFLEX. However, these differences in thermal and hydraulic process do not deny the capability of the MULTIFLEX code in its simulation of acoustic wave and its acoustic effect on two-phase flow. This will be discussed in detail in Section 6.6.

5.6 Conclusions

This section presents a summary of the adequacy of the TRANFLO code for its current applications. Blowdown test data of simulated reactor vessels validate the adequacy of the code in predicting the steam and water blowdown transient. The NRC has accepted the TRANFLO code in calculating mass and energy release to the containment during a steam generator blowdown due to feed or steam line break.

As part of its review, the NRC accepted the code's ability to accurately predict local thermal-hydraulics in the vessel. The calculated pressure agrees well with the measured vessel pressure. Flow through the internals of the steam generator depends on accurate prediction of pressure drops, which relies on the accuracy of the loss coefficients along the flow paths. Test data of pressure drops from model boiler and field steam generators have been applied to verify the correlations for the loss coefficients.

Westinghouse has made modifications to the code to better predict steam generator behavior following a SLB event. Westinghouse has performed the verification and validation consistent with the methods approved by the NRC staff for the original version.

To assess acoustic wave effects, the results between TRANFLO and MULTIFLEX have been compared. As expected for the steam environment and the diameter changes in the steam flow path (see Section 6.6), the MULTIFLEX results do not show any acoustic wave effects on the TSP loads. Thus acoustic wave effects do not need to be considered for the TSP loads. The minor differences between the TRANFLO and MULTIFLEX loads represent the sensitivity to the code used for the load analyses, and the differences between codes are bounded by the uncertainty factors applied to the TRANFLO TSP pressure drops.

In conclusion, the TRANFLO code is a verified program for adequately predicting thermal-hydraulic conditions during the blowdown transient of a steam generator due to a feed or steam line break.

Table 5-1

Hot Standby Pressure Drops Calculated by TRANFLO and MULTIFLEX

a,c

Table 5-2
TSP Pressure Drops and Ratios to Case 1 with Heat Transfer
(Hot Standby Conditions)

Peak Pressure Drop

a,c

Table 5-3

TSP Pressure Drops and Ratios to Case 2 with Heat Transfer
(Full Power Conditions)

Peak TSP Pressure Drop

a,c

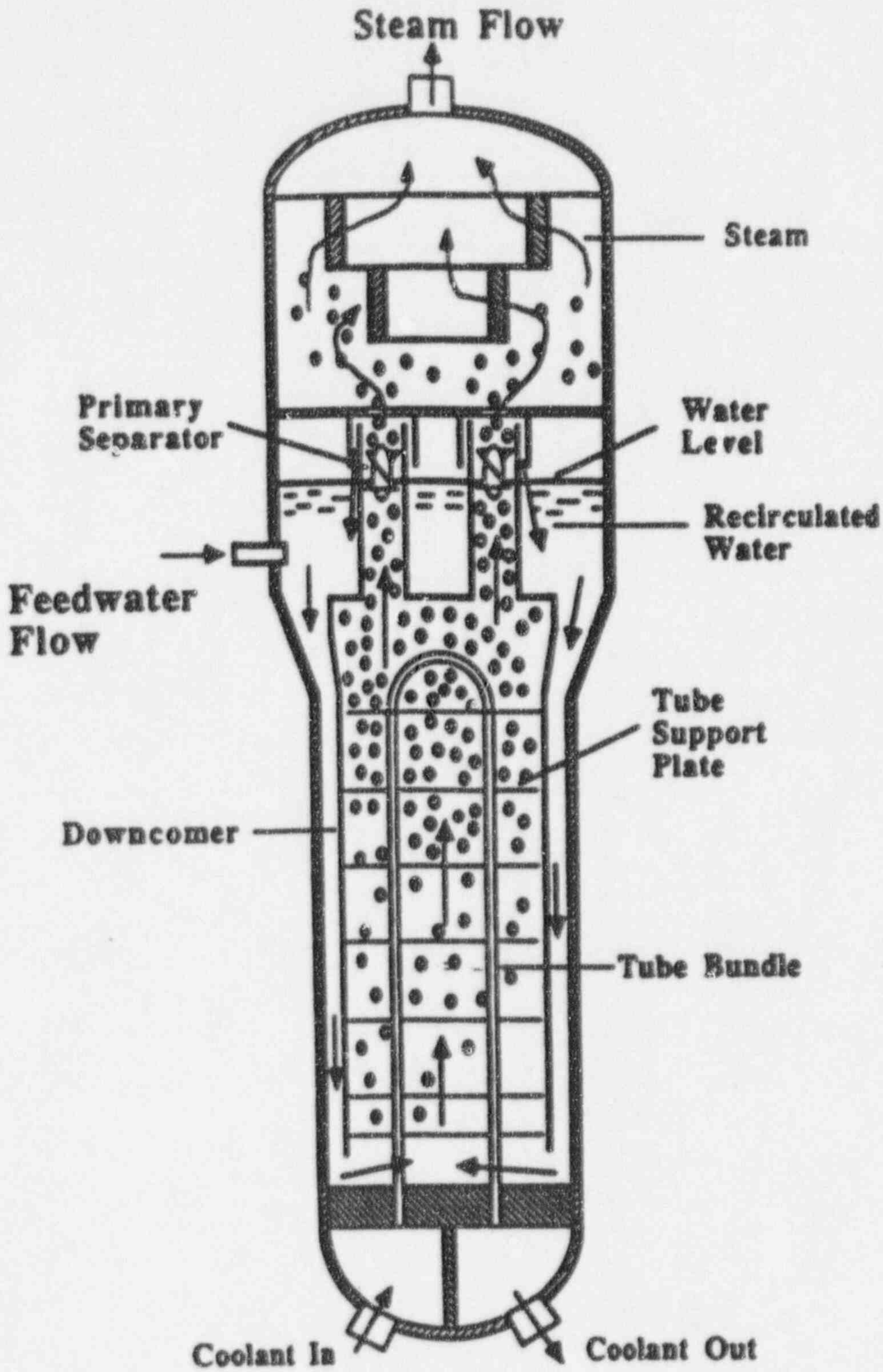

Figure 5-1. Diagram of Flow Circulation During Power Operation

a,b

Figure 5-2. Counterbored Structural Quatrefoil Loss Coefficients

a,b

Figure 5-3. GENF Verification, Circulation Ratio Versus Load

a

Figure 5-4. MULTIFLEX Model for Braidwood Unit 1 S/G

a,c

Figure 5-5. Pressure Drop Through Tube Support Plates M,N and P (Case 31 with Hot Standby, 487" Water Level, with Flow Limiter by MULTIFLEX Code)

a,c

Figure 5-6. Pressure Drop Through Tube Support Plates F, J and L (Case 31 with Hot Standby, 487" Water Level, with Flow Limiter by MULTIFLEX Code) a, c

Figure 5-7. Pressure Drop Through Tube Support Plates A and C (Case 31 with Hot Standby, 487" Water Level, with Flow Limiter by MULTIFLEX Code)

a,c

Figure 5-8. Pressure Drop Through Tube Support Plates M, N, and P
(Case 32 With Full Power, 487" Water Level by MULTIFLEX Code)

a,c

Figure 5-9. Pressure Drop Through Tube Support Plates F, J, and L (Case 32 With Full Power, 487" Water Level by MULTIFLEX Code)

a,c

Figure 5-10. Pressure Drop Through Tube Support Plates A and C (Case 32 With Full Power, 487" Water Level by MULTIFLEX Code)

a,b

Figure 5-11. Pressure Drop Through Tube Support Plates M, N and P
(Case 1 Without Heat Transfer)

a,c

[ ]

Figure 5-12. Pressure Drop Through Tube Support Plates F, J and L
(Case 1 Without Heat Transfer)

a,b

Figure 5-13. Pressure Drop Through Tube Support Plates A and C (Case 1 Without Heat Transfer)

a,c

[ ]

Figure 5-14. Pressure Drop Through Tube Support Plates M, N and P
(Case 2 Without Heat Transfer)

a,c

Figure 5-15. Pressure Drop Through Tube Support Plates F, J and L
(Case 2 Without Heat Transfer)

a,c

Figure 5-16. Pressure Drop Through Tube Support Plates A and C
(Case 2 Without Heat Transfer)

a,c

Figure 5-17. Transient of Steam Quality Immediately Upstream to Steam Nozzle

a,c

Figure 5-18. Break Flow of Braidwood Unit 1 (Water Level at 487")

a,c

Figure 5-19. Steam Pressure at Steam Nozzle of Braidwood Unit 1
(Water Level at 487")

a,c

Figure 5-20. Pressure Drop Through Tube Support Plate P of Braidwood Unit 1 (Water Level at 487")

a,c

Figure 5-21. Break Flow of Braidwood Unit 1
(Water Level at 544'")

a,c

Figure 5-22. Steam Pressure at Steam Nozzle of Braidwood Unit 1
(Water Level at 544")

a,c

Figure 5-23. Pressure Drop Through Tube Support Plate P of Braidwood Unit 1
(Water Level at 544")

a,c

Figure 5-24. Break Flow of Braidwood Unit 1
(Water Level at 474")

a,c

Figure 5-25. Steam Pressure at Steam Nozzle of Braidwood Unit 1
(Water Level at 474")

a,c

Figure 5-26. Pressure Drop Through Tube Support Plate P of Braidwood Unit 1 (Water Level at 474")

a,c

Figure 5-27. Break Flow of Braidwood Unit 1
(Water Level at 378")

a,c

Figure 5-28. Steam Pressure at Steam Nozzle of Braidwood Unit 1
(Water Level at 378")

a,c

Figure 5-29. Pressure Drop Through Tube Support Plate P of Braidwood Unit 1
(Water Level at 378")

a,c

[ ]

Figure 5-30. Break Flow of Braidwood Unit 1
(Hot Standby at a 280" Water Level)

a,c

Figure 5-31. Steam Pressure at Steam Nozzle of Braidwood Unit 1
(Hot Standby at a 280" Water Level)

a,c

Figure 5-32. Pressure Drop Through Tube Support Plate P of Braidwood Unit 1
(Hot Standby at a 280" Water Level)

6.0 HYDRAULIC SLB LOADS ON TSPs

6.1 Analysis Plan

The hydraulic, pressure drop loads on the TSPs in a SLB event are calculated with the TRANFLO computer code as described in Section 4. An extensive set of TRANFLO analyses was performed and the results of these analyses are reported in this section. The TRANFLO analyses include: reference analyses for a guillotine SLB both inside and outside containment at both hot standby and full power conditions; and a series of analyses to assess the sensitivity of the TSP loads to the most influential input parameters including the break size for a limited break, the S/G water level, the TSP pressure drop loss coefficient, the S/G downcomer loss coefficient and the Moody discharge coefficient. The results of the sensitivity analyses are used to define a conservative or bounding uncertainty factor which is applied to the reference analyses pressure drops to obtain a bounding set of loads for the TSP displacement analyses. The reference analysis loads on the TSPs and the bounding reference loads adjusted by the uncertainty factors are used to develop the expected and bounding TSP displacements in Section 8.

The TRANFLO analysis matrix is given in Table 6-1 and is described below:

<u>Reference Analyses</u>

The reference analyses, Cases 1 to 4 of Table 6-1, provide the expected TSP loads for a guillotine steamline break either inside containment at the exit of the S/G nozzle or at a location just outside of the containment building. The break at the S/G nozzle would result in a potential radiation release inside of containment, while the break outside containment represents containment bypass for the potential radiation release. In addition to the break size, the TRANFLO input parameters most influential on the TSP loads are the water level, the TSP loss coefficients, the downcomer loss coefficients and the Moody discharge coefficient. For the reference analyses, the expected values are used for the water level and the TSP/downcomer loss coefficients. The Moody discharge coefficient has been set at its maximum value (most conservative) of 1.0. The reference analyses thus lead to a moderately conservative representation of the expected TSP pressure drops, under hot standby and full power conditions, for a guillotine SLB inside and outside containment.

<u>TRANFLO Sensitivity Analyses</u>

TRANFLO sensitivity analyses were performed to assess the influence of the principal input parameters, individually and collectively, on the TSP pressure drops. The more limiting hot standby SLB event was used to determine the TSP load sensitivity to the break size (guillotine versus 1.5 ft^2), water level (expected 487" versus lower uncertainty level of about 466"), TSP loss coefficients (expected versus maximum values), downcomer loss coefficients (expected versus minimum values) and the Moody discharge coefficient (maximum 1.0 versus expected 0.84).

These analyses are represented by Cases 51 to 55 in Table 6-1. From these analyses, it was determined that the reduction in water level, the increased TSP loss coefficients and the reduced downcomer loss coefficients resulted in an increase in the TSP loads for the most limiting plates (plates C and J for TSP displacements) and typically for most other plates.

The above three input parameter changes that increase the TSP loads were then combined, in Cases 61 and 62, with the most limiting S/G guillotine break (with a Moody discharge coefficient of 1.0) to define a bounding set of loads to develop an uncertainty adjustment factor for the reference analyses. The uncertainty factor is a constant factor on the loads obtained to reasonably bound the ratio of the peak pressure drop for each plate from the combined analyses of Cases 61 and 62 to the reference analyses of Cases 1 and 2.

Reference Analyses with Uncertainty Adjustment

Cases 61 and 62 combine all the worst case or most limiting input parameters to define the combined uncertainty factor for each plate. It is extremely conservative to combine all the collective worst case input conditions in a single TSP load analysis. A more realistic bounding analysis would collectively combine intermediate (between expected and worst case) values for the input parameters in a single run, or would combine the resulting TSP loads by the square root of the sum of squares since all worst case conditions would not be expected to act simultaneously. However, it is the intent of these analyses to develop a very conservative set of bounding TSP loads, and the results of Cases 61 and 62 are used to define uncertainty factors. To further simplify the uncertainty factor approach, a constant uncertainty factor is developed based on the maximum ratio of the Case 61 to Case 1 and Case 62 to Case 2 pressure drops. As developed later in this section, this resulted in the Case 2, full power loads for all plates being increased by a factor of 1.75. For the Case 1, hot standby loads, the uncertainty factor applied was 2.0 for plates A to L (1 to 8) and 1.5 applied to plates M to P (9 to 11). Thus the reference analyses with the uncertainty adjustment provide a direct assessment of a constant factor increase in the loads. Cases 11 and 12 represent the adjusted load conditions and are considered to define an upper bound on the TSP pressure drops.

Case 21 provides a best estimate analysis for comparison with the reference analysis of Case 1 or the bounding analysis of Case 61. The best estimate conditions were selected to represent a more limited (than a guillotine break) SLB event with containment bypass and with the expected Moody discharge coefficient of 0.84. The analysis results, given later in this section, show that the best estimate loads of Case 21, representing a more likely SLB event, are typically about half the loads of Case 1 and about 1/4 the loads of the bounding Case 11. Since the loads of Case 11 are shown in Section 10 to result in acceptable tube burst probabilities for Braidwood-1 and Byron-1, it is clear that the more probable SLB event and expected S/G conditions would lead to small TSP displacements with a very low tube burst probability and would essentially eliminate tube burst as a concern for APC applications.

Cases 31 of Table 6-1 represents the MULTIFLEX computer code analysis described in Section 5 for qualification of the TRANFLO code. This analysis is used in Section 8 for TSP displacement analyses and is included in the table to define the complete analysis matrix.

The TSP loads for Cases 1, 2, 11, 12 and 31 are used in Section 8 to calculate the associated TSP displacements.

6.2 Reference Full Power and Hot Standby Loads

Case 1 is a reference analysis for SLB at hot standby with a guillotine break at the S/G outlet nozzle. Its water level is at the normal setting of 487 inches above the top of the tubesheet, and both TSP and downcomer loss coefficients are at nominal values. The Moody discharge coefficient for critical blowdown flow is set to be unity. Figures 6-1, 6-2 and 6-3 show the hydraulic loads through eight TSPs P, N, M, L, J, F, C and A.

Case 2 is equivalent to Case 1, except the SLB is initiated from full power operation. Figures 6-4, 6-5 and 6-6 show the hydraulic loads through eight TSPs P, N, M, L, J, F, C and A. As discussed in Section 5.5.4, both uniform and non-uniform temperature cases essentially give the same results, and we use the results from the uniform temperature case as the reference. Table 6-2 reports the results of the uniform temperature case.

Case 3 is identical to Case 1, but the guillotine break at hot standby is outside the containment building. Figures 6-7, 6-8 and 6-9 show the hydraulic loads through eight TSPs P, N, M, L, J, F, C and A.

Case 4 is equivalent to Case 3, except its initial condition is full power operation, not hot standby. Figures 6-10, 6-11 and 6-12 show the hydraulic loads through eight TSPs P, N, M, L, J, F, C and A.

For hot standby, a break at the S/G steam outlet nozzle generally yields higher loads than a break outside the containment. This is expected because of the additional flow resistance due to extra piping of about 120 feet and three 90° elbows between the steam outlet nozzle and the containment penetration. There is a flow split around the middle of tube bundle (between TSPs J and L). Flow is upward for TSP L and above (see Figure 4-1), and flow is downward for TSP J and below. Except for a low feedwater flow of 200 gpm through the auxiliary nozzle, the main feedwater nozzle is isolated during hot standby.

For full power operation, differences in hydraulic loads are negligible between a break at the S/G steam outlet nozzle and outside of the containment building.

Apparently, blowdown flow through the break has a negligible effect on the tube bundle flow for the full power mode, because there is not much water for flashing. During most of the transient, loads are more or less equal to those during steady state full power, because of continued feedwater flow through the main feedwater nozzle. Thus, there is no flow split within the tube bundle.

It is important to note that hot standby leads to higher loads on the TSPs than full power operation for both upper and lower TSPs, but middle TSPs tend to experience higher loads for full power than hot standby. Middle TSPs like J and L are where the flow split takes place for hot standby, and thus the flow rate in either direction tends to be small because they are not reaching fully developed conditions. Therefore, hot standby usually results in lower hydraulic loads at the middle TSPs than full power operation. Both upper and lower TSPs experience higher loads for hot standby than for full power. This is due to the difference in amount of water available for flashing, as discussed below.

Once a SLB event begins, it triggers a rapid depressurization, which leads to water flashing. The rapid water flashing generates water motion. Fluid velocity increases with an increase in the amount of water flashing. A higher water velocity will lead to a larger pressure drop across a TSP. In addition, when fluid moves in the tube bundle, water will exert a higher pressure drop across the TSP when compared to steam. Hot standby at zero power provides a solid water pool in the tube bundle, while power operation generates a steam and water mixture. Therefore, hot standby yields higher loads than full power operation.

6.3 SLB Load Dependence on Water Level

Sensitivity studies of water level on hydraulic loads on tube support plates have been performed and documented. Results show that the lower the water level, the larger the hydraulic loads on the TSPs. Figure 6-13 shows a relative load on the uppermost TSP with respect to the water level of a steam generator. This trend is expected, as explained below.

A postulated steam line break (SLB) event results in blowdown of steam and water out of the steam generator. The fluid blowdown depressurizes the secondary side fluid and thus causes the fluid to move. Fluid motion leads to pressure drops and thus hydraulic loads across the TSPs and baffle plates. Depressurization triggers rapid water flashing, mainly across the water level during the early part of the transient. The rapid water flashing generates water and steam motion, and the closer the tube support plate is to the water level, the higher the flow rate and thus the higher the pressure drop.

Therefore, a chosen water level being lower than the normal setting is most conservative in determining and providing hydraulic loads as input to displacement analysis of the TSPs. The normal water level setting at hot standby for a Model D4 S/G, including Braidwood- 1, is about 492 inches above the top of the tubesheet.

Braidwood Unit 1 actually controls at a level about 5 inches lower (or 487 inches above the top of the tubesheet); it is about 206 inches above the uppermost TSP. The span between the uppermost TSP and mid-deck is 264 inches, over which Braidwood Unit 1 has a 78% span.

The TRANFLO TSP loads at hot standby in WCAP-14046 are based on a water level at the uppermost TSP, which is excessively conservative. The control point water level of 487 inches above the tubesheet is the reference water level for the reference Braidwood-1 TRANFLO analyses (i.e., Cases 1, 2, 3 and 4 of Table 6-1). The uppermost TSP peak pressure drop for the Braidwood-1 updated analysis at the controlled water level is a factor of about 2.5 lower than the corresponding load given in WCAP-14046. The WCAP-14046 loads also include the additional conservatism of a feedwater transient coincident with the SLB. This combined event is considered to be a low probability event and the feedwater transient is not considered in the Braidwood-1 reference analyses for a SLB from hot standby.

6.4 Best Estimate Loads

As stated earlier, the hydraulic load varies with initial and boundary conditions of a SLB event. The best estimate case (i.e., Case 21 of Table 6-1) consists of the following:

Break outside containment
A limited break size of 1.5 ft^2
A nominal water level of 487 inches
Nominal correlation constant of TSP loss coefficient
Nominal downcomer loss coefficient
A Moody discharge coefficient of 0.84.

There has been no steam line break event on Westinghouse designed PWRs. Two main feedline pipe breaks have occurred on Westinghouse designed PWRs. These breaks were outside containment.

A guillotine break of a steam line results in a double-ended break and a break area of the total pipe cross section. The probability of a guillotine break is extremely low. In reality, the steam line would leak before breaking, and the break takes some finite time to open up to its final size. Therefore, the blowdown rate is limited at the beginning since it depends on the break area. By the time it reaches its final break size, the system pressure drops, on which the blowdown flow rate depends. The maximum likelihood of the break size could be less than half of the pipe cross section.

The TRANFLO code does not simulate the break size as a function of time during the break of the steam line. It will take the final size and apply it to the beginning of the breaking. Therefore, recognizing such a model and the nature of a non-guillotine break with gradual opening, we could consider a break size of 1.5 ft^2, about one third of the steam line flow area of 4.71 ft^2. Note that the throat area of the S/G steam nozzle is about 1.4 ft^2.

If the break were to occur at the exit of the steam generator, it is assumed to be three feet from the top of the steam nozzle.

TRANFLO uses the Moody model for calculation of break (or critical discharge) flow. Comparisons with measured break flows of pressure vessels have indicated the need to use a multiplier for the Moody model. The multiplier is less than unity, depending on the conditions of the two-phase flow and the geometry to and through the break. The multiplier can be as low as 0.55 and as high as 0.84.

Just the geometry alone, Moody model, like many critical flow models of two-phase flow discharge, considers a one-dimensional flow problem. In reality, it is not one dimensional flow. Consideration of two-dimensional flow demonstrates that a multiplier of about 0.84 is needed to achieve agreement with measured data. A multiplier of 0.84 is used as a best value for a SLB event for the Braidwood-1 and Byron-1 units. Figures 6-14, 6-15 and 6-16 show pressure drops through TSPs for this best estimate case. As expected, the pressure drops are smaller than those of Cases 1 and 3. The ratios to those of Case 1 range from about 0.4 to 0.8, depending on the individual TSP (see Table 6-2).

6.5 SLB Load Sensitivity Analyses

6.5.1 Break Size

According to Section 6.4, a break size of 1.5 ft^2 is considered at the exit of the S/G steam outlet nozzle.

The time histories of the pressure drops through various TSPs are similar to those of Figures 6-1, 6-2 and 6-3 for Case 1, but smaller as expected for a limited break size. Table 6-2 presents ratios of the peak values of the pressure drops between Case 51 and Case 1; the peaks are about 10 to 20% smaller for the limited break than a guillotine break.

6.5.2 Water Level

The normal water level setting at hot standby and full power operation is 487 inches above the top of the tubesheet for the Braidwood-1 steam generators. According to system control, the control is accurate within 1% of the 233 inch span of the narrow range taps. The water level for hot standby can drop below the normal setting due to steaming by the reactor residual heat. However, the water level is quickly restored within about 10 minutes at a typical flow rate of 200 gallons per minute. The cross sectional area of fluid space at this level is about 152 ft^2. This implies that the water level can momentarily drop by about 21 inches. In other words, we consider a drop of the water level from 487 inches to 466 inches.

For the minimum water level, Case 52, the pressure drops through the various TSPs are similar to those of Figures 6-1, 6-2 and 6-3 for Case 1, but higher as expected for a lower water level. Table 6-2 presents ratios of the peak value of pressure drops between Case 52 and Case 1; the peaks are about 10 to 30% higher for the water level of 466 inches than for 487 inches.

6.5.3 TSP Loss Coefficient

As shown in Figure 5-2, the best value of the correlation constant of the loss coefficient correlation is 1.1. Its upper and lower bounds are 1.4 and 0.8, respectively. Reference analyses of Cases 1 to 4 use the best estimate of 1.1. The upper bound of 1.4 is applied to assess the sensitivity of the TSP loss coefficient on pressure drops. Use of the upper bound of 1.4 leads to higher pressure drops.

For the maximum TSP loss coefficient, Case 53, the dynamic behavior of pressure drops through the various TSPs are similar to those of Figures 6-1 to 6-3 for Case 1, but higher in value as expected. Table 6-2 presents ratios of peak value of pressure drops between Case 53 and Case 1; the peaks are about 15 to 30% higher.

6.5.4 Downcomer Loss Coefficient

The loss coefficient of the downcomer consists of friction along the shell and wrapper, and form loss due to area changes and flow turns. The estimate of friction and form loss for the downcomer is straightforward, as it is within single phase (water) flow, and simple geometry; but, it can be subject to uncertainty, too. Its total drop is only about 0.6 psi during full power operation.

For sensitivity study, we will consider a possibility of a decrease of about 0.3 psi, or a 50% decrease in the downcomer pressure loss. This decrease is achieved by a decrease in the downcomer form loss coefficient. A decrease in downcomer loss will promote more tube bundle flow toward the tubesheet and then entering the tube bundle.

For the minimum downcomer loss coefficient, Case 54, the time histories of pressure drops through various TSPs are similar to those of Figures 6-1 to 6-3 for Case 1. Table 6-2 presents ratios of peak value of pressure drops between Case 54 and Case 1; the ratios depict that downward flow increases by a few percent for TSPs A, C, F and J. Indeed, the upward flow decreases slightly, 2% for TSP N and 1% for TSP P. These are expected because the downcomer loss is very small compared to the total loss through the whole bundle and separator.

6.5.5 Moody Discharge Coefficient

Pressure drop increases with an increase in flow rate, and vice versa. A decrease in break flow generally decreases the tube bundle flow and thus reduces the pressure drops across the TSPs. A Moody discharge coefficient of 0.84 reduces break flow compared to that of a coefficient of unity.

For the lower, 0.84 Moody discharge coefficient, Case 55, the pressure drop transients through various TSPs are similar to those of Figures 6-1 to 6-3 for Case 1, but essentially lower. Table 6-2 presents ratios of peak value of pressure drops between Case 55 and Case 1; the peaks are up to 20% smaller for Case 55 than for Case 1.

6.5.6 Combined Worst Conditions for Hot Standby

Combined worst conditions are given in Table 6-1; they are:

Break outside steam outlet nozzle
A guillotine break
A lower water level of 466 inches
An upper bound for correlation constant of TSP loss coefficient
Minimum loss coefficient
A Moody discharge coefficient of 1.0.

Figures 6-17, 6-18 and 6-19 depict pressure drops through the TSPs. As expected, they are higher than those of Cases 1 and 3. Their ratios to those of Case 1 range from about 1.4 to 2.1, depending on the individual TSP (see Table 6-2).

6.5.7 Combined Worst Conditions for Full Power

The combined worst conditions for full power are identical to those for hot standby (see Section 6.5.6). Figures 6-20, 6-21 and 6-22 show pressure drops through TSPs. As expected, they are higher than those of Case 2 (see Table 6-2).

6.6 Adjusted Full Power and Hot Standby Loads

Sensitivity analyses of SLB loads are discussed in detail in Section 6.5. In these sensitivity studies, we have considered uncertainties of the break size, water level, TSP loss coefficient, downcomer loss coefficient, Moody discharge coefficient, break location and break size. Based on these studies, we consider the combined worst conditions for hot standby (i.e., Case 61, see Table 6-1), and for full power (i.e., Case 62, see Table 6-1).

Results of Cases 61 and 62 are presented in Table 6-2. In the same table, we list results of reference loads from Cases 1 and 2 for hot standby and full power, respectively. Accordingly, a factor of 2 on the reference loads represents a conservative load adjustment factor that combines the uncertainties.

6.7 Acoustic Wave Consideration

A steam line break does generate a decompression wave, which can enter the steam generator. This pressure wave that starts at the break has to propagate through the tortuous path provided by the primary and secondary separators with their numerous area changes. It has to pass through the U-bend of the tube bundle. Before it reaches the uppermost or lowest TSP it will attenuate significantly along the path.

The MULTIFLEX calculation for Case 1 confirms that an acoustic wave due to a SLB event is indeed insignificant, as to be discussed below using the MULTIFLEX result.

In order to explain the results obtained, it is useful to first discuss what results would be obtained for a simplified, idealized case. The idealized case is a two foot long section of piping connected to the top of the steam generator. The area of the piping is 5 ft^2 while that of the steam generator is 99 ft^2. There is no flow restrictor, zero friction in the piping, constant fluid properties, the break occurs in zero time, and the pressure at the break plane remains constant. The break will generate a pressure wave of magnitude P = 1100 - 325 = 775 psi that has zero spatial length (a step change in pressure) and that will propagate at sonic speed to the steam generator. At an elapsed time of 0.00125 second (or t = L/c = 2 ft / 1605 fps), the wave will arrive at the steam generator. Because of the area change at the steam generator, the initial blowdown wave will be decomposed into a penetration wave and a reflected wave.

The penetration coefficient is as follows:

$$C_p = 2A_{pipe} / (A_{pipe} + A_{SG}) = 2(5 \text{ ft}^2) / (5 \text{ ft}^2 + 99 \text{ ft}^2) = 10\%$$

Therefore, the reflection coefficient is 1 - C_p = 90%. The penetration wave of magnitude P = 0.1(1100 - 325) = 78 psi will propagate into the steam generator, dropping the local pressure to a value of P = 1100 - 78 = 1022 psia. The reflection wave of magnitude P = 0.9(1100-325) = 697 psi will propagate back toward the break, increasing the local pressure to a value of P = 325 + 697 = 1022 psia. Again at an elapsed time of 0.00125 sec, the initial reflection wave will arrive at the break and be reflected again, back toward the steam generator. Since the break plane is essentially a constant pressure boundary condition, any wave reflected from it will have the same magnitude as the incident wave but opposite sign. Thus, at time 2(0.00125) = 0.00250 second, there is a wave of magnitude 697 psi propagating toward the steam generator, reducing the local pressure to P = 1022 - 697 = 325 psia. When this wave arrives at the steam generator it is decomposed into a penetration wave of magnitude 0.1(1022 - 325) = 70 psi and a reflection wave of magnitude 0.9(1022 - 325) = 627 psi. This precession of waves will continue in an analogous manner until a quasi steady-state flow condition is achieved. From the perspective of the pressure just inside the steam generator it can be seen that the initial blowdown depressurization wave of magnitude 775 psi is reduced to a series of depressurization waves of much smaller and diminishing magnitude (i.e. first 78 psi, then 70 psi etc.), each separated by a time interval of 0.00250 second.

For the steam generator model analyzed in this report, the following factors serve to modify the above behavior for an idealized case: the presence of the flow restrictor, friction at the pipe wall, a 1 msec break opening time, and the presence of many area changes within the flow path inside the steam generator. The effect of the flow restrictor, within the context of this discussion, is to provide an additional point of wave decomposition. Each wave which arrives at the flow restrictor is split into two waves in a manner which is similar to that described above. The effect of friction at the pipe wall is to stretch the acoustic waves over an increasing spatial length, thus changing the ideal step change in pressure to a spatial ramp in pressure. The effect of the 1 msec break opening time is to change the initial blowdown wave from a step change to a ramp over 1 msec (and a corresponding spatial length). The effect of the additional area changes within the steam generator is to further decompose the acoustic waves traveling inside the steam generator.

The combined effect of the above factors is to obscure the presence of individual acoustic waves, except for very early in the transient at locations relatively close to the break. After just a few milliseconds or at locations within the steam generator, the transient does not exhibit the characteristically rapid changes in pressure and mass flow associated with waterhammer, but rather appears as a relatively slow depressurization event. Due to friction primarily, the step changes in fluid parameters are transformed into linear ramps of finite spatial length. Because of the complex network of area changes and superposition of the resulting large number of individual acoustic waves, the individual linear ramps combine to result in continuous, smooth changes in fluid parameters rather than discrete step changes. The transient is still driven by the propagation of acoustic waves, but individual acoustic waves are not discernable except as noted above.

The following figures, taken from MULTIFLEX results for the Hot Standby Case 1, illustrate the foregoing discussion: Figures 6-23 and 6-24 are the pressure at the break plane, plotted against two time scales; Figures 6-25 and 6-26 are the pressure at the top of the steam generator, again for two time scales; and Figure 6-27 is the pressure at the upper surface of the uppermost tube support plate. Figure 6-24 shows that the initial blowdown wave is of magnitude P = (1106 - 910) = 196 psi with a duration of 1 msec. Figure 6-26 shows that the portion of the initial blowdown wave that penetrates the steam generator beginning at approximately 1 msec is of magnitude P = (1106 - 1091) = 15 psi, where 1091 is the pressure at time t = 0.0015 sec. The pressure at 0.0015 sec was used instead of the pressure at time t = L/C + 0.001 = 0.00225 second (wave propagation time plus break opening time) in order to ignore the secondary effect represented by the small peak between 0.0015 sec and 0.00225 sec.

Figure 6-27 shows no discernable step change in pressure associated with the initial blowdown wave. The small increase in pressure seen at the beginning of the transient in Figure 6-27 is a correction by the computer code for static pressure due to elevation head. Figures 6-25 and 6-27 show that, except for early in the transient, individual acoustic waves (of the classic step-change type) from the blowdown event are not discernable inside the steam generator.

As reported in Section 5.5.1, results of the pressure drop through the tube support plates for the case without the venturi flow limiter give values similar to those of the TRANFLO calculation with the flow limiter. For assessing the acoustic effect under the condition without the flow limiter, Figures 6-28 through 6-32 present the similar plots like Figures 6-23 through 6-27. There are no discernable acoustic effect inside the steam generator, too.

6.8 Conclusions

Considering the above discussion, we can draw the following conclusions.

1. SLB at hot standby generates higher pressure drops across tube support plates than SLB at full power operation. This trend is observed for most of TSPs, except for middle TSPs, such as Plates J and L (see Reference Cases 1 to 4 in Table 6-2).

2. The best estimate case (i.e., Case 21) of hot standby SLB has limited break outside the containment and a Moody discharge coefficient of 0.84, and results in smaller pressure drops than Case 1.

3. Sensitivity studies indicate that 1) a limited break is less severe in pressure drop than a guillotine break, 2) pressure drop increases with a decrease in water level, 3) an increase in TSP loss coefficient increases the pressure drop, 4) a decrease in downcomer loss coefficient has negligible effect on the pressure drop, and 5) a decrease in Moody discharge coefficient reduces the pressure drop.

4. Combined worst conditions were constructed from the sensitivity study. The sensitivity study has been applied to develop a bounding uncertainty factor on the TRANFLO TSP pressure drops. The resulting factors of 2.0 on hot standby loads and 1.75 on full power loads are applied to the reference Cases 1 and 2 loads for the TSP displacement analyses given in Section 8.

5. The effects of an acoustic wave initiated from the decompression at the break can penetrate into the steam generator but are less than 5% of the initial wave, and the acoustic wave effects dampen out within milliseconds. The penetrated waves do not travel deep into the tube bundle and are insignificant at the TSPs. The dynamic transient due to an SLB event is essentially a hydraulic process, not an acoustic one.

Table 6-1
TRANFLOW Analysis Matrix

a,c

Table 6-2

SLB Peak TSP Pressure Drops and Ratio of Each Case to Case 1

a,c

a

Figure 6-1. Pressure Drop Through Tube Support Plates M, N, and P - Case 1

a

Figure 6-2. Pressure Drop Through Tube Support Plates F, J, and L - Case 1

a

Figure 6-3. Pressure Drop Through Tube Support Plates A and C - Case 1

a

Figure 6-4. Pressure Drop Through Tube Support Plates M, N, and P (Case 2 With Full Power, 487" Water Level)

a

Figure 6-5. Pressure Drop Through Tube Support Plates F, J, and L
(Case 2 With Full Power, 487" Water Level)

a

Figure 6-6. Pressure Drop Through Tube Support Plates A and C
(Case 2 With Full Power, 487" Water Level)

a

Figure 6-7. Pressure Drop Through Tube Support Plates M, N, and P - Case 3

a

Figure 6-8. Pressure Drop Through Tube Support Plates F, J, and L - Case 3

a

Figure 6-9. Pressure Drop Through Tube Support Plates A and C - Case 3

a

Figure 6-10. Pressure Drop Through Tube Support Plates M, N, and P
(Case 4: Full Power, 487" Water Level)

a

Figure 6-11. Pressure Drop Through Tube Support Plates F, J, and L
(Case 4: Full Power, 487" Water Level)

a

Figure 6-12. Pressure Drop Through Tube Support Plates A and C
(Case 4: Full Power, 487" Water Level)

a

Figure 6-13. Relative Peak Pressure Drop Across the Uppermost TSP as a Function of Water Level Ranging from the Uppermost TSP (280") to the Mid-Deck (544") - Model D4 S/G

a

Figure 6-14. Pressure Drop Through Tube Support Plates M, N, and P - Case 21

a

Figure 6-15. Pressure Drop Through Tube Support Plates F, J, and L - Case 21

a

Figure 6-16. Pressure Drop Through Tube Support Plates A and C - Case 21

a

Figure 6-17. Pressure Drop Through Tube Support Plates M, N, and P - Case 61

a

Figure 6-18. Pressure Drop Through Tube Support Plates F, J, and L - Case 61

a

Figure 6-19. Pressure Drop Through Tube Support Plates A and C - Case 61

a

Figure 6-20. Pressure Drop Through Tube Support Plates M, N, and P
(Case 62 With Full Power, 466" Water Level)

a

Figure 6-21. Pressure Drop Through Tube Support Plates F, J, and L
(Case 62 With Full Power, 466" Water Level)

a

Figure 6-22. Pressure Drop Through Tube Support Plates A and C
(Case 62 With Full Power, 466" Water Level)

a

Figure 6-23. Pressure at Steam Nozzle Outlet Where Break Occurs

a

Figure 6-24. Pressure at Steam Nozzle Outlet
(Early Few Milliseconds)

a

Figure 6-25. Pressure Immediately Upstream of Steam Nozzle

a

Figure 6-26. Pressure Immediately Upstream of Steam Nozzle
(Early Few Milliseconds)

a

Figure 6-27. Pressure at the Top of Tube Support Plate P

a

Figure 6-28. Pressure at Steam Nozzle

a

Figure 6-29. Pressure at Steam Nozzle
(Early Few Milliseconds)

a

Figure 6-30. Pressure Immediately Upstream to Steam Nozzle

a

Figure 6-31. Pressure Immediately Upstream to Steam Nozzle
(Early Few Milliseconds)

a

Figure 6-32. Pressure at TSP P

7.0 STRUCTURAL MODELING FOR TSP DISPLACEMENTS

7.1 General Methodology

Section 7.0 summarizes the structural modeling of the Model D4 tube bundle to determine relative tube / plate motions under steam line break loads. The analysis involves the preparation of a tube bundle model for the hot leg side of the tube bundle, consisting of the flow distribution baffle, seven tube support plates, tierods and spacers, channel head, lower shell, and tubesheet. The WECAN computer code, a general purpose finite element code is used to develop the model. The model is composed mainly of shell elements, with beam elements used to model the tierods and spacers. Calculations are performed to define applicable dynamic degrees of freedom (DOF) for each plate. Once the DOF are defined, a global substructure is generated for the overall tube bundle. The dynamic response of the plates is then calculated using the special purpose computer program, ***pltdym***.

Additional details for all aspects of the structural modeling are provided in the following sections.

7.2 Component Materials

A specification of component materials is contained in Table 7-1, with the corresponding material properties summarized in Tables 7-2 through 7-7. The properties in these tables are taken from the 1971 edition (through summer 1972 addenda) of the ASME Code, the applicable code edition for Byron Unit 1 and Braidwood Unit 1. It should be noted that although the properties are provided over the temperature range 70°-700°F, the average temperature during the transient, based on the thermal hydraulic results is ≈550°F. Since temperature dependent properties cannot be used in substructures, properties for the finite element model correspond to the values at 550°F. In addition, the material properties for the tubesheet and tube support plates must be modified to account for the tube penetrations and flow holes, and to account for added mass effects of the secondary side fluid. Additional details of the material property modifications are provided later in Section 7.5.

7.3 TSP Support System and Tube Expansion

The various TSPs and baffle plates are supported vertically using several support mechanisms. A schematic of the tube bundle region is shown in Figure 7-1, with each of the plates identified. All of the plates are supported by three tierods/spacers in each of the plate quadrants. In addition, plates C (3H), F (5H), and J (7H) (where the Braidwood-1 and Byron-1 plate numbers are in parentheses), in the preheater region, are supported at their center by a vertical bar welded to the partition plate, while the plates above the preheater, L (8H), M (9H), N (10H), and P (11H), are supported at their center by a central tierod and spacer. Additional support is also provided to the plates by vertical bars welded to the wrapper and / or partition plate immediately above and below the plates.[1]

This analysis also accounts for the beneficial effects of tube expansion relative to providing support for the plates against vertical motion under accident condition loads. The number and location of the tube expansions varies from plate to plate depending on the number and location of other plate supports, and the magnitude and direction of the applied pressure loading.

The support locations for the plates are shown in Figures 7-2 through 7-10. The location of the tierods and spacers is shown in Figure 7-2, while the plate / wrapper support locations, including tube expansion locations, are shown in Figures 7-3 through 7-10. The configuration of the tierod / spacer supports is shown in Figure 7-11, with the vertical bar / plate interface shown in Figure 7-12.

The in-plane support for the TSPs is provided by wedges located around the circumference of each plate. In all cases, the wedges are welded to the wrapper. The wedges are intended to provide in-plane support for the plates. However, since the wedges are welded to the wrapper, there is resistance to upward vertical motion, due to the sloped face of the wedge (see Figure 7-12). In evaluating a preliminary set of transients (without tube expansion), vertical support provided by the wedges was not included. However, the resulting displacements showed that for the limiting plates, the maximum displacements occur near the tube lane at the outer edge of the plate. Thus, in evaluating subsequent sets of loads, wedge support (in the up direction only) is included at the 10° location for the plates showing the highest deflections in this area, Plates A (1H), C (3H), and J (7H). When the hydraulic laods are in the downward direction, the wedges at the corners of these plates do not provide vertical support and, as shown in Section 8, the maximum TSP displacements occur at the corners along the tubelane in the downward direction. All other plates have vertical bar supports at the corners and smaller displacements are found for these plates.

---

[1] For the Model D3 steam generator, the vertical bars are present only for some of the plates in the preheater region, and only along the partition plate. Vertical support for the periphery of the plates is limited to the tierods and spacers, and in some cases local vertical support is provided by wedges welded to the wrapper. The wedges for the Model D3 steam generators are not welded to the wrapper in all cases. For a number of the plates, the wedges are welded to the TSPs and / or baffle plates. For cases where the wedges are not welded to the wrapper, they are unable to provide resistance to upward movement by the plates.

Regarding the tierods and spacers, the tierods are bars that are threaded into the tubesheet and run the full height of the tube bundle with a nut on the upper side of the top TSP, Plate P (11H). (For the central tierod, the lower end is threaded into a special coupling welded to the top of the partition plate at Plate L (8H).) Around the outside of the tierods are spacers that are located between each of the support plates. For the central tierod, the spacers are welded to each of the TSPs. For the spacers located at the periphery of the TSPs, however, there is no rigid link between the spacer and the support plates.

The lack of a rigid link between the spacers and TSPs for the outer tierods / spacers results in a non-linear dynamic system. The TSP / spacer non-linearities are included in the dynamic solution. The tierods / spacers have different stiffness characteristics for upward and downward loads, and these differences are incorporated into the model. For the up direction, the load path is through the spacers from the loaded plate to the one above it, up through the bundle to the top plate, where the load is transferred to the tierod and down to the tubesheet. For the down direction, the load path is through the spacers from the loaded plate to the one below it down through the bundle to the tubesheet. As a means of comparison, the combined tierod / spacer stiffnesses for the outer tierod / spacers are summarized in Tables 7-8 and 7-9. Table 7-8 provides the stiffness values for the "upward" load path, and Table 7-9 for the "downward" load path. In general, the down load path is several times as stiff as the up load path. The combined tierod / spacer stiffnesses for the central tierod / spacer are summarized in Table 7-10. Recall that the central tierod / spacer runs from Plate L (8H) to Plate P (11H). As will be shown later, the loads for these plates all act in the upward direction, so the combined stiffness is based on a load path up through the spacers to Plate P (11H), and then down to the coupling at the top of the partition plate, just below Plate L (8H). A summary of the spacer stiffnesses for the individual tube passes is provided in Table 7-11. These stiffnesses are incorporated in the dyamic model for the non-linear TSP / spacer interface.

For the expanded tube locations, the stiffness of the tubes is incorporated in the dynamic analysis through axial stiffness members. The prescribed stiffness for these members is the combined stiffnesses of the tube section and the expanded joint, which was determined through a test program. Based on preliminary qualification tests, a conservative axial stiffness for the expanded joint was determined to be [ ]^{a,b,c} lb/inch. A summary of the resulting stiffnesses for the various tube sections is provided in Table 7-12.

As a result of the plate deflection and rotation under SLB loads, the potential exists for interaction between the TSP and the tubes. These interaction effects have been incorporated in the analysis. If the plate rotates locally such that the top surface of the plate contacts the tube on one side while the bottom surface of the plate contacts the tube on the other side, then the tube will bind up in the plate and restrict further deflection of the plate. The amount of rotation necessary to cause tube / plate interaction is summarized in Figure 7-13.

7.4 Finite Element Model

The overall finite element model is shown in Figure 7-14. With the exception of the tierods, all of the structural components are modeled using three dimensional shell elements. The tierods are modeled using three-dimensional beam elements. The spacers are incorporated in the dynamics code through stiffnesses that are coupled to the various plate elements when the corresponding gaps are closed.

In modeling the plates, the various cutouts along the tubelane, the cutout for the FDB in the center of the hot-leg, and the cutouts at the outer edges of Plates N (10H) and P(11H), are accounted for. In terms of material properties, equivalent properties are specified only in the tubed regions of the plate. Actual plate properties are used along the tubelane and at the periphery of the plates.

7.5 Revised Material Properties

As noted earlier, the material properties for the tubesheet and TSPs are modified to account for the tube penetrations, flow holes, and various cutouts. The properties that are modified are Young's modulus, Poisson's ratio, and the material density. In the case of the TSPs, the density is additionally modified to account for the added mass of the secondary side fluid.

<u>Young's Modulus / Poisson's Ratio</u>
Due to the presence of flow holes in the TSPs, but not in the FDB, separate formulations are used to modify the material properties. Although different formulations are used for the two components, the same methodology is used in each case. Due to the square penetration pattern, different properties exist in the pitch and diagonal directions. The first step is to establish equivalent parameters for Young's modulus and Poisson's ratio in the pitch and diagonal directions (E_p^*/E, E_d^*/E, ν_d^*, ν_p^*), respectively. The equivalent Young's modulus for the overall plate is taken as the average of the pitch and diagonal directions. The next step in the process is to determine an equivalent value for the shear modulus, G^*/G, for the plate. This is done in a similar manner as for Young's modulus, starting with values in the pitch and diagonal directions, and then taking an average of the two values. The final equivalent value for Poisson's ratio is determined from the relationship between Young's modulus and the shear modulus.

A summary of the resulting effective plate properties for Young's Modulus and Poisson's ratio is shown in Table 7-13.

<u>Material Density</u>
There are two aspects to revising the plate density. The first is based on a ratio of solid plate area to the modeled area. The second aspect corresponds to the plate

moving through and displacing the secondary side fluid, creating an "added mass" effect. In calculating the added mass, the formulation shown below is used.

$$m_a = \rho_f \left(\frac{A_e^2}{A_h} \right) l_{eff}$$

$$l_{eff} = l + \left(\frac{8d}{3\pi} \right) \left(1 - \frac{d}{2b} \right)$$

where,

ρ_f = fluid density
A_e = solid area of plate
A_h = flow area
l = hole length (plate thickness)
d = hole diameter
b = hole pitch

The first step in the process of calculating revised densities for the plates is to determine the applicable areas for the metal and the fluid. Summaries of the actual and modeled plate areas are provided in Table 7-14. Summarized in Table 7-15 are the corresponding flow areas.

The resulting added mass is a direct function of the fluid density. Because the dynamic analysis cannot account for the change in fluid density with time, the analysis uses an average density value for the transient. Variations in the fluid density as a function of elevation in the tube bundle are accounted for by calculating an average fluid density for each plate.

Two sets of calculations are performed for added mass corresponding to whether the transient initiates from hot standby or full power. For transients initiating from full power, the secondary fluid has a much lower fluid density and a lower added mass. Summaries of the resulting fluid and structural masses, together with the resulting effective densities are summarized in Tables 7-16 and 7-17.

Note that the density modification for the tubesheet is based solely on an area ratio of the actual perforated tubesheet to the equivalent solid plate.

7.6 Dynamic Degrees of Freedom

In setting up the global substructure, it is necessary to define the dynamic degrees of freedom. In order to define dynamic degrees of freedom for the TSPs, two sets of modal calculations are performed for each of the plates. The first set of calculations determine plate mode shapes and frequencies using a large number of degrees of freedom (approximately 120 per plate). The second set of calculations involves repeating the modal analysis, using a significantly reduced set of degrees of freedom (DOF). The reduced DOF are selected to predict all frequencies for a given plate below 70 hertz to within 10% of the frequencies for the large set of DOF.[2] A frequency of 70 hertz was selected as a cutoff, as it is judged that higher frequencies will have a small energy content compared to the lower frequencies. This can be confirmed by noting that the frequency content for the dominant peak in the pressure time histories is typically less than 10 hertz.[3] For each of the modal runs, symmetry boundary conditions are prescribed along the "Y-axis", and vertical restraint at vertical bar locations. Actual stiffness properties are incorporated for both the tierods/spacers and the expanded tubes.

A sample set of mode shape plots for Plate A (1H) for the full set of DOF are provided in Figures 7-15 through 7-17, while mode shapes for the reduced set of DOF are shown in Figures 7-18 through 7-20. A comparison of the natural frequencies for the full and reduced sets of DOF for the plates (with tube expansion included) is provided in Table 7-18. Based on the tabular summary, the reduced set of DOF are concluded to provide a good approximation of the plate response.

The reduced set of DOF consists typically of 15 or 16 DOF for each of the plates. Plots showing the resulting DOF for each of the plates are shown in Figures 7-21 through 7-28. The analysis of the plate dynamics without tube expansion use a slightly different set of DOF. Plots showing the DOF used for those calculations are provided in Reference 13.1.

7.7 Displacement Boundary Conditions

The displacement boundary conditions for the substructure generation consist primarily of prescribing symmetry conditions along the "X" and "Y" axes for each of the components. Vertical constraint is provided where the plates are constrained by the vertical bars welded to the partition plate and wrapper, and for

---

[2] For the analysis without tube expansion (Reference 13.1), a cutoff frequency of 50 hertz was used. However, with the additional support provided by the tube expansions, the frequencies of response of the plates are higher. With the increased response frequencies, it was judged that a higher cutoff frequency should be used, and the 70 hertz value was selected. Again, the frequency content for the dominant peak in the pressure time history is less than 10 hertz, thus the higher frequency modes will have lower energy content than the lower modes of response.

[3] Pressure time curves for each of the transient conditions are presented in Section 6.

the channel head at the locations corresponding to its interaction with the interfacing support structure. For the TSPs, rotations normal to the plate surface are also constrained, as required by the stiffness representation for the plate elements.

7.8 Integration Time Step / Structural Damping

The dynamic time step used in evaluating the SLB transients is 0.0002 second. This time step was selected based on analyses using similar models and loadings where various time steps were considered, and 0.0002 second was shown to result in a converged solution. The analysis incorporates structural damping of 4%, which is judged to be a conservative value for the type of dynamic loading and response (movement of the plates through the secondary fluid) being considered.

7.9 Application of Pressure Loads

The SLB pressure loads act on each of the TSPs. To accommodate the variation in load from plate to plate, load vectors are prescribed for each of the plates using a reference load of 1 psi. The reference loads are then scaled during the dynamic analysis to the actual time-history (transient) loading conditions. The transient pressures summarized in Section 6 are relative to the control volume for the thermal hydraulic analysis. The area over which the hydraulic pressure acts corresponds to the area inside the wrapper minus the tube area. Before applying the pressure time histories to the structural model, they are scaled based on a ratio of the plate area in the structural model to the control volume area in the hydraulic model.

Table 7-1

Summary of Component Materials

a,c

Table 7-2

Summary of Material Properties
SA-285, Gr. C

		TEMPERATURE						
PROPERTY	CODE ED.	70	200	300	400	500	600	700
Young's Modulus	71	27.90	27.70	27.40	27.00	26.40	25.70	24.80
Coefficient of Thermal Expansion	71	6.07	6.38	6.60	6.82	7.02	7.23	7.44
Density	---	0.284 7.35	0.283 7.33	0.283 7.32	0.282 7.30	0.281 7.28	0.281 7.26	0.280 7.25

PROPERTY	UNITS
Young's Modulus	psi x 1.0E06
Coefficient of Thermal Expansion	in/in/deg. F x 1.0E-06
Density	lb/in^3 lb-sec^2/in^4 x 1.0E-4

Table 7-3

Summary of Material Properties
SA-106, Gr. B

		TEMPERATURE						
PROPERTY	CODE ED.	70	200	300	400	500	600	700
Young's Modulus	71	27.90	27.70	27.40	27.00	26.40	25.70	24.80
Coefficient of Thermal Expansion	71	6.07	6.38	6.60	6.82	7.02	7.23	7.44
Density	---	0.284 7.35	0.283 7.33	0.283 7.32	0.282 7.30	0.281 7.28	0.281 7.26	0.280 7.25

PROPERTY	UNITS
Young's Modulus	psi x 1.0E06
Coefficient of Thermal Expansion	in/in/deg. F x 1.0E-06
Density	lb/in^3 lb-sec^2/in^4 x 1.0E-4

Table 7-4

Summary of Material Properties
SB-163

PROPERTY	CODE ED.	TEMPERATURE 70	200	300	400	500	600	700
Young's Modulus	71	31.70	30.90	30.50	30.00	29.60	29.20	28.60
Coefficient of Thermal Expansion	71	7.13	7.40	7.56	7.70	7.80	7.90	8.00
Density	---	---	0.306	0.305	0.305	0.304	0.303	0.302
		---	7.923	7.905	7.886	7.867	7.847	7.828

PROPERTY	UNITS
Young's Modulus	psi x 1.0E06
Coefficient of Thermal Expansion	in/in/deg. F x 1.0E-06
Density	lb/in^3 lb-sec^2/in^4 x 1.0E-4

Table 7-5

Summary of Material Properties
SA-216, Gr. WCC

		TEMPERATURE						
PROPERTY	CODE ED.	70	200	300	400	500	600	700
Young's Modulus	71	27.90	27.70	27.40	27.00	26.40	25.70	24.80
Coefficient of Thermal Expansion	71	6.07	6.38	6.60	6.82	7.02	7.23	7.44
Density	---	0.283 7.324	0.282 7.303	0.282 7.287	0.281 7.269	0.280 7.252	0.280 7.234	0.279 7.215

PROPERTY	UNITS
Young's Modulus	psi x 1.0E06
Coefficient of Thermal Expansion	in/in/deg. F x 1.0E-06
Density	lb/in^3 lb-sec^2/in^4 x 1.0E-4

Table 7-6

Summary of Material Properties
SA-508, Class 2a

		TEMPERATURE						
PROPERTY	CODE ED.	70	200	300	400	500	600	700
Young's Modulus	71	29.90	29.50	29.00	28.60	28.00	27.40	26.60
Coefficient of Thermal Expansion	71	6.07	6.38	6.60	6.82	7.02	7.23	7.44
Density	---	0.283 7.324	0.282 7.303	0.282 7.287	0.281 7.269	0.280 7.252	0.280 7.234	0.279 7.215

PROPERTY	UNITS
Young's Modulus	psi x 1.0E06
Coefficient of Thermal Expansion	in/in/deg. F x 1.0E-06
Density	lb/in^3 lb-sec^2/in^4 x 1.0E-4

Table 7-7

Summary of Material Properties
SA-533, Grade A Class 2

PROPERTY	CODE ED.	TEMPERATURE 70	200	300	400	500	600	700
Young's Modulus	71	29.90	29.50	29.00	28.60	28.00	27.40	26.60
Coefficient of Thermal Expansion	71	6.07	6.38	6.60	6.82	7.02	7.23	7.44
Density	---	0.283 7.324	0.282 7.303	0.282 7.287	0.281 7.269	0.280 7.252	0.280 7.234	0.279 7.215

PROPERTY	UNITS
Young's Modulus	psi x 1.0E06
Coefficient of Thermal Expansion	in/in/deg. F x 1.0E-06
Density	lb/in^3 lb-sec^2/in^4 x 1.0E-4

Table 7-8

Summary of Combined Tierod / Spacer Stiffnesses
Outer Tierod / Spacer

Up Loads

a,c

Table 7-9

Summary of Combined Tierod / Spacer Stiffnesses
Outer Tierod / Spacer

Down Loads

a,c

Table 7-10

Summary of Combined Tierod / Spacer Stiffnesses
Central Tierod / Spacer

a,c

Table 7-11

Summary of Spacer Stiffnesses

a,c

Table 7-12

Summary of Combined Tube / Expansion Zone Stiffnesses

a,c

Table 7-13

Summary of Equivalent Plate Properties

a,c

Table 7-14

Summary of Plate Areas

a,c

Table 7-15

Summary of Flow Areas

a,c

Table 7-16

Summary of Effective Densities
SLB Initiating from Hot Standby

a,c

Table 7-17

Summary of Effective Densities
SLB Iniating from Full Power

a,c

Table 7-18

Comparison of Natural Frequencies
Full Versus Reduced DOF

a,c

a,c

Figure 7-1. Tube Bundle Geometry

a,c

Figure 7-2. Tierod / Spacer Locations

a,c

Figure 7-3. Plate A (1H) Support Locations

a,c

Figure 7-4. Plate C (3H) Support Locations

a,c

Figure 7-5. Plate F (5H) Support Locations

a,c

Figure 7-6. Plate J (7H) Support Locations

a,c

Figure 7-7. Plate L (8H) Support Locations

a,c

Figure 7-8. Plate M (9H) Support Locations

a,c

Figure 7-9. Plate N (10H) Support Locations

a,c

Figure 7-10. Plate P (11H) Support Locations

a,c

Figure 7-11. Configuration of Tierod / Spacer Supports

a,c

Figure 7-12. Configuration of Vertical Bar / Wedge Supports

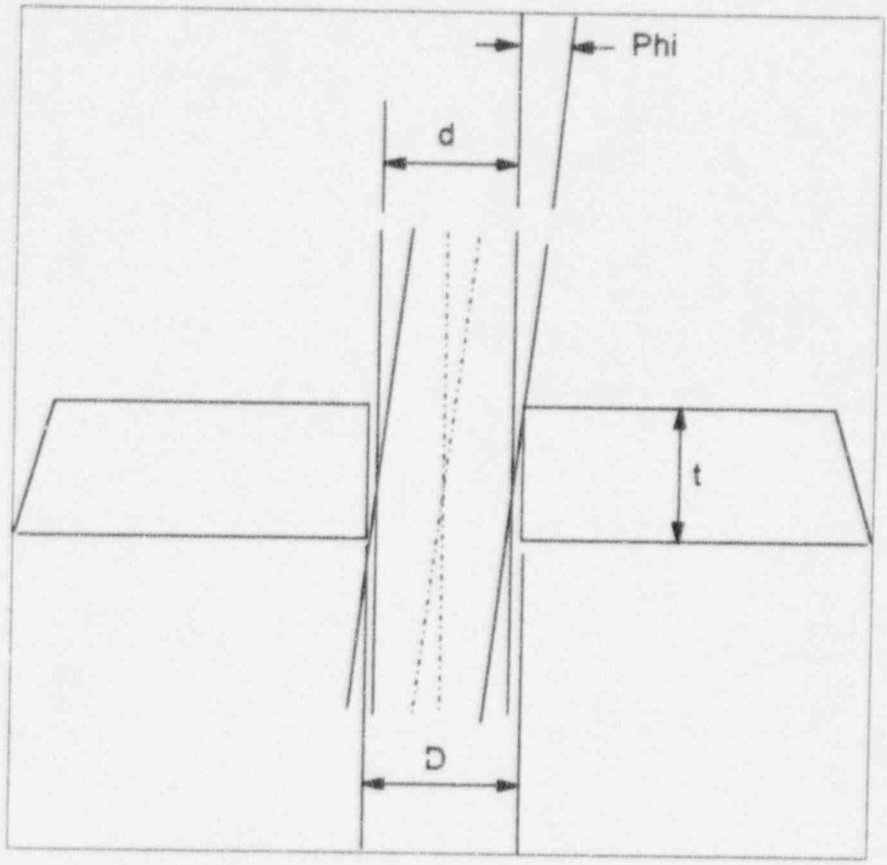

a

Figure 7-13. Summary of Plate Rotation to Cause Two-Edged Contact

a,c

Figure 7-14. Overall Finite Element Model Geometry

a,c

Figure 7-15. Mode Shape Plot - Plate A (1H)
Full Set of DOF
Mode 1

a,c

Figure 7-16. Mode Shape Plot - Plate A (1H)
Full Set of DOF
Mode 2

a.c

Figure 7-17. Mode Shape Plot - Plate A (1H)
Full Set of DOF
Mode 3

a,c

Figure 7-18. Mode Shape Plot - Plate A (1H)
Reduced Set of DOF
Mode 1

a,c

Figure 7-19. Mode Shape Plot - Plate A (1H)
Reduced Set of DOF
Mode 2

a,c

Figure 7-20. Mode Shape Plot - Plate A (1H)
Reduced Set of DOF
Mode 3

a,c

Figure 7-21. Dynamic Degrees of Freedom
Plate A (1H)

a,c

Figure 7-22. Dynamic Degrees of Freedom Plate C (3H)

a,c

Figure 7-23. Dynamic Degrees of Freedom
Plate F (5H)

a,c

Figure 7-24. Dynamic Degrees of Freedom Plate J (7H)

a,c

Figure 7-25. Dynamic Degrees of Freedom
Plate L (8H)

a,c

**Figure 7-26. Dynamic Degrees of Freedom
Plate M (9H)**

a,c

**Figure 7-27. Dynamic Degrees of Freedom
Plate N (10H)**

a,c

**Figure 7-28. Dynamic Degrees of Freedom
Plate P (11H)**

8.0 TSP DISPLACEMENT ANALYSIS RESULTS

8.1 Analysis Approach

Section 8 provides a summary of the displacement results for the limiting SLB load cases presented in Section 6 both with and without the effects of tube expansion. The cases analyzed without the effects of tube expansion are summarized in the table below. In evaluating the effects of tube expansion only one case, Case 11, was considered.

Case	Initial Conditions	Break Location	Uncertainty Factor	T/H Code
1	Hot Standby	S/G Nozzle	----	TRANFLO
2	Full Power	S/G Nozzle	----	TRANFLO
11	Hot Standby	S/G Nozzle	2.0	TRANFLO
12	Full Power	S/G Nozzle	1.75	TRANFLO
31	Hot Standby	S/G Nozzle	----	MULTIFLEX

The objective of the time history analysis for the case without tube expansion is to define the number of tube locations where displacement amplitudes exceed 0.100 inch. For the case with tube expansion, the objective of the analysis is to show that the relative plate / tubesheet displacements are less than 0.100 inch for all of the plates. In both cases, these results are supplied as input to the evaluation to establish burst probabilities as a result of tube support plate motions under SLB loads. In evaluating the displacements, the first step is to generate displacement time histories for each plate for all of the degrees of freedom (DOF). Using the displacement time histories, maximum displacements and corresponding times are determined for each of the support plates. For the case without tube expansion, full plate displacements are then calculated for the limiting plates at the critical times and superimposed on a tube map for local regions of the plates . Displacements are calculated at each tube location within the local region by interpolating the displacements of the closest nodes, and placed into groups based on the amplitude of the displacement. The number of tubes with a given relative tube / plate displacement amplitude is then determined and provided as input to the tube burst analysis.

It is the relative plate / tube displacement that is of interest, with the tube and plate positions at the start of the SLB transient defined as the reference position. At hot standby, the TSP positions relative to cracks inside the TSP are essentially the same as at cold shutdown. Every known SG cold condition inspection shows ODSCC cracks within the non-dented TSP with a trend towards being centered within the TSP. Therefore, the cold condition TSP location relative to the tubes is essentially the same as for the full power condition where the cracks formed, which is also the position during hot shutdown. These inspections indicate that there is little relative movement between the tubes and plates throughout the operating cycle. Thus, this analysis calculates relative tube / TSP motions based on the tube / plate positions at the initiation of the SLB transient.

Calculations are also performed to demonstrate the applicability of the elastic analysis approach in determining the resulting displacements. These calculations consist of showing that the tierods / spacers remain elastic throughout the transient, that significant yielding of the tube support plates does not occur, and that the welds joining vertical bars (that provide vertical restraint for the plates) to the partition plate and wrapper remain intact.

8.2 TSP Displacements Without Tube Expansion

As discussed above, several sets of SLB loads have been considered. An overall summary of the limiting displacements for each of the plates is provided in Table 8-1. Three sets of displacement results are presented. The first set, the top set in Table 8-1, are the plate displacements relative to their initial installation (zero displacement) position. The second set of displacements, the middle set in Table 8-1, are the relative plate / tubesheet displacements (i.e. plate - tubesheet, since the tubesheet displacements also represent the tube displacements at the TSP elevation). The third and final set of displacements, shown at the bottom of Table 8-1, are the change in the relative plate / tubesheet displacements from the start of the transient. It is the final set of displacements that represent the relative plate / tube motion and the potential for uncovering cracks that could potentially exist in the tube inside the TSP.

Displacement time histories for each of the SLB cases, showing the displacement time history for the limiting location for each plate, are provided in Figures 8-1 through 8-10. Two plots are provided for each transient. The first plot shows the response of the bottom four plates, Plates A(1H), C(3H), F(5H), and J(7H), while the second plot shows the response of the top four plates, Plates L(8H), M(9H), N(10H), and P(11H). These plots show the change in relative plate / tubesheet displacements from the initiation of the transient. The analysis results show Case 11 (SLB initiating from hot standby with the break at the steam generator nozzle and an uncertainty factor of 2.0 applied) to be limiting. The results further show Plates A(1H), C(3H), and J(7H) for Case 11 to experience the largest deflections. The results for the other plates are judged to not be significant relative to the limiting plates.

In comparing the results for the TRANFLO and MULTIFLEX cases, Cases 1 and 31, the MULTIFLEX case is found to result in somewhat higher displacements. Although the pressure loads were close in terms of individual plate loads, the different frequency content of the loads results in displacements that are somewhat higher for the MULTIFLEX case.

In reviewing the results for Case 11 relative to the other cases, it is noted for Plate C(3H) that the displacement for the limiting location does not return to its initial starting position at the end of the transient (or nearly so), as for the other plates. This is a result of the plate interacting with a tube as discussed in Section 7.3. The response of the plate is such that once tube / plate interaction occurs due to local plate rotations, the tube and plate remain in contact throughout the remainder of the transient. The nature of the overall plate response is shown in Figures 8-11 and 8-12, where the time history response of all of the Plate C(3H) DOF is shown. (In conjunction with these plots, nodal locations for Plate C(3H) are shown in Figure 8-13.) The tube / plate interaction occurs at node 736.[1] Referring to Figure 8-11, it is observed that nodes adjacent to the tube contact location, Nodes 797 and 817, reach their maximum deflection shortly after tube contact occurs, and begin to return to the unloaded position, which increases the local plate rotations, maintaining the plate / tube interaction. A plot of the local plate rotations is shown in Figure 8-14, and shows results consistent with the displacement pattern of Figure 8-11. Thus, once tube / plate contact is initiated, it remains throughout the remainder of the transient for this particular loading and plate geometry.

The limiting plate displacements in all cases occur over a small region of the plate located near the tube lane at the outer edge of the plate, where the distance between vertical supports is greatest. Displaced geometry plots for Plates A(1H), C(3H), and J(7H) for the limiting set of loads, Case 11, are shown in Figures 8-15 through 8-17. The consistent displacement pattern is apparent for each of the plates.

8.3 SLB TSP Displacements By Tube Location Without Tube Expansion

In order to establish probabilities for tube burst as a result of relative plate / tube movement, calculations are performed to determine how many tubes are associated with a given displacement magnitude for a given plate. The plate displacements are categorized into groups, starting at 0.10 inch, and increasing in 0.05 inch increments to a maximum displacement > 0.55 inch.

---

[1] In referring to Figure 8-11, it is observed that Node 717 has a higher deflection than Node 736, and would also be expected to interact with tubes. Node 717, however, is located at the outer edge of Plate C(3H) and there are no tubes adjacent to this node. Node 736 represents the outermost node location that is adjacent to a tube. Thus, Node 736 was selected as the site for potential plate / tube interaction

The calculations to estimate the SLB tube burst probabilities are based on the change in the relative plate/tube position from their positions at the initiation of the SLB transient. The ODSCC indications are formed on the tube within the TSP at normal operating conditions. Relative to cold shutdown conditions, the TSP is displaced (relative to a fixed location on the tube) by the net effect of the secondary flow pressure difference across the plate plus the bow of the tubesheet. (Thermal expansion effects also marginally influence the TSP/tube displacements relative to cold shutdown, but these effects are negligible for SLB displacements at normal operating conditions.) The tubesheet bow displaces all axial locations on the tubes by the amount of the bow, while the TSP displacements closely match the bow of the tubesheet only at the locations of the tierods. The secondary flow pressure difference across the TSP tends to displace the plate in the upward direction relative to the tube. The net displacement of the plate is the sum of the tubesheet bow interaction through the tierods and the pressure differential. Therefore, the movement of the plate relative to the tube is the difference between the net plate displacement and tubesheet bow. For the Model D4 SG, the relative plate to tube displacements at normal operating conditions are not large, typically $\leq$ 0.06 inch, for the location with maximum SLB displacement. The relative displacements for hot standby conditions are not significantly different, which indicates that the full power TSP displacements due to the pressure differential across the plate are not large. Thus, it would be expected for the Model D4 SGs that the indications would be inside the TSP at both cold and hot conditions, independent of whether or not the plates are effectively clamped to the tubes as a result of crevice deposits. The net SLB displacement of the plate relative to the ODSCC on the tube is then the change in relative plate to tube (or tubesheet) displacement between a time in the SLB and time = 0.

The algorithm for calculating the relative displacements is as follows:

$$\Delta D = (D_{t=T} - D_{t=0})_{Plate} - (D_{t=T} - D_{t=0})_{Tubesheet}, \text{ where}$$

D_{Plate} = Plate Displacement

$D_{Tubesheet}$ = Tubesheet Displacement

T = Time of maximum displacement from dynamic analysis

In order to calculate the relative displacements across the full plate, displacement (stress) solutions are performed for the limiting plates at the times of maximum displacement.

The displacement solutions are performed using the finite element representations for the plates. Displacements for the dynamic degrees of freedom for the limiting plates (and tubesheet) are extracted at the times of interest from a file containing the DOF displacements for the full transient. These displacements are applied to the finite element model as boundary conditions (along with any other appropriate boundary conditions representing symmetry or ground locations), and displacements for the entire plate (and tubesheet) are calculated. Using the algorithm above, the relative plate / tubesheet displacements are calculated.

The next step in calculating displacements at individual node locations is to determine where in the model node layout each tube is located. Shown in Figure 8-18 is an overlay of the tube pattern on the finite element grid for the critical plate region. Once the four nodes surrounding a given tube location is known, the displacement at the tube location is calculated by interpolating the nodal displacements using the following algorithm. where,

$$d_1 = d_B + \left[\left(\frac{Y_T - Y_B}{Y_C - Y_B}\right)(d_C - d_B)\right]$$

$$d_2 = d_A + \left[\left(\frac{Y_T - Y_A}{Y_D - Y_A}\right)(d_D - d_A)\right]$$

$$d_T = d_2 + \left[\left(\frac{X_T - X_A}{X_B - X_A}\right)(d_1 - d_2)\right]$$

A, B, C, D correspond to the four element nodes
X_A, X_B, ... Y_A, Y_B, ... correspond to the coordinate locations of the nodes
X_T, Y_T, ... correspond to the coordinate locations of the tube
d_A, d_B, ... correspond to the displacements at the four corner nodes
d_1, d_2, are the interpolated displacements in the Y-direction at the tube location
d_T corresponds to the final interpolated tube displacement

As an example of the calculation methodology, sample results are provided for Plate C(3H) for the limiting set of SLB loads. Shown in Table 8-2 are the nodal displacements at time = 0.0, and at the limiting transient time, 2.600 seconds, for Plate C(3H) and for the corresponding tubesheet nodes. Also shown in the far right hand column are the relative plate / tubesheet displacements with respect to time = 0.0, calculated using the above algorithm. A summary of the nodes associated with selected tube locations is provided in Table 8-3. Referring to Table 8-3, on the left hand side of the table is the row and column number of the tube in question, and its coordinate location relative to the plate center. Next, for each of the four nodal locations surrounding the tube position are the node number, nodal coordinates, and the relative plate / tubesheet displacements from Table 8-2 (Note that C1, C2, C3, C4, in Table 8-3 correspond to the four element nodes A, B, C, and D in the above algorithm.) Finally, shown in Table 8-4 are the interpolated tube displacements for tube rows 1 and 2 in the vicinity of the limiting plate displacement, and the categorization of the tube displacements into the appropriate displacement group. In Table 8-4, d_1 and d_2 correspond to the intermediate interpolated displacements, with d_T being the final interpolated displacement. Similar calculations are performed for all of the tube locations in the vicinity of the maximum plate displacements, and an overall sum of the number of tubes in each displacement grouping is obtained.

A summary of the number of tubes falling into each of the displacement groupings for the limiting plates for each of the load cases is provided in Table 8-5. Note that the numbers of tubes in Table 8-5 correspond to the full plate. The number of tubes in each plate quadrant is one-half of the values listed.

Summarized in Table 8-6 is a comparison of the maximum plate displacement to the plate displacement at the limiting tube location (the tube having the highest displacement), R1C1. As can be observed in the displaced geometry plots in Figures 8-15 through 8-17, the displacement gradients at the corner of the plate are high, so the maximum differential displacement at R1C1 is less than the maximum plate displacement reported in Table 8-1.

8.4 Optimization of Tube Locations for Tube Expansion

As stated above, the analysis of the effects of tube expansion is performed for the Case 11 SLB loads. Using the displacement results for the case without expansion, a preliminary set of locations for expansion was selected at the positions of highest displacement. Incorporating the appropriate expanded tube stiffnesses into the dynamic solution, an initial set of displacements was obtained. The expansion locations were then modified to add / move expansion positions for the locations of highest displacement. A new displacement solution was obtained, and the process continued until plate displacements were all calculated to be less than the 0.100 inch objective.

Stress solutions were then obtained for the limiting plates and times in the dynamic solution. (Further discussion regarding plate stresses is provided in Section 8.10). For Plate P, the stress results indicated that yielding of the plate in the vicinity of the cutouts along the tube lane would potentially result in increased plate displacements. Thus, a pinned connection was assumed for the critical locations, and a new dynamic solution was obtained. The results indicated that an additional tube expansion along the tube lane was necessary, and two final expansion locations (one on each side of the bundle) was added to the expansion matrix. (In later discussions, the expansion locations added due to the plate stresses are identified as "structural" expansions.)

The final locations selected for tube expansion are shown in Figures 7-22 through 7-28 (there are no tube expansions for Plate A (1H) due to the oversized tube holes in this plate). Although not shown on these figures, there are several locations where two tubes are to be expanded. Further discussion of the number and location of the tube expansions is provided below.

8.5 TSP Displacements With Tube Expansion

A summary of the resulting displacements including the effects of tube expansion are summarized in Table 8-7. The displacements for the case without expansion are also shown for comparison. The effects of tube expansion are dramatic for the lower plates that experience high displacements at the corners of the plates without expansion. For the upper plates, and in particular Plate P (11H), tube expansion has a significant effect, but is not as dramatic as for the lower plates. Expansion is not as effective for the upper plate due to the reduced stiffness of the expanded tube for the upper plate as compared to the lower plates. The reduced stiffness is due to the significantly increased tube span between the tubesheet and the top plate.

8.6 Redundant Tube Expansions for Postulated Circumferential Cracking

In order to provide redundancy at the most critical expansion locations, a second tube is specified for expansion for Plates C (3H) and F (5H) in the corner region, and for Plates N (10H) and P (11H) in the central region of the plate. The expansion of the additional tube at these locations is to provide added assurance of an effective expansion in the unlikely event of a circumferential crack developing with the subsequent loss of load carrying capability of the expanded tube. A summary of the resulting maximum displacements including the redundant tube expansions are summarized in Table 8-8. It can be observed by comparing the results for the reference and redundant sets of expansions that the redundant tubes do not significantly reduce the limiting displacements for the reference expansions. The intent of these expansions, however, is to provide redundancy, and not a further reduction of the limiting displacements.

8.7 TSP Displacements for Postulated Circumferential Cracking

In order to assess the sensitivity of the plate displacements to losing support from one or more tubes due to postulated circumferential cracking, calculations were performed assuming various support conditions. For the first case, expansions for the lower plates, Plates C (3H), F (5H), and J (7H) were assumed to crack, with the exception for locations where more than one tube is expanded. For these locations, it is assumed that one of the expansions remains intact. Also for this case, a postulated crack at one of the lower plates also effectively eliminates that tube for the upper plates as well, except that the plate-to-plate interaction remains in place (between the upper plates only). For the second case, the expansions for the upper plates, Plates L (8H) through P (11H), are assumed to be lost. Again, duplicate expansions at a given location are assumed to remain intact. Finally, for the third case, all expansions are assumed to be lost with the exception of locations where duplicate expansions exist. A comparison of the resulting displacements for the various cases is provided in Table 8-9. Note that the "structural" tube expansions discussed above are not included in the dynamic solutions for Cases 74 - 78 in Table 8-9. This is not considered significant relative to the sensitivity of the dynamic solutions to the conditions being evaluated.

One additional case not related to circumferential cracking was run to provide a sensitivity of the displacement results to load amplitude. The results above are with a load factor of 2.0 applied to the loads predicted by TRANFLO. For the sensitivity run, the load factor was increased to 4.0. The resulting displacements are summarized in Table 8-9, and show that the peak displacements to be essentially linear with load amplitude, given that the frequency content of the loads does not change.

8.8 Sensitivity of TSP Displacements to Expanded Tube Location

In order to allow for plant specific selection of the exact tube locations to be expanded, a set of calculations was performed where the expansion locations were shifted slightly from the reference position. In general, the locations were shifted one node point (in the finite element model) away from the reference position. The direction of the movement was based on a review of the displacement results to determine what would be the most effective alternate positions. Movement of the expansion location one node point in the model is approximately equal to three tube pitches.

Based on initial results for determining the sensitivity of the displacements to tube expansion position, one additional tube was added to the matrix of expansion locations. However, the sensitivity runs discussed above were not rerun, as adding one additional expansion location would not significantly alter the results. The run for the redundant expansion case was rerun, however, and the revised results along with the results for the alternate tube positions are summarized in Table 8-10. The results show the shifted locations to also satisfy the 0.100 inch requirement.

The limiting displacement time histories for each of the plates are shown in Figures 8-19 through 8-21 for the shifted expansion location case, which is the bounding displacement case. (Note that Plate A (1H) is shown on a separate plot in order to better visualize the results for Plates C (3H), F (5H), and J (7H), which have much smaller displacements than Plate A (1H). There is very little change to the Plate A (1H) displacements from the unexpanded case, which is expected since there are no expansions for this plate. Plots of the distorted geometries for Plates A (1H), C (3H), and J (7H) are provided in Figures 8-22 through 8-24, and can be compared to the plots for the unexpanded case to see how the high corner displacements have been eliminated. The distorted geometry for Plate P (11H), the limiting plate for expansion conditions (excluding Plate A (1H)), is shown in Figure 8-25.

One effect that has not been accounted for in the analysis, is the influence of the displacement of the cold leg side of the plates on the hot leg displacements for the plates above the preheater, where tube expansion does not exist. Cases 76 and 78 in Table 8-9, where the upper plate tube expansions have been deactivated, show the maximum relative tube / TSP displacement to be on the order of 0.200 inch for Plate P (11H). Thus, it would be anticipated that the relative tube / TSP displacements along the tube lane for this plate would be on the order of 0.150 inch, the approximate average of the two displacement results. The other plates are also effected, but based on the results in Table 8-9, the effect is judged to be less significant.

8.9 Tube Locations and TSP Elevations for TSP Expansions

Based on the results of the above calculations, the number and location of the tube expansions is summarized in Table 8-11. The tube locations identified in the table represent the expansion positions considered in the reference dynamic solution. Based on the dynamic solution to evaluate the sensitivity of the TSP displacements to expanded tube position, a group of tubes has been defined for use in selecting the final tube expansion matrix for a given steam generator. These groups of tubes are shown in Figure 8-26.

At some plate locations, multiple tube expansions are required. The locations for multiple tube expansions are of two types. The first type corresponds to locations of redundant tube expansion. Referring to Table 8-11, these locations are R6-C7, R6-C108, and either R19-C56 or R19-C59. (R19-C56 and R19-C59 are in the center of the bundle and expansion is required at only one of the two locations.) These locations correspond to the most critical expansion positions. Only one of the tube expansions is required to limit the plate displacement at these locations to less than 0.100 inch. However, if loss of tube support would occur at these locations, the maximum plate displacements would approach those for the unexpanded case. Thus, a second, redundant, expansion has been defined. Again, referring to Table 8-11, the remaining locations for multiple expansions, R26-C22, R19-C41, R26-C93, and R19-C74, correspond to positions where two tubes are required to meet the 0.100 inch criteria. At these positions, loss of one of the tubes due to postulated cracking would result in plate displacements that exceed 0.100 inch by only a small amount (<0.025 inch).

An example of an expanded tube matrix based on the results of the analysis is summarized in Section 2. The tubes identified in this table represent one of many possible permutations that could be defined. A final matrix will be defined on a plant specific basis.

8.10 Summary of Stress Results

Since the dynamic analysis is based on elastic response, calculations were performed to assure that the various structural members remain elastic throughout the transient. The stress results reported below are for the dynamic solution to determine sensitivity of plate displacements to expanded tube position. This case represents the limiting solution for the expanded tube condition.

The first component evaluated is the tierods. The analysis results establish that the tierods do, in fact, remain elastic throughout the transient. The 0.2% offset yield point corresponds to an elongation of the outer tierods (that run from the tubesheet to the top TSP) of [ ]^{a,c} inch, and an elongation of the central tierod (that runs from Plate L(8H) to Plate P(11H)) of [ ]^{a,c} inch. The maximum elongations calculated during the limiting SLB are [ ]^{a,c} inch for the outer stayrods, and [ ]^{a,c} inch for the central stayrods. In both instances, these elongations are well below the yield point for the stayrods. Similarly, for the spacers that are located on the outside of the tierods between the support plates, the maximum compressive stress in the tierods is on the order of [ ]^{a,c} psi, which is well below the yield stress of 23,400 psi.

Also relevant in assessing the appropriateness of the elastic solution, are the stresses in the plates. Thus, in conjunction with the displacement results from the dynamic analysis, stresses are calculated for the hot leg plates at the times corresponding to the maximum plate displacements. The stresses are calculated by extracting displacements from the dynamic analysis for each plate degree of freedom, and then applying those displacements to the finite element model. The finite element code then back-calculates the displacements and stresses for the overall plate model.

Additional boundary conditions corresponding to lines of symmetry and appropriate rotational constraints are also applied to the model. The finite element results give a set of displacement and stress results for the overall plate. The resulting plate stresses, however, correspond to the effective Young's modulus, and must be multiplied by the inverse ratio of effective-to-actual Young's modulus to get the correct plate stresses.

Stresses are calculated for Plates A (1H), C (3H), J (7H), and P (11H) for the limiting set of loads. In order to interpret the stress results, stress contour plots for the maximum and minimum stress intensities have been made for each plate. Plots showing the maximum and minimum stress intensities are shown in Figures 8-27 to 8-34, for Plates A (1H), C (3H), J (7H), and P (11H), respectively. These plots show the distribution of stress throughout the plate. As expected, the maximum stresses occur near the locations of vertical support, the tierod / spacers and vertical bars. The ASME Code minimum yield strength for the TSP material is 23.4 ksi. The results for Plate A show the stresses to be elastic throughout the plate. For Plates C(3H), J(7H), and P (11H), there are local areas near the tierods, where the surface (bending) stresses exceed the yield stress. As discussed earlier, the boundary conditions for Plate P (11H) account for yielding of the "tabs" in those locations where high bending stresses were present in tabs along the tube lane in the initial solution.

The plate stresses cannot be compared directly to the material yield strength, as these stresses correspond to an equivalent solid plate. In order to arrive at the plate ligament stresses, additional detailed stress analysis of the plates is required. Such an analysis is outside the scope of this program. The equivalent plate stresses do provide a general guideline as to those areas of the plate that are most limiting from a stress viewpoint. The plate stresses are meaningful in that they indicate that the stresses are generally low throughout the plate, and that the elastic analysis is a good approximation of the transient plate response. In general, local yielding of the plates near the tierods will not lead to a significant change in the maximum displacements as they are limited by the tube / plate interactions.

Calculations have also been performed to determine the stresses in the welds between the vertical bars and the partition plate and wrapper. The loads at the various support points are extracted from the static WECAN runs in the form of reaction forces at the times of maximum plate deflection. Loads have been extracted for the limiting plates (based on plate motions) for the limiting set of SLB loads. Calculations are also performed for the limiting plate above the preheater, Plate P (11H), as these plates have a somewhat different support arrangement than the lower plates.

The vertical bars are generally [ ]^{a} inches in length. except for the bars underneath Plate A(1H), which are only [ ]^{a} long. The bars are welded to the partition plate and / or wrapper using a full length [ ]^{a} fillet weld along both edges of the bar. The stresses in the welds act in the shear direction. The weld throat area is simply the throat width times the height of the weld [ ]^{a}. The corresponding stress intensity is twice the shear stress.

A summary of the reaction forces and corresponding stresses for each of the bar locations for the locations considered is provided in Table 8-12. The results show all of the stresses to be low (<3 ksi) for a faulted event. The allowable stress for the welds is based on $2.4S_m$ x 1.5 x 0.35 (for fillet welds with visual examination) for carbon steel. S_m at 550°F is 15.5 ksi. The resulting allowable stress intensity is 19.53 ksi, and the weld stresses are acceptable.

Calculations were also performed to determine the axial force in the expanded tubes as a result of the SLB event. A summary of the maximum forces for each of the expansion regions is provided in Table 8-13, and shows the forces in these tubes to be quite low (<500 lb).

8.11 S/G Structural Effects of Expanded Tubes

The influence of tube expansion on the structural integrity of the tube bundle assembly and its attachments to the shell are considered in light of the two conditions that may exist: 1) The TSP tube crevices are open or packed with minimal tube to TSP contact force and the tubes move freely (except for normal contact friction) through the TSPs and 2) The tubes are assumed to be locked to the TSPs as a result of a range of TSP packing and/or denting. It is shown that with the TSP crevices open, the expanded tubes function as an additional stayrod and introduce no new significant loading conditions. With the tubes effectively locked at the TSPs, the expanded tubes are equivalent to another plugged tube under a tube to TSP condition for which tube expansion is not required to limit TSP displacements.

Nominal Bundle Conditions - Minimal Tube/TSP Contact Force

In the model D-4 steam generators, the TSP axial position is determined by 12 stayrods and spacers connecting the tubesheet to each of the TSPs, and by positioning blocks, "backup bars", that are welded to the wrapper and the divider plate above and below the TSPs (see Section 7). The addition of expanded tubes is similar to addition of more stayrods, except that an expanded tube is significantly less stiff (more than an order of magnitude) than a stayrod. The net effect of adding 21 expanded tubes is to reduce the flexibility of the TSPs.

No significant loads are applied to the TSPs by implementation of tube expansion. The expansion process may cause small axial forces on the TSPs due to residual axial strains in the expanded tubes. Management of the expansion sequence will prevent buildup of these strains. These forces will be partially relaxed during rise to power due to differential thermal expansion between the Alloy 600 tubes and the carbon steel stayrods.

In summary, the addition of expanded tubes does not add any significant new loading mechanisms to the TSPs for normal operation of the S/Gs. The net effect of the expanded tubes is to add out-of-plane stiffness to the TSPs to limit plate deflection during postulated SLB conditions, as discussed previously. Interaction of the TSPs with the wrapper remains primarily influenced by the 12 stayrods with an order of magnitude higher stiffness than the expanded tubes, and the backup bars and wedges.

Tube/TSP Lockup Condition

Field inspection data indicate that the case of tubes locked to the support plate is the prevalent case. Tube inspections have shown that the incidence of ODSCC is always within the span of the TSPs at cold conditions, independent of axial position of the TSP within the tube bundle and radial position of the tube in the TSP. That this occurs, particularly at the upper TSPs in the bundle, is a firm indication that the TSPs and the tubes are locked together, and that lockup occurred at hot, operating conditions. If relative motion occurred between the tubes and the TSPs due to thermal contraction from operating conditions to the cold conditions for inspection, the TSP and the degradation indication would be expected to be overlapped or separated, most noticeably at the upper TSP.

The lockup condition requires that many tubes participate, sufficient in number that the stiffness of the aggregate tube is greater than the bundle wrapper stiffness. This is consistent with both the inspection observations as noted above, and phenomenological considerations of packed crevices and denting. The conditions leading to tube/TSP lockup are bulk conditions that would affect many tubes at approximately the same time rather than isolated tubes. This has been shown to be true in older operating plants, typically with model 44 and model 51 S/Gs, where denting occurred at a relatively large number of tubes simultaneously.

The lockup condition does not require denting. Test were performed (Ref 13.5) to determine the forces required to pull lightly dented tubes (or incipient denting with no deformation) from simulated support plates. Both bobbin voltages and dent dimension were recorded. All dents were measured to be less than 1 mil, radial. For dents less than 5 volts, pull forces up to 700 lbs. were measured. The tube pull force was also measured during the tube pull of a non-dented tube in Plant L. Without any contribution from the tubesheet, the force required to pull the tube through two support plates was approximately 4000 lbs. Conservatively estimating an average lockup force of 500 lbs. per tube, the net reaction capability of a TSP assumed to have packed crevices but no denting at all tube intersections is approximately 2.3×10^6 lbs.

The lockup condition causes interactions among the tubes, TSPs, wrapper, wrapper support structure and the tubesheet as a result of changes in the thermal condition of the S/G. Interactions with plugged tubes also occur as noted below. The reference condition is the hot, operating state as noted above. In this condition, the interaction stresses are nominally zero. During cooldown, interaction stresses build up due to differential thermal contraction between the tubes and the TSPs. Because the tubes are locked to the TSPs, TSP bending occurs that is maximum at the top TSP, and incrementally smaller at each lower TSP. Further, since the TSPs are axially fixed to the stayrods and the wrapper, the stayrods and the wrapper react the TSP forces. Local bending of the TSP is expected at the stayrod locations and at the wrapper TSP backup bars. Since the tubes are anchored at the tubesheet, the net effect is to load the wrapper to shell support structure to react the wrapper loads, and the tubesheet to react the stayrod forces.

Tube expansion is implemented at cold conditions; therefore, for the TSP lockup condition, expanded tubes are equivalent to tubes plugged after lockup has occurred. This includes most tubes plugged for ODSCC at the TSPs. The number of tubes that will be expanded is much smaller than the number of plugged tubes. No adverse structural effects during rise to power and operation have been observed for plugged tubes; thus, no adverse structural effect is expected for the expanded tubes.

During the rise to operating temperature, differential thermal expansion between the active tubes and the expanded or plugged tubes will cause axial forces on the TSP at the location of these tubes. The magnitude of these forces is much smaller than the forces applied by the stayrods during the descent from power to cold conditions. Thus, tube expansions introduce no significant new loading mechanisms for S/G structural considerations for the tube/TSP lockup condition.

Summary

Since the tube expansions do not introduce any significant new loading mechanism for either the case of free tube expansion or tube/TSP lockup conditions, and operation with expanded tubes is enveloped by existing conditions, additional analyses are not required to support operation with expanded tubes. Acceptable operation under lockup conditions has been demonstrated by the field experience of operating S/Gs which have been shown in EC inspections to be in the lockup condition.

8.12 Conclusions

Based on the above results, it is concluded that expansion of selected tubes at each of the tube support plates (excluding Plate A (1H)) is effective in reducing tube support plate displacements under steam line break loads. With the possible exception of the top plate, Plate P (11H), along the tube lane, the displacements are limited to 0.100 inch or less. Based on an evaluation of the resulting stresses, it is concluded that the elastic analysis provides a good approximation of the dynamic response of the TSPs to the applied loading.

Stress levels in the tubes, plates and supporting components were analyzed and found to be acceptable. It is also shown that the tube expansions do not introduce any significant new loading mechanisms on the TSP or the TSP support structures for either the case of free tube expansion (low tube/TSP contact forces) or the case of tube/TSP lockup conditions. Additional analyses are not required to support operation with expanded tubes.

Table 8-1

Summary of Maximum TSP Displacements for Postulated SLB Events for D4 Steam Generators

a,c

Table 8-2

Summary of Relative Plate / Tubesheet Displacements
Model D4 Steam Generator
SLB Initiating From Hot Standby
Break at Steam Generator Nozzle

Plate C

a,c

Table 8-3

Summary of Nodal Displacements
Model D4 Steam Generator
SLB Initiating From Hot Standby
Break at Steam Generator Nozzle

Plate C

a,c

Table 8-4

Summary of Relative Plate / Tube Displacements
Model D4 Steam Generator
SLB Initiating From Hot Standby
Break at Steam Generator Nozzle

Plate C

a,c

Table 8-5

Summary of Number of Tubes Having Different Displacement Magnitudes
Model D4 Steam Generator
Steam Line Break Load Cases

a,c

Table 8-6

Comparison of Maximum Displacement at Plate Edge and at Limiting Tube Location

a,c

Table 8-7

**Summary of Limiting Displacements
Model D4 Steam Generators
Including Tube Expansion Effects**

a,c

Table 8-8

Summary of Limiting Displacements
Model D4 Steam Generators
Including Redundant Tube Expansion Effects

a,c

Table 8-9

Summary of Limiting Displacements
Model D4 Steam Generators
Tube Expansion With Postulated Circumferential Cracking

a,c

Table 8-10

Summary of Limiting Displacements
Model D4 Steam Generators
Sensitivity of Displacements to Tube Expansion Location

a,c

Table 8-11

Summary of Tube Expansion Locations

a,c

[ ]

Table 8-12

Summary of Vertical Bar Stresses
SLB Transient
Model D4 Steam Generators

a,c

Table 8-13

Summary of Axial Forces in Expanded Tubes
SLB Transient
Model D4 Steam Generators

a,c

a,c

Figure 8-1. Relative Plate / Tubesheet Displacement Time History Response
SLB from Hot Standby
Break at Steam Generator Nozzle
Plates A(1H), C(3H), F(5H), J(7H)

a,c

Figure 8-2. Relative Plate / Tubesheet Displacement Time History Response
SLB from Hot Standby
Break at Steam Generator Nozzle
Plates L(8H), M(9H), N(10H), P(11H)

a,c

Figure 8-3. Relative Plate / Tubesheet Displacement Time History Response
SLB from Full Power
Break at Steam Generator Nozzle
Plates A(1H), C(3H), F(5H), J(7H)

a,c

Figure 8-4. Displacement Time History Response
SLB from Full Power
Break at Steam Generator Nozzle
Plates L(8H), M(9H), N(10H), P(11H)

a,c

Figure 8-5. Relative Plate / Tubesheet Displacement Time History Response
SLB from Hot Standby
Break at Steam Generator Nozzle
Uncertainty Factor of 2.0
Plates A(1H), C(3H), F(5H), J(7H)

a,c

Figure 8-6. Relative Plate / Tubesheet Displacement Time History Response
SLB from Hot Standby
Break at Steam Generator Nozzle
Uncertainty Factor of 2.0
Plates L(8H), M(9H), N(10H), P(11H)

a,c

Figure 8-7. Relative Plate / Tubesheet Displacement Time History Response
SLB from Full Power
Break at Steam Generator Nozzle
Uncertainty Factor of 1.75
Plates A(1H), C(3H), F(5H), J(7H)

a,c

Figure 8-8. Relative Plate / Tubesheet Displacement Time History Response
SLB from Full Power
Break at Steam Generator Nozzle
Uncertainty Factor of 1.75
Plates L(8H), M(9H), N(10H), P(11H)

a,c

Figure 8-9. Relative Plate / Tubesheet Displacement Time History Response
SLB from Hot Standby
Break at Steam Generator Nozzle
MULTIFLEX Loads
Plates A(1H), C(3H), F(5H), J(7H)

a,c

Figure 8-10. Relative Plate / Tubesheet Displacement Time History Response
SLB from Hot Standby
Break at Steam Generator Nozzle
MULTIFLEX Loads
Plates L(8H), M(9H), N(10H), P(11H)

a,c

Figure 8-11. Relative Plate / Tubesheet Displacement Time History Response
SLB from Hot Standby
Break at Steam Generator Nozzle
Uncertainty Factor of 2.0
Plate C(3H) Degrees of Freedom

a,c

Figure 8-12. Relative Plate / Tubesheet Displacement Time History Response
SLB from Hot Standby
Break at Steam Generator Nozzle
Uncertainty Factor of 2.0
Plate C(3H) Degrees of Freedom

a,c

Figure 8-13. Plate C(3H) Node Numbers

a,c

Figure 8-14. Plate C(3H) Local Plate Rotations
SLB from Hot Standby
Break at Steam Generator Nozzle
Uncertainty Factor of 2.0

a,c

Figure 8-15. Displaced Geometry
Plate A(1H) : Time = 2.572 sec
SLB from Hot Standby
Break at Steam Generator Nozzle
Uncertainty Factor of 2.0

a,c

Figure 8-16. Displaced Geometry
Plate C(3H) : Time = 2.600 sec
SLB from Hot Standby
Break at Steam Generator Nozzle
Uncertainty Factor of 2.0

a,c

Figure 8-17. Displaced Geometry
Plate J(7H) : Time = 2.656 sec
SLB from Hot Standby
Break at Steam Generator Nozzle
Uncertainty Factor of 2.0

a,c

Figure 8-18. Tube Position Relative to Model Node Location

a,c

Figure 8-19. Relative Plate / Tubesheet Displacement Time History Response
SLB from Hot Standby
Break at Steam Generator Nozzle
Uncertainty Factor of 2.0
Tube Expansion Included
Plate A(1H)

a,c

Figure 8-20. Relative Plate / Tubesheet Displacement Time History Response
SLB from Hot Standby
Break at Steam Generator Nozzle
Uncertainty Factor of 2.0
Tube Expansion Included
Plates C(3H), F(5H), J(7H)

a,c

Figure 8-21. Relative Plate / Tubesheet Displacement Time History Response
SLB from Hot Standby
Break at Steam Generator Nozzle
Uncertainty Factor of 2.0
Tube Expansion Included
Plates L(8H), M(9H), N(10H), P(11H)

a,c

Figure 8-22. Displaced Geometry
Plate A(1H) : Time = 2.572 sec
SLB from Hot Standby
Break at Steam Generator Nozzle
Uncertainty Factor of 2.0
Tube Expansion Included

a,c

Figure 8-23. Displaced Geometry
Plate C(3H) : Time = 2.592 sec
SLB from Hot Standby
Break at Steam Generator Nozzle
Uncertainty Factor of 2.0
Tube Expansion Included

a,c

Figure 8-24. Displaced Geometry
Plate J(7H) : Time = 2.640 sec
SLB from Hot Standby
Break at Steam Generator Nozzle
Uncertainty Factor of 2.0
Tube Expansion Included

a,c

Figure 8-25. Displaced Geometry
Plate P(11H) : Time = 0.4480 sec
SLB from Hot Standby
Break at Steam Generator Nozzle
Uncertainty Factor of 2.0
Tube Expansion Included

a,c

Figure 8-26. Map of Tube Expansion Locations

a,c

Figure 8-27. Maximum Stress Intensity
SLB from Hot Standby
Break at Steam Generator Nozzle
Uncertainty Factor of 2.0
Plate A(1H)
Tube Expansion Included

a,c

Figure 8-28. Minimum Stress Intensity
SLB from Hot Standby
Break at Steam Generator Nozzle
Uncertainty Factor of 2.0
Plate A(1H)
Tube Expansion Included

a,c

Figure 8-29. Maximum Stress Intensity
SLB from Hot Standby
Break at Steam Generator Nozzle
Uncertainty Factor of 2.0
Plate C(3H)
Tube Expansion Included

a,c

Figure 8-30. Minimum Stress Intensity
SLB from Hot Standby
Break at Steam Generator Nozzle
Uncertainty Factor of 2.0
Plate C(3H)
Tube Expansion Included

a,c

Figure 8-31. Maximum Stress Intensity
SLB from Hot Standby
Break at Steam Generator Nozzle
Uncertainty Factor of 2.0
Plate J(7H)
Tube Expansion Included

a,c

Figure 8-32. Minimum Stress Intensity
SLB from Hot Standby
Break at Steam Generator Nozzle
Uncertainty Factor of 2.0
Plate J(7H)
Tube Expansion Included

a,c

Figure 8-33. Maximum Stress Intensity
SLB from Hot Standby
Break at Steam Generator Nozzle
Uncertainty Factor of 2.0
Plate P(11H)
Tube Expansion Included

a,c

Figure 8-34. Minimum Stress Intensity
SLB from Hot Standby
Break at Steam Generator Nozzle
Uncertainty Factor of 2.0
Plate P(11H)
Tube Expansion Included

9.0 ANALYSIS METHODS FOR TUBE BURST & LEAKAGE WITH LIMITED TSP DISPLACEMENTS

Since the TSPs do not undergo any displacement relative to indications developed within the upper and lower planes of the TSPs during normal operation, tube burst at pressures less than three times the normal operating differential pressure is obviated by the presence of the TSP. Thus, the RG 1.121 requirement relative to $3 \cdot \Delta P$ is inherently met. Hence, the considerations documented in this section are limited to determining the margin against tube burst during a postulated Steam Line Break (SLB).

9.1 General Description of Analysis Methods

The essentials of the analyses consist of consideration of correlations of the burst pressure of throughwall cracks relative to crack length and the burst pressure of ODSCC TSP indications relative to the NDE ECT amplitude, i.e., the bobbin voltage. The concern for the potential of tube rupture during a SLB is based on the consideration that the pressure gradient in the SG will cause the TSPs to deform out of plane and expose TSP intersection tube ODSCC indications such that they behave as free-span indications without the constraint of the TSP. The evaluation of the likelihood of tube rupture is based on the calculated deformations of the plates to determine the magnitude of potential exposure, the correlation of the burst pressure of tubes with free-span ODSCC indications to bobbin voltage, and the correlation of the burst pressure of tubes with free-span axial cracks to crack length.

Most of the ODSCC TSP tube indications in a SG occur at row and column locations where the TSP undergoes relatively minor displacement, say ≤ 0.1", during a SLB. Since the thickness of the TSP is 3/4", it is unrealistic to treat each indication as though it would be fully exposed during a SLB. In this case the expected burst pressure can be calculated by considering a throughwall crack which is exposed by an amount equal to the deformation of the plate. The probability of burst (PoB) for such a crack can be calculated based on the correlation of the burst pressure to the crack length. For larger deformations the PoB is calculated as the lesser value obtained by using both correlations. While the PoB may increase significantly for longer throughwall cracks, the actual PoB would be limited by that for a free-span ODSCC indication.

9.2 Burst Pressure versus Through-Wall Crack Length Correlation

Since an essential part of the mehodology involves the correlation of the burst pressure to the potentially exposed crack length, it is appropriate to first consider the relationship of the burst pressure to crack length for a free-span indication. This relationship forms the basis for estimating the probability of burst as a function of the exposed crack length, i.e., in subsequent sections the relationship of burst to exposed crack length is developed relative to the free-span correlation.

Recent analysis of burst test data for a variety of tube sizes indicates a strong correlation between the burst pressure, P_b, and the throughwall crack length, a, using an exponential relationship, i.e.,

a, c, g

(9.1)

where t and R_m are the thickness and the mean radius of the tube, and S_Y and S_U are the yield and ultimate tensile strength of the tube material. The term in brackets is usually referred to as the normalized or non-dimensionalized burst pressure, P_N, i.e.,

$$P_N = \frac{P_B r_m}{2 S_f t}. \tag{9.2}$$

Thus, P_N is the ratio of the maximum Tresca stress intensity (taking the average compressive stress in the tube to be $P_B/2$), to twice the flow stress, S_f, of the material, taken as $\frac{1}{2}(S_Y+S_U)$ for Alloy 600. The exponent term, λ, is referred to as the normalized crack length, where

$$\lambda = \frac{a}{\sqrt{R_m t}}. \tag{9.3}$$

The coefficients of equation (9.1) were found by performing a non-linear regression of P_N on λ, i.e,

$$P_N = g_1 + g_2 e^{g_3 \lambda}. \tag{9.4}$$

The index of determination of the regression was found to be 99.1% with a standard error of 0.0176. The p values for each of the coefficients was significantly less than 0.1%. The distribution of the residuals was found to be approximately normal. A plot of the resulting relation corresponding to the form of equation (9.1) is provided on Figure 9-1, for a nominal flow stress of 71.6 ksi, the average of the Westinghouse database for tubes at 650°F. Also shown on Figure 9-1 is the regression curve adjusted for lower 95%/95% tolerance limit material properties at 650°F. It is noted that equation (9.1) yields estimates of the critical crack length for burst during SLB of 0.75" for the actual SLB differential pressure and 0.51" for a margin of 1.4 times the SLB differential pressure for material considered to have lower tolerance limit (LTL) yield plus ultimate tensile strength at 650°F.

9.3 Burst Pressure vs. Length for Cracks Extending Outside TSPs

The results of burst testing of tubes with throughwall axial cracks has demonstrated a correlation between the burst pressure, or burst strength, and the crack length. A discussion of the form of the correlation is deferred to Section 9.4, where the probability of burst for throughwall cracks is evaluated. For tubes in which a portion of the length of the crack is restrained in the radial and circumferential directions, i.e., as would exist within a hole in a TSP, the burst pressure correlates with the exposed crack length. This is because the local condition for burst is the achievement of a critical opening of the crack at the crack tip. For throughwall cracks in thin walled tubing the critical crack tip opening displacement (CTOD) is on the order of the thickness of the tube, i.e., about 40 mils. In essence, the clearance between the OD of the tube and the ID of a TSP hole is not sufficient to permit the achievement of the critical CTOD for the end of the crack within the TSP at the pressures which would lead to the burst of cracks of significant length.[1] Hence, within the TSP, the crack would not be expected to extend beyond that associated with minor blunting of the crack tip.

To evaluate the strengthening effect of the constraint afforded by the TSP, a series of burst tests was performed to provide a direct comparison between the free-span burst strength and the TSP constrained burst strength. The results from the tests are summarized in Table 9-1 and Table 9-2, and illustrated on Figure 9-2. Free-span burst tests were performed for a range of throughwall crack lengths, simulated by narrow EDM slits, from 0.15" to 0.70". For TSP confined tests, the crack length was always 0.70", and exposure of the crack beyond the TSP boundary ranged from 0.15" to 0.50". For the TSP constrained burst tests the presence of the TSP is simulated by a round collar which is sized to provide a radial stiffness equal to the average radial stiffness of the TSP. For the series of tests performed the diametral clearance between the tube and the TSP hole ranged from [ ]^{a,c,e} mils, or about [ ]^{a,c,e} mils on the circumference. The results from the tests employing the smaller gap, see Figure 9-2, verify the expectation that the burst pressure for a long crack with a portion of the crack constrained by the TSP would be similar to that of a free-span crack with a total length equal to the exposed length of the constrained crack. Hence, if the clearance in the S/G is small, i.e., on the order of 13 mils or less, the throughwall burst pressure correlation may be used to evaluate the probability of burst of exposed cracks as a function of the length exposed.

Specific data relating to the as-built dimensions of the TSP holes in the Model D4 S/Gs is not currently available. Hence, information was developed to indirectly support the selection of the collar inside diameter for the test program. The Model D4 TSP drawings indicate a tolerance for the tube hole size of ["]^{a,c,e}, with a reference dimension of [ ]^{a,c,e}. It may be concluded that the drill size

[1] Specimens with 3/4" long cracks, entirely confined with the TSP exhibit burst pressures well above 8500 psi.

used for the D4 TSPs was either a standard [ ]^{a,c,e} diameter. Random sampling data from TSP holes drilled for another model S/G indicated that the average hole diameter is]^{a,c,e} larger than the drill size, and that the standard deviation of the hole diameter is [ ]^{a,c,e} mils. A sample of hole diameters in the tubesheet of a Model 51F S/G were found to have a standard deviation of [ ]^{a,c,e} mils. Based on the average and standard deviation of the sample data, holes drilled with a [ ]^{a,c,e} diameter drill would be expected to have a 95% confidence upper bound of [ ]^{a,c,e}, or clearances ranging from [ ]^{a,c,e} mils. If the drill size was [ ]^{a,c,e}, the corresponding clearance range would be from [ ]^{a,c,e} mils. For the larger clearances it would be expected that the strengthening due to the TSP constraint would be significant, but not as significant as for the small clearance range. The results illustrated on Figure 9-2 confirm this supposition. Over the range of exposure of interest, the effect of the larger clearance is to diminish the burst pressure as predicted by equation (9.1) by about [ ]^{a,c,e}.

9.4 SLB Burst Probability as a Function of Throughwall Crack Length

A generalized form of equation (9.1) can be written as,

$$P_B = \left(\frac{2\,t}{R_m}\right) P_N S_f \,. \tag{9.5}$$

Equation (9.5) may be used to estimate the probability of burst based on the variance of the estimate of P_N about the regression equation and the variance of S_f from a large database of measured properties of tubing installed in Westinghouse steam generators. An unbiased estimate of the variance, **V**, of P_B is given by

$$\mathbf{V}(P_B) = \left(\frac{2\,t}{R_m}\right)^2 \left[P_N^2\, \mathbf{V}(\sigma_f) + \sigma_f^2\, \mathbf{V}(P_N) - \mathbf{V}(\sigma_f)\, \mathbf{V}(P_N) \right]. \tag{9.6}$$

The standard deviation of the burst pressure, σ_P, is taken as the square root of $\mathbf{V}(P_B)$. If P_A is an actual burst pressure, it is assumed that the statistic

$$t = \frac{(P_B - P_A)}{\sigma_P}, \tag{9.7}$$

is distributed as a Student's t distribution with degrees of freedom equal to the degrees of freedom ([ ]^{e}) used for the regression of P_N on λ.

Taking P_A equal to the SLB pressure, a t variate is calculated from equation (9.7). The probability of randomly obtaining a t variate as large at that obtained is then calculated from the cumulative Student's t distribution. A plot of probability of burst as a function of crack length using this approach is provided as Figure 9-3. This is then taken probability of burst (PoB) during a postulated SLB for a tube with a throughwall crack length of a.

In actuality, the distribution of P_B does not follow a Student's t distribution. Monte Carlo simulations of the burst pressures have resulted in distributions which appear close to the form of a Student's t distribution, but which have a longer tail in the higher burst pressure range, i.e., they are skewed right. Hence, the use of equation (9.7) is expected to be conservative. Comparison of individual 95% upper bound Monte Carlo results with predictions from equation (9.7) indicate a small level of conservatism for high probabilities of burst, e.g., PoB greater than 0.1, and an order of magnitude difference for low probabilities of burst, e.g., on the order of 10^{-6}.

The above equations apply to calculating the PoB for a single throughwall crack or indication. For multiple indications the PoB of one or more of those indications is found as one minus the probability that none of them burst. The probability of no burst, or survival, for any single indication is one minus the PoB, thus the probability of burst of one or more of m indications is given as,

$$\mathrm{PoB(m\ indications)} = 1 - \prod_{k=1}^{m} \left(1 - \mathrm{PoB}_k\right) < \sum_{k=1}^{m} \mathrm{PoB}_k , \tag{9.8}$$

where PoB_k is the probability of burst of the k^{th} indication. In practice, the indications are segregated into crack length bins with all indications in one bin considered to have the length of the upper bound of the bin. Thus, the PoB for all indications in the same bin is the same. By multiple application of equation (9.8), the PoB of one or more of all of the indications in the n bins is,

$$\mathrm{PoB(n\ bins)} < \sum_{i=1}^{n} r_i \, \mathrm{PoB}_i , \tag{9.9}$$

where r_i is the number of indications in bin i and PoB_i is now the probability of burst for an indication in the i^{th} bin.

It is admitted that this practice omits consideration of the uncertainties of the parameters of the regression equation. However, formation of the normalized burst pressures from the test data includes an uncertainty of the material properties of the test specimens. Thus, the variance of an actual P_N about its predicted P_N includes a contribution from the variation of material properties associated with repeated measurements of tensile specimens from the same tube. This, combined with the observation that equation (9.7) always yields conservative results relative to Monte Carlo simulations is judged to outweigh the effect of omitting the uncertainty in the estimate of the coefficients.

9.5 Modelling for Burst Probability with Limited TSP Displacements

One model was considered for the evaluation of the burst probability given the relative displacements of the TSPs during a postulated SLB. This model is based solely on the TSP displacements and estimates the PoB by assuming every intersection to have a throughwall crack equal to the thickness of the TSP. Thus, every intersection is considered to have a throughwall crack exposed by the magnitude of the displacement at each intersection. The prediction of the PoB of a single indication can be estimated using the methods described in the previous section of this report, however, in this case the predicted burst pressure for nominal material would be reduced by [ ]a,c,e, i.e., the value of the t distribution variate would be calculated as,

a,c,e

[ ]

instead of using equation (9.7). This approach implicitly assumes that the standard error of the burst pressure based on performing many tests would be the same as that obtained from the testing of free-span cracks. Given the large database from the fre-span burst tests, this is not an unreasonable assumption. Details and results of the application of the model are discussed in Section 11.0 of this report.

A more realistic estimate of the PoB could be obtained by considering only the estimated number of indications and the spatial distribution of those indications in a steam generator. Furthermore, assessment of the PoB of a tube at SLB conditions for limited TSP displacement only requires an estimate of the probability of a large indication occurring at the corners of the TSP where the TSP displacements are significant. Only plates 3 and 7 have significant TSP displacements such that a burst assessment is appropriate.

Although the flow distribution baffle (FDB, plate 1) has a few TSP intersections with significant displacements, no bobbin indications have been found at the FDB. The FDB in the Model D4 S/Gs has large tube to FDB gaps (nominally [ ]a,c,e diametral clearance toward the center of the plate and [ ]a,c,e with radialized holes for the outer region). Thus, there is a significantly lower likelihood of packed crevices with associated tube corrosion at the FDB intersections. Since no indications at the FDB have been found at either Braidwood 1 or Byron 1, the FDB is not included in the tube burst assessment.

9.6 SLB Leak Rates Based on Assumed Free Span Indications

A discussion of the methods employed to evaluate the leak rate from tubes during a postulated SLB are given in Reference 13.19. A linear model relating the common logarithm of the leak rate from a tube at SLB conditions to the common logarithm of the bobbin amplitude of an ODSCC indication is used. The relationship was developed and verified to be valid in accord with the requirements of the NRC generic letter, Reference 13.2. The use of the model to develop EOC total S/G leak rates by appropriately simulating the parametric uncertainties is also described in Reference 13.19, and are also in accord with the requirements of the NRC generic letter. The data and the results of the analyses are discussed in a later section relative to the potential leak rate from indications at TSP elevations.

9.7 SLB Leak Rate Analyses for Overpressurized Tubes

This section describes the results of a Westinghouse analysis for SLB leak rates from an overpressurized tube which expands within the TSP until the crack face contacts the ID of the TSP drilled hole. The results of these analyses are compared with a NRC sponsored analysis and a recommended leak rate for overpressurized tubes is developed.

Westinghouse Analysis

A tube is assumed to develop a large crack opening within the confines of a tube support plate due to overpressurization of the crack indication. The presence of the tube support will limit the opening and the flow rate which can leak from the opening. It is of interest to determine the maximum flow possible under these circumstances.

For large cracks in the free span, leak mass velocity approaches a limit as the friction and form losses become small. For steam line break, this is the critical or "choked" mass velocity. This limiting mass velocity, Figure 9-4, can be used in conjunction with the minimum area along the leak flow path between the primary and secondary side. The product of the limiting mass velocity and the minimum flow area give the maximum leak rate. By applying the limiting mass velocity developed for large cracks to small cracks, the leak rates for the small cracks are conservatively estimated.

At fixed primary to secondary conditions, the leak rate for a free span crack increases with crack length. The flow rate is proportional to the crack opening area which increases rapidly as a function of crack length. Flow is limited by friction and form losses in the crack flow path. For large cracks these losses become small and the flow per unit crack area, mass velocity, approaches the limiting critical flow value. Figure 9-4 illustrates a plot the mass velocity as a function of crack length, as calculated by CRACKFLO. The figure shows that the values of mass velocity remain below a selected limiting value of G_{max} = [ ]^{a,c,e} lbm/ft^2-sec.

Use of this limiting mass velocity conservatively neglects turning, form and friction losses on the leak flow path. For a crack within a tube support plate, the crack opening is limited. More importantly, the flow path area is restricted by the presence of the tube support plate. This flow path area combined with the maximum mass velocity, [ ]^{a,c,e} lbm/ft^2-sec, sets the maximum leak rate for a crack within a tube support plate.

Figure 9-5 displays the crack configuration which might exist within a tube support, postulating an overpressurization of the crack indication. The tube crack edges are conservatively assumed to contact the tube support only at the center of the crack length, L. For crack lengths long enough to burst at SLB conditions, it would be expected that a significant fraction of the crack face would contact the TSP hold ID and the leak rate would be lower than estimated by this analysis. At the ends of the crack, no tube diameter deformation is assumed, leaving the full diametral clearance, c, open to leak flow. The crack opening area, Figure 9-5, is characterized by a crack opening displacement, COD, and the crack opening area is given by $A_c = L(\mathrm{COD})/2$. The leak flow from this crack, however, must flow into the annular space between the overpressurized tube and the plate tube hole. This flow area, for the flow in one direction from the center point of the crack, is

$$L_b = \left(\frac{G_{max}}{\rho}\right) A_a = \left(\frac{G_{max}}{\rho}\right) cL \tag{9.11}$$

displayed in Figure 9-5. The total flow area into the annulus, twice the flow area displayed, is given by $A_a = cL$. The bounding volumetric flow rate (gpm) is,

[ ]^{a,c,e}

Manufacturing data on hot leg TSP drilled hole diameters were reviewed (Section 9.2) to characterize the hole diameter distribution. These data indicate that the median and average hole diameter is [ ]^{a,c,e} inch resulting in an expected tube to TSP diametral hole clearance of [ ]^{a,c,e} inch. At 95% confidence on manufacturing tolerances on the hole diameter, the diameter is [ ]^{a,c,e} inch. For added margin, an upper bound diametral clearance of [ ]^{a,c,e} inch is applied to obtain the leak rates for the overpressurized indications. The limiting flow rate is plotted in Figure 9-7, as a function of crack length for average and minimum diametral clearance values of [ ]^{a,c,e} inches. For a free span throughwall crack of about 0.55 inch length, the crack opening width is about [ ]^{a,c,e}. Consequently, free span cracks greater than about 0.55 inch long would leak more than the same crack overpressurized within the TSP while overpressurized indications less than about [ ]^{a,c,e} inch long would leak more than the free span indication of the same length.

NRC Analysis for Leak Rate from an Over-Pressurized Tube

As a part of the NRC task team effort reviewing the APC and developing draft NUREG-1477, a conservative estimate (Reference 13.8) of the SLB leak rate from an overpressurized tube was performed. This analysis assumed that the crack opening width was limited by the circumferential expansion of the tube required to fill the TSP hole. This assumption of uniform diametral expansion is not typical of overpressurized cracks which tend to result in fishmouth crack openings and most of the diametral expansion near the crack face. For the uniform diametral expansion assumption, the crack opening area is approximately the crack opening width times the crack length. This NRC model assumes no flow restriction due to the TSP hole geometry and the leak rate as calculated based upon free span leakage with the modified crack opening area. The crack opening area for this model is:

$$A_a = \pi (D_{hole} - D_{tube}) L = \pi c L . \qquad (9.13)$$

where D_{hole} and D_{tube} are the respective diameters of the TSP hole and the outside of the tube. Thus the NRC model, which ignores the flow restriction provided by the TSP hole ID, results in a factor of π larger leak rates than the Westinghouse model described above. The referenced NRC analyses were performed for $\pi c = 0.06$ inches or a hole clearance of about [ ][a,c,e] mils. The NRC SLB leak rates given in Reference 13.8 are slightly more than a factor of π larger than the above Westinghouse results. This may be due to a larger pressure differential assumed in the NRC analyses, differences in computer models for leak rates and/or the NRC results may represent gpm at operating temperature while the Westinghouse results are in gpm at room temperature which is the basis used for calculating the allowable SLB leak rates. It is believed that the Westinghouse model described above provides a more realistic estimate of the bounding leak rate from an over pressurized tube and is applied for the leak rate analyses of this report.

Bounding SLB Leak Rates for Over-Pressurized Indications

This model develops the bounding leak rates as a function of the throughwall crack length while the leak rates as a function of voltage are required for APC applications. A relation between bobbin voltage and throughwall crack length was developed in the EPRI database report of Reference 13.6. The fit to the data of this report was updated to include all pulled tube data for 3/4 inch diameter tubing available through January, 1995. The functional relation and results of the latest regression analysis for the data are:

[ ] a,c,e

where L is the throughwall crack length and V is the bobbin voltage. In fitting the functional relation, V_0 which represents a lower voltage estimate for throughwall penetration was set at [ ]^{a,c,e} volts for the regression analysis. The results of the regression analysis are shown in Figure 9-8 including the mean regression line and the upper/lower 90% confidence limits on the mean correlation.

The lower 90% confidence bound on the Figure 9-8 correlation was used to convert the crack lengths of Figure 9-5 to bobbin voltage and obtain the bounding leak rates for the overpressurized tube condition with a [ ]^{a,c,e} inch diametral clearance as a function of voltage. The resulting bounding leak rates are shown in Figure 9-9 and compared with the free span leak rate correlation. It is seen that bounding leak rate approaches the free span leak rate at higher voltages approaching about 20 volts. It would be expected that the bounding leak rate would be about equal to the mean regression line at about 20 volts which is consistent with the free span leakage exceeding the overpressurized leak rate above about 0.55 inch throughwall cracks.

The bounding leak rate can be represented as a linear curve in logarithmic coordinates as,

[ ]^{a,c,e}

where LR_b is the bounding leak rate in liters per hour. This leak rate formulation is used for the overpressurized indication analysis described in the following section.

9.8 Leak Rate Analysis Methods with Tube Expansion

The aim of expanding selected tubes is to suppress the potential motion of the TSPs during a postulated SLB. This allows the voltage limits of the alternate plugging criteria to increase without increasing the probability of a free-span burst of a tube. However, the probability of occurrence of indications with higher PoBs if they were free-span indications is increased. Thus, even though constrained, the probability of occurrence of indications which could experience increased crack flank deflections, referred to as overpressurization, is increased. Therefore, it is appropriate to modify the prediction methodology to account for the leak rate from potentially overpressurized tubes. The standard APC leak rate prediction methodology is described in detail in Reference 13.19. The modified methodology would consist of the following steps:

1) Simulate the POD, inspection uncertainties and growth of the indications using the methods described in Reference 13.19.

2) For each indication, determine a random exposure of a potential 0.7" long crack at the elevation of the TSP.

3) For each indication, estimate a random burst pressure based on the simulated exposure length, and determine whether or not the crack is overpressurized, i.e., a predicted burst pressure less than the SLB differential pressure.

4) If the crack is not overpressurized, the leak rate is estimated, i.e., simulated as described in Reference 13.19. If the crack is overpressurized, the leak rate is estimated utilizing the results from the previous section of this report, i.e., using the bounding leak rate curve shown on Figure 9-8.

The total leak rate from all of the indications in the S/G is calculated and retained. The 95% confidence bound on the total leak rate would then be found using the ordered array of total leak rates from all of the simulations of the S/G as described in Reference 13.19.

9.9 Potential Structural Limit for Indications at TSP Intersections

For free-span indications, the structural limit that determines tube repair limits is based on satisfying R.G.1.121 margins for burst of a tube. With the limited TSP displacements resulting from the tube expansion process, the constraint of the TSP reduces the tube burst probability to negligible levels (see Section 11) and tube repair limits are not required to prevent tube burst. For the limited TSP displacement and the expected tube degradation, the need for tube repair is dictated by the need to satisfy allowable SLB leakage limits (see Section 12). However, at some level of cellular or IGA corrosion, it becomes possible for the axial loads resulting from the pressure differential across the tube to result in axial tensile severing of the tube. This tensile load requirement establishes the applicable structural limit for tube expansion based on
limited TSP displacement.

Significant IGA depths have not been found for tubes pulled from TSP intersections which have not been plugged for at least two years prior to the tube pull. Even for prior plugged tubes, only Plant L tube R12C8, TSP 1 has been found with significant IGA. Thus, cellular corrosion is the expected crack morphology that might lead to tensile load limits. Conceptually, circumferential cracks could also limit the axial tensile capability of the tube. However, circumferential cracks have not been found at non-dented TSP locations and would not be expected. In addition, the APC of this report would require tube plugging of any tube with a circumferential crack even if it should occur. Therefore, the appropriate structural limit with tube expansion should be based on cellular corrosion.

For conservatism, both cellular and IGA corrosion are evaluated in this section to estimate a lower bound to the structural limit. This lower bound structural limit can be applied to restrict the upper range for tube repair limits until additional data are obtained to refine the structural limit. An assessment of this lower bound structural limit is provided in this section.

Data utilized to support a lower bound structural limit are:

1. Plant E-4 Pulled Tube Tensile Test Results for Cellular Corrosion

   These tensile tests, performed to measure the force required to sever a tube with cellular corrosion patches, are the most direct measurements required to establish a structural limit. These data, available for 9 pulled tubes from Plant E-4, are used to calculate the apparent tube residual cross section (RCS), based on specific tensile strength data developed for these tubes.

2. Pulled Tubes With Measured Uncorroded Tube Cross Section Profiles (Plant E-4 and Plant L)

   For some pulled tubes with cellular and/or IGA tube degradation, the corrosion depths have been measured around the circumference of the tube through the cellular or IGA degradation. Assuming that the degraded depths do not contribute to the axial load capability of the tube, the depth measurements yield the residual cross section directly. For these indications, the tensile capability of the tube can be conservatively calculated from the uncorroded cross-section of the tube, using lower bound material tensile properties.

   For Byron Unit 1 and Braidwood Unit 1, pulled tube data are available for six TSP intersections. The size (angular extent and depth) degraded areas of the TSP intersections were determined in metallographic examination. Conservative estimates were made of the average depth. For these data, the residual cross sections are calculated directly.

   For Plant L, TSP 1, the circumferential depth profile of the degradation was determined in destructive examination for the entire circumference. The RCS for this specimen is thus directly determined. For Plant L, TSP 2 and 3, destructive examination showed a large number (50 and 85, respectively) of axial cracks distributed around the tube circumference. For these sections, the residual cross section was calculated assuming uniform degradation of a depth equal to the average depth of the observed cracks. This is conservative in that the ligaments between the cracks that would contribute to the axial load capability of the tube are neglected.

3. Laboratory IGA Specimens With Known (Measured) IGA Depths

calculated directly as the ratio of the undegraded section to the nominal tube metal cross section.

For the IGA specimens, where specimen specific material tensile properties were not available, the mean tensile strength data of Reference 13.5 was used. Similarly, for the pulled tube TSP constrained burst data, the RCS is calculated as the required section to support the measured burst pressure based on the mean ultimate strength from Reference 13.5. In all cases, nominal tube dimension were assumed.

The available cellular and IGA corrosion data outlined above are summarized on Table 9-2.

Figure 9-8 shows the linear regression fit of the RCS for the Byron 1, Braidwood 1, Plant E-4 and Plant L data for which the RCS can be directly calculated or inferred based on actual measurements. The lower 95% confidence interval for the data fit is also shown, as well as a correction to this lower 95% confidence interval for temperature. The temperature correction applied is the ratio of the 650°F flow stress to the room temperature flow stress of the material as noted in Reference 13.5. The required minimum RCS for $3 \cdot \Delta P_{NO}$ loading shown on Figure 9-8 is based on the LTL flow stress at 650°F. The intersection of the temperature corrected lower 95% confidence limit of the fit with the required minimum RCS indicates an acceptable bobbin voltage structural limit of approximately 37 volts.

Also shown on Figure 9-8, but not included in the data correlation, are the calculated RCS for the available data for IGA degradation and TSP constrained burst tests. Both the IGA data and the burst test data support the correlation of the cellular corrosion data. Significant IGA has not been found in pulled tubes and is thus not considered a credible contributor to a potential failure mode. However, for the available IGA data, Figure 9-9 shows a correlation of the cellular plus IGA corrosion vs bobbin voltage. The resulting correlation, together with confidence limit and temperature correction as described above, is essentially the same as the correlation of only the cellular data. For this combined data correlation, a bobbin voltage limit of 35 volts is indicated.

The TSP constrained burst data provide a conservative lower bound estimate for the structural limit. In these test, axial burst occurred without evidence of circumferential rupture. Within the range of the bobbin voltages of the available indications, the burst test data support the structural limits suggested by Figure 9.9, in that axial tube burst is expected to occur prior to circumferential fracture, and neither axial nor circumferential burst is expected at the $3 \cdot \Delta P_{NO}$ loading condition.

More data are needed to refine an estimate for the pressure differential structural limit. However, the data show that the bobbin voltage for the $3 \cdot \Delta P_{NO}$ structural limit is beyond the range of voltages expected for the tube repair limits of about 10

Laboratory IGA specimens have been prepared with nearly uniform IGA depths. NDE (bobbin coil) data were obtained and the tubes were destructively examined to obtain the depths and therefore, the residual tube cross section. For these specimens, the tensile load capability can be adequately and conservatively calculated from the uncorroded cross section of the tube, assuming LTL material properties.

4. Laboratory IGA Specimens Not Destructively Examined

Some IGA specimens have been prepared as NDE library samples which have not been destructively examined. From IGA specimens prepared at the same time, although without NDE data, it was shown that the specimens were prepared with reasonably uniform IGA depths. Depths can be estimated from the NDE data. The residual cross section was conservatively estimated assuming uniform circumferential degradation at the maximum depth estimated from the NDE data plus a 5% uncertainty factor.

Although this group of data is less reliable than items 1 to 3 above, these data are included for comparison purposes.

5. Pulled Tubes for Burst Test for Indications Within TSPs

Although pulled tubes that were burst tested with TSP constraint do not provide a direct estimate of tube axial load capability, they provide a conservative lower bound estimate of that capability. Since the tubes burst axially and include the axial pressure loads, it is clear that the axial load capability is greater than the burst pressure. These tubes, some of which have indications greater than 30 volts (bobbin) were subjected to internal pressure well in excess of the required $3 \cdot \Delta P_{NO}$ pressure. In all cases, the tubes burst without evidence of axial separation. In two cases, the tubes burst in the freespan outside the TSP constraint. Relevant pulled tube data are available from Plants E-4, J-1, P-1 and D-2.

The approach to developing a structural limit for cellular corrosion is to compare a correlation of the residual strength of tubes from items 1 and 2 above, expressed as a residual undegraded metal cross section vs. bobbin voltage, with the minimum metal cross section required for $3 \cdot \Delta P_{NO}$ loading at temperature, assuming that the tube is laterally constrained. The assumption of lateral constraint is reasonable since the degradation mechanism, cellular corrosion, occurs within the span of the TSP.

For the Plant E-4 tensile specimens (open symbol in Figure 9-8), for which tube specific material ultimate strength and fracture loads are available, the residual cross sections (RCS) are the ratio of the fracture load to the measured ultimate strength. For the pulled tube specimens with measured cross sections, the RCS is

Table 9-1: Burst Pressure as a Function of Crack Length
and Crack Extension Outside of the TSP
Series 1

a,c,e

to 15 volts, and may exceed 35 volts. Thus, structural limits are not likely to be required for APCs based on tube expansion.

With application of the progressively increasing tube repair limits with implementation of tube expansion, axial tensile tests of pulled tube indications will be included in the destructive examination program. The destructive exams would include free-span burst testing followed by an axial tensile test of the indication and fractography for both the burst crack and the tensile break face to define corrosion depth versus length. Fractography would include the depth profile for cellular and IGA corrosion since the axial cracks would not sufficiently influence the axial load capability of the indication.

With the data of Figure 9-8 supporting very high structural limits and a progressively increasing data base from pulled tube results as the repair limits increase, updates to Figure 9-8 can be expected to demonstrate axial load capability much higher than any expected EOC degradation. This progressive approach will demonstrate that structural considerations, as contrasted to leakage considerations, do not limit the tube repair limits with tube expansion.

9.10 Conclusions

A conservative estimate of the probability of burst of one or more indications in a S/G during a postulated SLB event indicates a likelihood of burst less than that required in the NRC's draft Generic Letter on Alternate Plugging Criteria for tube ODSCC indications at the elevations of the TSPs. Consideration of the aggregate of the largest individual indications in the Braidwood 1 and Byron 1 S/Gs results in an expected probability of burst of one or more tubes at either plant of approximately five and three orders of magnitude less than the requirement of the draft Generic Letter respectively.

Table 9-3
Summary of Cellular/IGA Corrosion Data

a,c,e

IGADATA.XLSTbl9

Table 9-2: Burst Pressure as a Function of Crack Length
and Crack Extension Outside of the TSP
Series 2

a,c,e

Figure 9-2: Burst Pressure vs Crack Length for Probability of Burst
3/4" x 0.043", Alloy 600 MA SG Tubes, Average Material @ 650°F

Burst Pressure (ksi)

Crack or Exposure Length (inch)

a,c,e

Figure 9-1: Burst Pressure vs. Crack Length

3/4" x 0.043", Alloy 600 MA SG Tubes, σ_f = 71.6 ksi

Burst Pressure (ksi)

Axial Crack Length (inch)

a,c,e

[PBRVSLAM.XLS] 34.Tubes

RFK: 2/6/95, 9:52 AM

Figure 9.4. Mass Velocity for Large Cracks

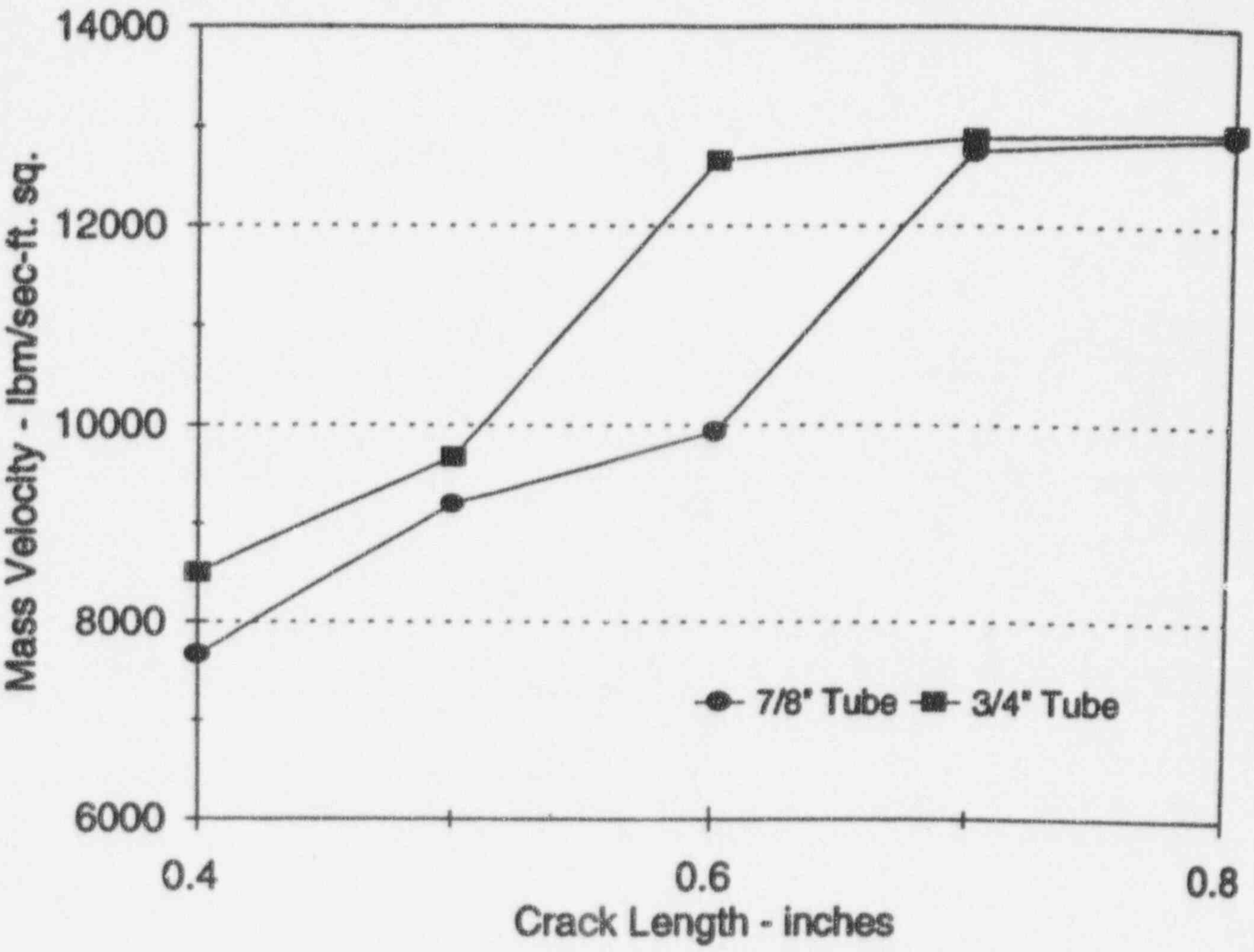

Figure 9-3: Effect of TSP Clearance on the Probability of Burst
3/4" x 0.043", Alloy 600 MA Steam Generator Tubes

a,c,e

Probability of Burst

Crack Length or Exposure (inch)

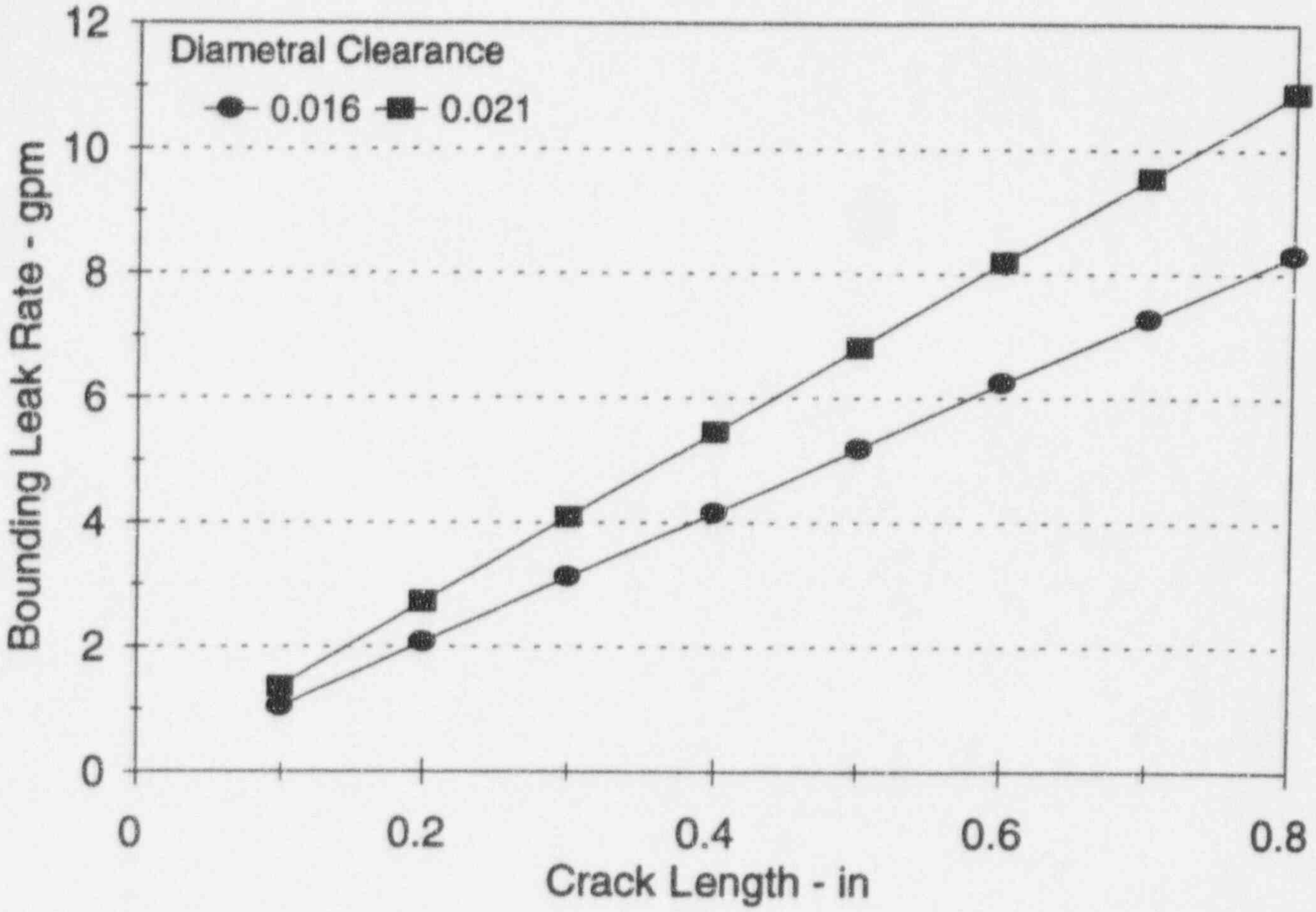

Figure 9-6. Bounding Leak Rate vs. Through Wall Crack Length

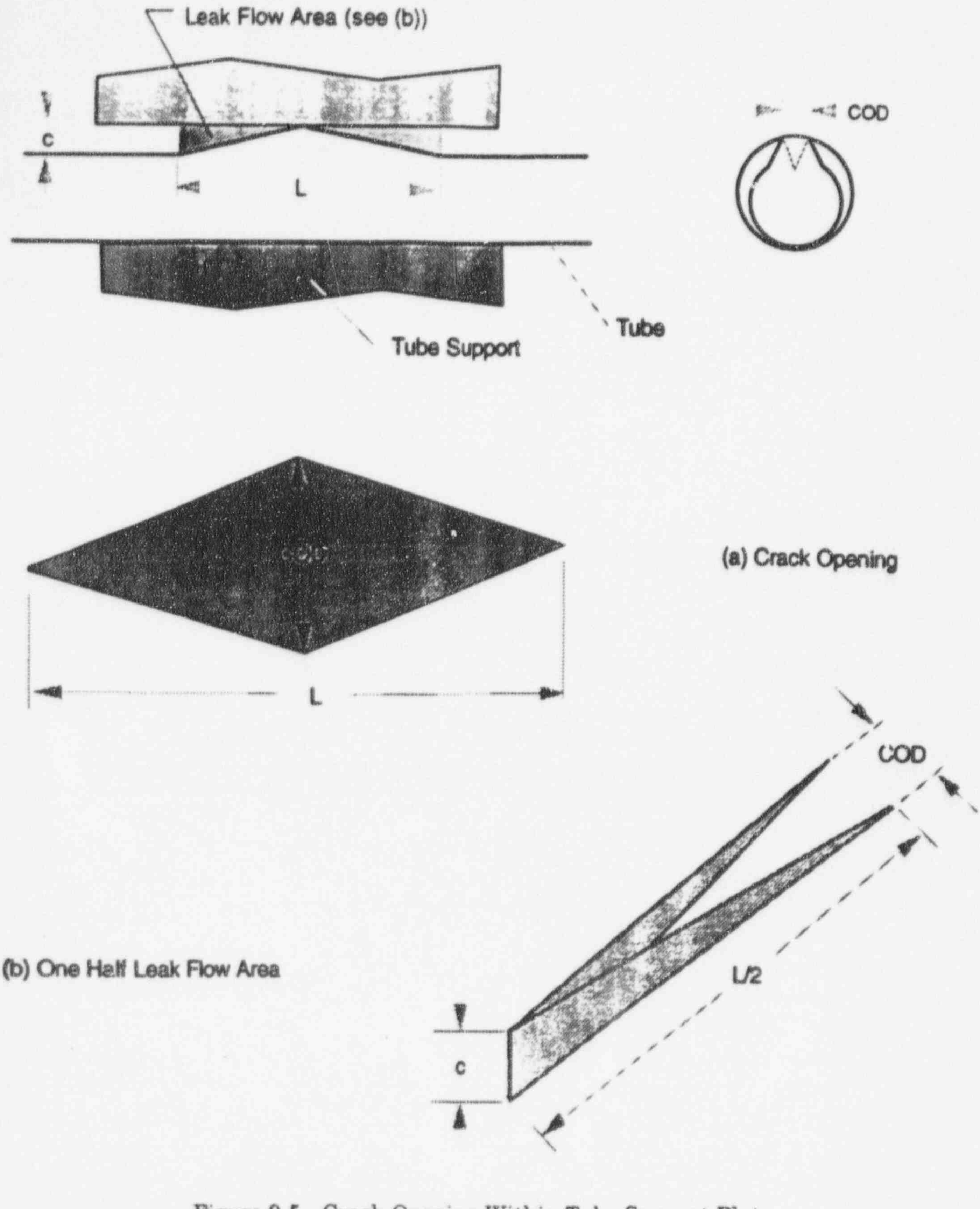

Figure 9-5. Crack Opening Within Tube Support Plate

Figure 9-8: SLB Leak Rate vs. Bobbin Amplitude
3/4" x 0.043" Alloy 600 SG Tubes @ 650°F, ΔP = 2560 psi

SLB Leak Rate @ 2560 psi (l/hr)

Bobbin Amplitude (Volts)

a,c,e

[34QV_TSP.XLS] QvsV.Bound

RFK: 1/29/95, 3:48 PM

Figure 9-7: Correlation of Bobbin Volts to Throughwall Crack Length

Bobbin Amplitude (Volts)

Throughwall Crack Length (inch)

a,c,e

[V-TWCORD.XLS] VvsL.Plot

RFK: 2/6/95, 7:10 PM

Figure 9-10
Residual Strength of Tubes with Cellular and IGA Corrosion

Residual Tube Cross Section (%)

Bobbin Volts

a,c,e

Ch-SummryIGADATA.XLS

Figure 9-9
Residual Strength of Tubes with Cellular Corrosion
(Data Fit Excludes IGA and Burst Data)

Residual Tube Cross Section (%)

Bobbin Volts

a,c,e

Ch-Sumry2IGADATA.XLS

10.0 TUBE EXPANSION PROCESS AND TEST/ANALYSIS SUPPORT

Since the TSPs do not undergo any displacement relative to indications developed within the TSPs during normal operation, tube burst at these locations is unrealistic so the burst capability requirement of three times the normal operating differential pressure is obviated by the presence of the TSP. Thus, the RG 1.121 requirement relative to $3 \cdot \Delta P_{NO}$ is inherently met. If the TSPs did not undergo displacements during a postulated SLB event, the same would be true of the RG 1.121 requirement relative to $1.43 \cdot \Delta P_{SLB}$. However, the TSPs are subjected to significant out-of-plane loads during a SLB and TSP displacements are predicted to occur at locations relatively remote from the stayrods and remote from TSP supports (wedges, support bars) at the edges of the plate. To minimize the potential for tube burst and for significant tube leakage, a modification to the S/Gs is performed to limit TSP displacements to insignificant levels. A selected number of tubes on the hot leg side of the S/G will be expanded with sleeves installed for tube stabilization and added stiffness at the elevations of the TSPs. The sleeves and the tubes will be expanded adjacent to the top and bottom sides of the plate to a diameter larger than the tube holes in the TSP. This essentially converts the tube into a stayrod, and significantly restricts the potential out-of-plane motion of the TSPs. A description of the design and testing of the expansion process is provided in this section, along with a discussion of the potential effects of the process and limitations with regard to application.

10.1 Tube Expansion Process Requirements

The fundamental requirement of the modification is to restrict TSP motion to a level that results in a non-significant probability of burst (POB) during a postulated SLB event. The modification design to accomplish this consists of expanding the tube, with an internal sleeve installed, into an hourglass shape at the elevations of the TSPs, such that the TSP is captured by the tube/sleeve combination. This is illustrated on Figure 10-1.

The overall requirements for the application of tube expansion are summarized in Section 12.0 and Table 12-2 of this report. If TSP motion is restricted to less than or equal to 0.31" during a postulated SLB, the probability of burst will be less than 10^{-5} under the assumption that all tubes have throughwall indications at all of the hot leg TSP intersections. If the motion is further restricted to less than or equal to 0.1", the likely probability of burst is estimated to be less than 10^{-10}. Under this second restriction, the leakage from cracked tubes would be expected to be significantly reduced relative to the free-span rates currently employed for alternate plugging criteria applications. An implicit requirement of the modification is that the integrity of the expansions must be such that they perform their intended function after long periods of exposure to the secondary side environment. A sleeve is expanded with the parent tube expansion to function as a tube stabilizer (prevent potential damage to adjacent tube assuming a tube is severed at the expansion) and to increase the stiffness of the combined parent tube/sleeve expansion against TSP displacement. A feature of the current design is that the tube being expanded will be removed from service by plugging, hence there will be no exposure to primary water unless the tube selected for expansion has a throughwall defect at the time of the tube expansion/plugging.

The results of the thermal/hydraulic and structural analyses described in previous sections of this report, coupled with conservative bounds on those results, have led to the following requirements.

1) The stiffness of the expansion shall be such that the TSP will experience resistance to motion of [ ].^{a,b,c} The associated stiffness of the expansion relative to plate motion shall be]^{a,b,c} when averaged over the initial 0.20 inch of TSP displacement as determined by TSP pull force versus displacement tests on expanded joints.

2) The stiffness of the expansion shall be such that the TSP will experience resistance to motion of [ ].^{a,b,c}

3) The expansion shall be performed above and below the TSP by a hydraulic expansion process with a sleeve stabilizer installed at and above/below the parent tube expansion.

4) The expansion process shall be designed to achieve maximum expanded tube diametral increases of less than or equal to [ ]^{a,b,c} mils when applied over the expected range of material properties and TSP conditions. This limit on the expansion diameter is a design goal to limit residual stresses in the expanded tube but does not represent an unacceptable diameter for field implementation.

In order to provide a sufficient level of axial load resistive capability at each expanded intersection, the resistive level of [ ]^{a,b,c} of TSP motion was established. This value was established based on a dynamic evaluation of the Model D4 TSPs during a postulated SLB. At this relative stiffness level, [ ]^{a,b,c}, the tubes identified in Section 8 will effectively prevent the TSP from deflecting more than 0.1 inch during the blowdown phase of the event. The tube stiffness requirement applies at operating temperatures. When adjusted for operating temperatures, the room temperature test requirement is a pull force capability of [.]^{a,b,c} Additionally, the program had to result in sufficiently small tube OD changes such that the residual tube stresses between expansions do not represent a short term stress corrosion cracking concern.

Testing of the design modification has demonstrated this capability as described in the following sections.

10.2 Tube Expansion Process Description

The tube expansion process is performed using existing Westinghouse 3/4 inch tube sleeving hydraulic expansion equipment and a modified sleeve delivery mandrel. The expansion is generated by supplying high pressure water to an expansion mandrel/bladder system. The same length bladder, [ ],[a,c] used for sleeve expansion in the laser welded sleeving system is used for the tube expansion process. In order to increase the radial stiffness of the tube and therefore increase the resistive load capabilities of the expansion, a surrogate sleeve is used. This sleeve also provides tube stabilization under the assumption of a severed parent tube at the expansion. An integral eddy current coil senses the edge of the TSP and the tool automatically strokes into the installation/expansion position. The sleeve delivery mandrel has been modified to adequately position the [ ].[a,c] For development testing purposes the tubes, sleeves, and TSP collars were manually positioned. The sleeve sections used were actual TSP laser welded sleeves cut to an overall length of approximately [ ].[a,c] The sleeve OD was [ ].[a,b,c]

Based on the tests performed, a maximum expansion pressure of [ ][a,b,c] was established. This pressure is applied to the ID surface of the expansion bladder. For the heats of tube material used, this expansion pressure results in a maximum tube OD change of approximately [ ].[a,b,c] The low yield strength heat of tube material used are approximately equal to the expected lower bound of 3/4 inch tube heats while the high yield strength tube heat used is approximately 10% larger in yield strength than the expected upper bound of Braidwood-1 tube yield strengths. As the test results will show, there is a relationship between tube OD change, tube flow stress and resistive force capability of the expansion.

The tube expansion process uses computer control to develop the desired tube OD changes, and is independent of tubing yield strength. The computer control [

]^{a,c} A typical expansion curve is provided in Figure 10-2.

As shown in Section 10.6, there is a negligible potential for circumferential cracking in the hydraulic expanded tubes in the plugged tube condition. Even with this low potential for circumferential cracking, additional design margins for allowances for cracking have been included in the design process. Sleeves expanded with the tube provide tube stabilization under the postulate of a severed tube and permit the expansion to perform its intended function at the lower TSP elevations with downward loads on the TSPs even if the tube becomes severed at the expansion. In addition, redundant tube expansions have been included in the expansion matrix to accommodate postulated severed expansions. Based on these design margins, there is no need for heat treatment of the expansions to further reduce the potential for circumferential indications at the expansions.

TSP intersections with axial ODSCC indications can be expanded since axial cracking does not affect the expanded joint stiffness. The expansion process results in an overpressurization of the pre-existing indication within the confines of the TSP. The expansion process expands the tube to close the tube to TSP crevice, which can result in opening the crack face by up to the tube to TSP diametral clearance. The actual opening of the crack face is also a function of the thinning of the tube wall from the expansion process. Some degree of tearing at the crack tips to extend the crack length may occur from the expansion process. Burst tests for indications within the TSP generally show little or no crack extension and similar results can be expected from the tube expansion process. Even if crack tearing should occur at pre-existing axial indications and extend outside the TSP, the axial indications would not significantly affect the stiffness of the expansion for resisting axial displacement of the TSP. Thus, pre-existing ODSCC is acceptable at TSP intersections selected for expansion and would not significantly affect the functional cabability of the expansion. From an expansion process efficiency consideration, the simultaneous expansion of the sleeve and bladder prevents premature failure of the bladder as the crack opens up within the TSP. Without the sleeve, the bladder can extrude through the crack opening and rupture prior to achieving an acceptable expansion, similar to that occurring in tube burst tests without a foil insert.

10.3 Tube Expansion Process Test and Analysis Results

10.3.1 Tube Expansion Process Test Results

Test specimens were prepared at various expansion pressures to establish a relationship between expansion pressure and projected tube OD and also to establish a relationship between tube OD and resistive load capability at varying TSP deflection levels.

Test specimens used [ ]a,c in addition to TSP collar simulants with ID dimensions considered to conservatively represent the upper bound for TSP holes. Testing has shown the TSP hole diameter has an effect upon resistive load capacity. The center of the TSP collar was located approximately 3 inches from the end of the tube, and the end of the sleeve and tube end were coincident. Expansions were performed at various maximum pressure levels, and from these expansion curves, [ ].a,c Tubes and sleeves were expanded into TSP collar simulants manufactured from carbon steel. Two sets of TSP collar simulants were used; one with the ID representative of a slightly oversized non-packed crevice, and the other representative of packed crevices. The reason for using the two different ID sizes was to determine if the crevice condition had an effect upon the resultant expansion diameters. The TSP collar OD dimension was determined based on a finite element analysis of the TSP. Using this analysis, a collar OD dimension of [ ]a,c was established. This OD dimension will result in a TSP collar simulant with approximately the same radial stiffness as the actual TSP. During testing the OD dimensions of some of the TSP simulant collars was measured and recorded. No change in collar OD dimension was detectable after expansion. Therefore, it can be concluded that the expansion process will not affect the integrity of the TSP or result in localized yielding of the TSP in the direction of the flow holes, which represents the minimum ligament dimension, [ ]a,b,c. Additionally, [

]a,b,c A prototypic expansion was also performed in a TSP section which included the tube hole to be expanded, surrounding flow holes and adjacent tube holes. The hole patterns were produced for two complete pitches around the tube hole being expanded. The pre-expansion diameters of the adjacent tube and flow holes on perpendicular axes were recorded. One axis was inline with the minimum ligament dimension, the other was perpendicular to this axis. After expansion, no detectable diameter change was recorded. Therefore, the conclusion can be made that the diameter of the TSP simulant collars were infact representative of the actual TSP radial stiffness.

Test specimens were mechanically tested in a MTS® 55 Kip tensile testing machine. The bottom of the tube was inserted into an outside diameter gripping fixture. At the specimen top, a steel plate with a clearance hole in the center was positioned immediately below the TSP collar. This plate was mechanically coupled to a similar plate using 1.00 inch rods. The upper fixture plate was attached to the load cell of the testing machine. Total system displacement was plotted versus load for each specimen. System displacement feedback is provided by a linear displacement transducer located in the movable machine base. As will be discussed later, these displacement values are conservative in that the displacement feedback represents total system displacement, which includes the actual TSP collar displacement and any test rig elasticity/slippage.

The test sequence involved fine adjustment of the stroke control to a "touch" condition with the TSP collar to reduce any fitup conditions which could adversely affect the test results (i.e., loose threaded connections in the test rig, etc.). The machine was then activated in a stroke control mode at a rate of 0.5 inch/second. The resistive load developed by the interaction between the TSP collar and tube expansion was recorded by the load cell. Testing was also performed at a rate of 1 inch/second using 7/8 inch specimens from a similar program for 7/8 inch tubing; results indicate no difference in the resistive load capabilities for similar sized expansions and it was then concluded that the testing rate of 0.5 inch/second was adequate to appropriately model the TSP response during a postulated SLB event. Similar conclusions were also developed for the 7/8 inch specimens tested with [ ]^{a,c} wall thickness sleeve sections in the bladder area.

Force versus tube OD change curves (bulge size) were established for 3/4 inch OD specimens at displacement values of 1/8 inch, 1/4 inch, and 3/8 inch. A sample of these curves is given on Figure 10-3. As shown in this figure, an expansion of approximately [

]^{a,b,c} should be adequate to bound all field tube heats, since this value corresponds to a tube yield of 73 Ksi. These bulge sizes also meet the 3,500 lb_f requirement at 3/8 inch deflection. It should be noted that based on the expansion process development efforts, actual bulge sizes in the tubes were several mils larger than the minimum values listed above. Therefore, margin will inherently be provided if nominal sized bulges (based on the computer control expansion program) are achieved.

The elasticity of the test fixture, which produced about 0.01 to 0.02 inches of deflection over the pull force range and slippage of the grips during pull are not subtracted from the pull force curves, thereby adding conservatism to the force-deflection curves. The grips are a three piece construction. The body of the grips has an 8.5° taper which mates to the gripper jaw. As the grip body is pulled downwards, slippage between the grip body and jaw produces a transverse movement of the gripper jaws. The forces developed then cause the jaws to bite into the tube wall. Estimated depth of the jaw bite was up to 0.005 inch. At this bite depth, about 0.033 inch of relative motion between the jaw and grip are required. Since the deflection plotted on the force-deflection curves represents total machine motion, the deflection of the test rig, slippage of the grips, and actual motion of the collar are all included in the deflection response. Some pull force curves showed a noted "slippage" in the 250 to 500 lb range. This slippage, which nominally represents about 1/32 inch, is believed to be activation of the grips, producing the bite into the tube wall by the gripper jaws. Not removing the combined test rig deflection and gripper slippage (up to about 0.05 inch) provides a large conservatism in the force-deflection curve. As stated previously, these error points are not eliminated from the calculation of the expanded joint stiffness, which results in significant conservatism in process verification that the joint stiffness requirements are satisfied. If the force values from the curves are examined at an additional 0.05 inch of total deflection past 1/8 inch, which could represent a true TSP collar deflection of 1/8 inch since the measured deflection represents total machine motion, the force values are about 10 to 20% larger. Therefore, there is a margin built into the force vs. bulge size relationship due to not eliminating the system elasticities and slippage noted above. Note that the TSP dynamic displacement analysis assumes all expanded tubes provide only the minimum acceptable stiffness of [ ][a,c]. The relationship between bulge size and resistive load capacity at 1/8 inch TSP deflection for low and high yield strength tubing is provided in Figure 10-4. It is seen from this figure that expansion diametral increases of [ ][a,b,c] provide the required room temperature pull force capability of [ ][a,c] at 1/8". The discussion regarding field measurement of expansion I.D.s and relation to tube material yield strength is furnished in Section 10.4.3.

A subset of pull force was selectively removed from the data base. In these specimens exceptionally large pull forces were evidenced, and in some case, the tube failed in tension at about 10,000 lb_f. Apparently a small machining burr was left at the edge of the collar after chamfering. The effect of this burr was to act as a dull cutting tool, and paper thin sections of tube were actually sheared from the tube O.D. during the pull testing. Pull force values for these specimens is approximately 25% to 50% higher than other specimens over the first 1/8 inch of displacement, and therefore removed from the data base. The effects of the burr were most pronounced at larger displacement values. Instead of the resistive load peaking at about 1/2 inch displacement and dropping as the collar is pulled over the bulge, the load continued to escalate rapidly. The effect of including these points would be to support a smaller minimum bulge size. However, the existence of this burr in the field cannot be verified, so it was not included in the analysis.

10.3.2 TSP Stresses Produced by Tube Expansion

A finite element analysis has been performed to determine the effect of tube expansion on the tube support plates. The basic finite element model is shown in Figure 10-5. Included in this model is a quarter-symmetric section of the TSP next to the expanded sleeve and tube, along with dented tubes in the holes adjacent to the expanded tube. The elements representing the dented tubes can be selectively deactivated to remove them from consideration when desired. The finite element model has been used, with appropriate modifications, to determine the stresses produced in the TSP by tube expansion, the minimum ligament permitted adjacent to the expanded tube, and the maximum dent size for TSP integrity considerations. The analyses with this model for the maximum dent size for tube integrity considerations are given in Section 10.7.

During the tube expansion process, the TSP is not loaded until the tube O.D. has expanded to reach the hole I.D. Up to the point of contact, the expansion pressure is used to first expand the sleeve, and then the sleeve and tube. Subsequent to contact between the tube and TSP, part of the additional pressure further expands the sleeve and tube, with the rest acting on the TSP hole I.D. Since both the sleeve and tube are deforming plastically at this stage of the expansion, their material properties must be adjusted to provide the proper resistance to additional expansion. The expansion tests provide the data needed to determine the effective stiffness of the sleeve and tube when they are in contact with the TSP.

Inflection points in the pressure vs time curve of the expansion process indicate the pressure when the sleeve contacts the tube, when the tube starts to deform plastically, and when the tube contacts the TSP. Assuming that the tube deforms plastically from its initial contact with the sleeve yields a conservative value for the effective radial stiffness of the combined sleeve and tube. Taking the data for specimen 34HE006 gives:

$$\frac{\Delta P}{\Delta R} = \frac{(17{,}200 - 14{,}800)}{(0.387 - 0.37565)} = 211{,}454 \text{ psi/in} \qquad (10.1)$$

Standard thick cylinder equations for deformation caused by internal pressure may be used to calculate an effective elastic modulus corresponding to this stiffness:

$$R = Pc\left[\frac{2b^2}{(c^2 - b^2)}\right]\frac{1}{E_{equiv}}, \tag{10.2}$$

or,

$$E_{equiv} = c\left[\frac{2b^2}{(c^2 - b^2)}\right]\frac{P}{R}, \tag{10.3}$$

where: E_{equiv} = Effective elastic modulus of sleeve and tube,
b = Inside radius of the tube, and
c = Outside radius of the tube.

The resulting effective modulus for the sleeve and tube is:

$$E_{equiv} = 559{,}183 \text{ psi}$$

Figure 10-6 shows an enlargement of a section of the finite element model, along with the boundary conditions and coupled nodes for tube expansion with no denting. Note that the dented tubes of Figure 10-5 have been deactivated. The pressure acting on the I.D. of the sleeve is 4000 psi, which represents the pressure increase in the expansion test for specimen 34HE006 between contact with the TSP and the end of the test.

The stress intensity contours of the region next to the expanded tube are shown in Figure 10-7. The peak stress intensity in the TSP caused by the tube expansion is 19.41 ksi, which is well below the 30 ksi minimum yield strength of the TSP.

Denting of tubes in adjacent holes is simulated by imposing a thermal expansion of the tubes relative to the TSP equal to the size of the dent. The largest operating plant TSP dent for which profile data were available had a 15.4 diametral dent. The combination of coefficient of thermal expansion and temperature to achieve a thermal expansion equal to this dent was assigned to the materials representing the dented tubes. The effective stiffness of the dented tubes was determined using a procedure similar to that above for the expanded sleeve and tube. An inelastic analysis of tube expansion under internal radial pressure was performed to obtain the relationship between pressure and radial expansion. The data bracketing the dent size was used to determine P/R. Since the tube will be acted on by external pressure, the expression for the equivalent elastic modulus is given by:

$$E_{equiv} = c\left[\frac{(c^2 + b^2)}{(c^2 - b^2)}\right]\frac{-P}{R}, \tag{10.4}$$

which results in:

$$E_{equiv} = 508{,}398 \text{ psi}$$

Four denting combinations were considered. These were:

1. All eight tubes adjacent to the expanded tube.
2. The four adjacent tubes in the pitch direction.
3. The four adjacent tubes in the diagonal direction.
4. Two adjacent tubes in the pitch direction.

The maximum stress intensities along each of the four ligaments near the expanded tube identified in Figure 10-8 are listed in Table 10-1 for the undented and dented cases. The stress intensity contours for the maximum of these cases, case 3, are shown in Figures 10-9. As can be seen, the presence of dented tubes adjacent to the expanded tube has only a minor effect on the maximum stress intensity in the TSP.

10.3.3 Minimum TSP Ligament for Tube Expansion

The finite element model of Figure 10-5 was modified to reduce the size of the ligament between the expanded tube and the flow hole (ligament 1) in order to determine the minimum ligament that could be subjected to tube expansion without exceeding the yield strength of the TSP. Instead of a nominal ligament of 0.11 inch, the ligament in this model was 0.0723 inch, achieved by moving the flow hole closer to the expanded tube. The rest of the model was unchanged.

The stress intensity contours throughout the region next to the expanded tube for this case are given in Figure 10-10. The peak stress intensity in the TSP caused by the tube expansion is 29.60 ksi, which is slightly below the 30 ksi minimum yield strength of the TSP.

This case did not consider denting. If denting were present, the minimum ligament size would have to be increased by approximately five per cent. Therefore, tube expansion may be performed as long as the minimum ligament size adjacent to the tube is greater than 0.075 inch.

10.4 NDE Support for Tube Expansion

The expanded tubes will be inspected following application of the process to verify that the expansion, or bulge, sizes have been achieved. If the expansion size has not been achieved, one option is to attempt the expansion again. Due to tooling limitations, this may only be attempted if the expansion is small both above and below the TSP. Post-process diameter verification of the expansions is required to ensure that the maximum stiffness requirements are provided. A standard bobbin coil will be used to determine the mean diameter of the expansion maxima (above and below the TSP). If the minimum diameter requirements are not achieved, additional tubes will be expanded. This section describes the application of bobbin coil profilometry to measure the expansion diameters and the comparison of the eddy current measurements with direct measurements of the expansions.

10.4.1 Principles of Bobbin Profilometry

Eddy current bobbin profilometry has been commonly used for expansion verification in the nuclear industry. Typical applications have been to measure the expansion diameter and placement for full-depth expanded tube sheets and the hydraulic and hard roll expansion diameters for sleeves in steam generator tubing.

The technique involves the use of a bobbin coil probe excited in differential and absolute modes at multiple frequencies, typically ranging from 10 kHz to 630 kHz. The lowest frequency penetrates outside of the sleeved tube and is used for steam generator landmark detection. The highest frequency has a very shallow depth of penetration and is used for the measurement of the diameter of the expansion. The bobbin probe integrates the signal response about the circumference of the tube and yields a mean diameter measurement at a given axial location.

For the profiling of the tube diameter, the absolute mode of excitation is used. The absolute mode of excitation shows a change in the operating point of the probe as the diameter changes. At high frequencies this 'fill factor' effect is reasonably linear over fairly wide ranges and can be used to establish a relationship between tube inner diameter and the change in operating point of the coil. A standard with expansions of known diameter is used to construct a calibration table which relates the diameter of the tube to the voltage of the eddy current response. Figure 10-11 shows a typical sleeve expansion standard with both hydraulic and hard rolled expansions. The calibration standard for this process will have expansions of diameters which are close to the expected process result in order to achieve the most accurate measurement possible. Figure 10-12 shows the profile of a tube with multiple expansions at tube supports.

10.4.2 Verification of Test Sample Diameters

Expansion samples were tested using a bobbin probe to measure expansion diameters. Profilometry calibrations were performed using an expansion sample. A profilometry calibration was performed using known expansion minimum and maximum calculated values. This calibration was then used to measure the remaining expansions.

Since the bobbin probe measures the I.D. of the sleeve, it is necessary to establish the difference between the expansion O.D. and the sleeve I.D. Calculations of the wall thickness in the expansion maxima (based on strain) were performed to be subtracted from the measured outer diameters for the samples in order to achieve expected final inner diameter measurements. Table 10-2 shows the actual and calculated I.D's for ten locations. The calculated I.D.'s average 0.001" greater than the measured values. The calculated I.D. measurements are in excellent agreement with the actual values. This demonstrates that the expected I.D. may be calculated using the strain achieved during the expansion process.

Tables 10-3 and 10-4 shows the results of the evaluation of the expansions for both 7/8 and 3/4 inch diameter tubing along with the calculated bulge I.D.'s based on the O.D. measurements and the expansion strain. These tables show that the eddy current measurement of the inner diameter, on the average, meets the expected value within ± 0.002" (range -0.0051" to +0.0038"). This uncertainty on the bobbin profilometry results is acceptable and no adjustments are necessary to the bobbin data for field process applications. This shows that the tube I.D. can be reliably measured using eddy current methods. This measurement coupled with the knowledge of the strain experienced during the expansion process can be used to verify that the O.D of the bulge falls within the desired process range.

10.4.3 Field Application of Eddy Current Diameter Verification

As stated previously, the expansion I.D. dimensions will be established for each field expansion. Since the pull force testing has established a relationship between material flow stress, bulge size and available resistive load capacity, acceptance of field expansions will involve estimation of material yield strength from the expansion curve, and verification of minimum acceptable bulge size for that material yield strength estimation. Expansion profile curves indicate a noted difference in combined tube/sleeve yield point. Based upon the value of this pressure value, the tube yield point will be estimated. Typical expansion curves for the high yield heat used show a tube/sleeve yield point of approximately [ ][a,b,c] while the corresponding value for low yield tubing was found to be approximately [ ][a,b,c]. Since the sleeves used for testing were all manufactured from the same heat of material, their relatively yield point will remain constant, and a relationship can be developed between the available test data to adequately determine tube yield in the field.

Based on the excellent correlation between calculated and mechanically measured expansion I.D.s, a similar calculation can be performed to establish the resultant tube O.D. Comparison of calculated and mechanically measured specimen I.D.s showed that in most cases the difference between the two values was less than 0.001 inch. Since the sleeves to be used in the field will each have an individual serial number, accurate calculation of sleeve hoop strain can be performed, and the tube O.D. calculated using both the measured tube I.D. from the eddy current trace and an assumed wall thickness of 0.043 inch.

10.4.4 NDE Capability for Assessing TSP Integrity

Although the assessments of Sections 10.3 and 10.7 indicate that TSP integrity will be maintained with tube expansion in S/Gs that are not heavily dented, an evaluation was made of the NDE capability to inspect the TSP for integrity considerations such as cracked ligaments. This inspection would utilize low frequency (10kHz) bobbin data to examine for responses typical of cracked TSP ligaments with or without the presence of magnetite. Laboratory tests were performed to evaluate bobbin probe capability for inspecting the TSPs. To assess this bobbin probe capability, the following tube/TSP configurations were manufactured:

1. As-built nominal tube holes with no simulated cracks

2. Tube holes with slotted ligaments including 100% over the full TSP thickness and 100% over half the TSP thickness

A comparison of the low frequency responses from these mockups with those obtained from Braidwood-1 TSP intersections was performed to assess the ability to distinguish the slotted ligaments from as built, undegraded holes and typical field TSP responses. Data from a mid-range bobbin probe was collected at 10 kHz and at 130 or 150 kHz. At these frequencies, the presence of significant disruptions in the azimuthal continuity of the carbon steel bore surrounding the tube were not easily distinquished from the normal hole response. By comparison with the response of the as-built or normal hole (Figure 10-13 upper), it was possible to discriminate the presence of two half TSP thickness slots (Figure 10-13 lower), but the single full length 100% slot (Figure 10-14 lower) was easy to confuse with the as-built TSP. When field bobbin data from expansion candidate intersections were reviewed at 10 kHz or 130 kHz, it was observed that one of the normal TSP exit lobes on the ASME standard (Figure 10-14 upper) produced signatures very similar to those produced by the half TSP thickness slots. Moreover, the typical TSP signatures in the field data (Figure 10-15) all exhibited the asymmetric features observed for the field standard and the half thickness slots. It is not clear whether or not the field TSP responses were influenced by magnetite although the responses are comparable to that obtained with the ASME standard without magnetite. If the bobbin inspection for cracked TSP ligaments had proven more feasible, the influence of magnetite in the crevice would also have to be evaluated.

At very low frequencies, the tube is essentially transparent to the eddy current signals and even dents or tube cracks would not be expected to seriously interfere with the TSP response. However, given the lack of discriminability described above, it is concluded that the normal mid-range bobbin probes used for IPC inspections will not provide a reliable NDE technique to detect cracked ligaments at the expansion candidate intersections. Therefore, an eddy current inspection for TSP integrity is not recommended for selecting candidate tubes for expansion.

10.5 Tube Stabilization with an Expanded Sleeve

Should circumferential cracking of the tube be postulated to occur in the original tube, sufficient restraint is provided by the sleeve. If it is postulated that a crack forms at the top edge of the TSP, the interaction between the tube and sleeve in the expanded area provide for a rigid interaction point. Expanded specimens cut apart in the expansion region indicate intimate contact between the tube and sleeve. The expanded sleeve provides a relatively rigid structure with the tube even if it is assumed that the tube is severed at the upper edge of the bulge. The tube at this point still acts as though it is fixed due to the stiffness of the sleeve and the interaction of the tube and sleeve with the TSP. The potential for fluidelastic vibration of the tube is negligible. If the tube is postulated to separate at the upper edge of the expansion, the tube end is effectively restrained by the sleeve extension above the expanded region. At the intersection between the tube and sleeve, the gap is zero and progresses to a maximum of 0.026 inch in the unexpanded area. Lateral motion of the tube end is limited to the size of the gap, and the stiffness of the sleeve is sufficient to restrain further lateral motion of the tube, such that contact with adjacent tubes is precluded. The bending stiffness of the sleeve is large enough that any operational loading due to flow effects is negated by the sleeve stiffness, and tube-to-tube contact will not occur. With the limited range of motion of the tube end, the end condition is similar to a pinned connection when contact with the sleeve occurs. As long as some boundary condition fixity is provided, the potential for fluidelastic excitation is minimal.

In summary the sleeve provides effective tube stabilization under the assumption that the parent tube is severed in the region of the expansion. The sleeve functions to essentially eliminate the likelihood of fluidelastic vibration of a severed parent tube and provides lateral restraint to prevent the assumed severed tube end from contacting adjacent tubes.

10.6 Potential for Circumferential Cracking in Expanded and Plugged Tubes

The potential for circumferential cracking in expanded and plugged tubes can be evaluated utilizing laboratory tests for bulged hydraulic expansions and steam generator operating experience for circumferential cracking at tubesheet transitions and small row number tubes, and comparison of the principal factors, stress and temperature, that determine SCC behavior. In addition, repairs that utilize tube expansions that were implemented in operating steam generators provide a basis for estimating the potential for circumferential cracking of tube expansions. Laboratory test data are available that provide comparative data for the onset of corrosion for different stress and operating conditions and these data are used to provide an estimate of the potential for circumferential cracking of the tube expansions. Figure 10-16 shows potential locations for PWSCC or ODSCC in the expanded tube.

As noted in Section 10.2, the hydraulic tube expansions will result in diametral changes in the tube in the range of [ ]^{a,c} inch. In comparison, tubesheet hydraulic expansions result in a diameter increase of nominally <0.020 inch. Field repairs have been made for active tubes that included approximately 0.040 inch diameter increase. Laboratory tests have been performed to evaluate the SCC behavior of tubes hydraulically expanded by more than 0.125 inch.

Since the expanded tubes will be plugged, the operating conditions of the expanded tubes are dictated by the secondary coolant conditions. Thus, the temperature of the expanded tubes will be the saturation temperature of the steam water mixture, in the range of 522°F to 540°F for a T_{hot} of 600°F to 618°F, respectively.

ODSCC occurs at normal operating temperatures as a result of concentration of corrodents in crevices due to superheat in the crevices. Since the expanded tubes will be plugged, there will be no heat transfer through the tube. Although secondary coolant ingress into the tube, and therefore the expansion crevice, cannot be excluded in all cases (some degraded tubes may be used for tube expansion), the corrodent concentration cannot increase due to the absence of heat transfer through the tube/sleeve crevice. Therefore, the corrosion potential of the expansions in the tube is extremely small. However, it is expected that most tubes to be expanded will not include throughwall degradation. Thus the primary side of the expanded tube would not be exposed to primary or secondary water such that PWSCC would not be expected.

Similarly, the corrosion progression of a previously degraded intersection will be effectively halted. The existence of prior corrosion implies that the tube crevice is at least partially packed. Tube expansion is expected to decrease or eliminate the remaining crevice. Consequently, neither the mechanism (heat transfer) nor an available crevice exist for further concentration of corrodents. Rather, it would be expected that existing corrodents in the crevice would be diluted over a period of time due to the coolant flow.

10.6.1 Operating Experience for Circumferential Cracking

<u>Tubesheet Expansion Region</u>

There has been relatively modest occurrence in terms of the number of tubes with circumferential cracking in operating steam generators. Table 10-5 summarizes the known operating plant experience to date for circumferential cracking at the tubesheet expansions. The observed cracks are predominantly associated with explosive tubesheet expansion, and somewhat less frequently with mechanical tube expansion. All of the cracks have been found on the hot leg of the steam generators. Thus, the temperature conditions on the cold leg have not led to circumferential SCC in the tube expansion region at this time.

Circumferential cracking has not been observed in plants with hydraulic tubesheet expansions. These plants have accumulated up to 12 years operation since the start of commercial operations. Although the plants with hydraulic tubesheet expansions utilize primarily Alloy 600 TT tubes, approximately 74% of the tubes are Alloy 600 MA in plant FC. This plant had accumulated approximately 8 years operation without plugging any tubes due to ODSCC or PWSCC prior to shotpeening the tubes.

The absence of circumferential cracking in hydraulically expanded tubes is consistent with laboratory data for accelerated corrosion tests and stress indexing tests noted below.

Tubesheet region corrosion in a highly caustic environment was shown to be arrested at a temperature of 557°F, while increasing corrosion rates were found at temperatures of 575°F and 595°F. This observation results from Plant M-1 operation where a short term reduction in T_{hot} was implemented to determine its effect on IGA in the tubesheet crevice which had been observed during normal power operations. During operation at the reduced temperature, no significant increase in SCC was detected. Upon return to the initial T_{hot}, significant increase in the incidence of SCC in the tubesheet crevice was again found.

Similar reduction in the PWSCC behavior with temperature was found in tests described below.

Other Regions

Table 10-3 also summarizes the operating data for circumferential cracking in areas other then the tubesheet expansion. The non-tubesheet circumferential cracks occur at a tube support plate and are due ODSCC at dented TSPS and to a few occurrences of fatigue loading. Only a single plant has identified OD initiated circumferential cracks at dented TSPs to date in operating steam generators.

10.6.2 Laboratory Data on Cracking of Expanded Tubes

PWSCC Temperature Sensitivity Tests (1)

Tests were performed to determine the temperature effect of PWSCC for a temperature range of 590°F to 626°F, typical of the T_{hot} of operating plants. In this range of temperatures, approximately a factor of 2 increase in exposure time to initiation of PWSCC was found when the test temperature was reduced by 10°C (18°F) from 626°F. Evaluated in terms of activation energy, the resulting activation energies for these data are consistent with the activation energy ranges reported in the literature. Thus, a reduction from normal operating temperature to plugged tube conditions of approximately 78°F is expected to result in a factor of greater than 16 increase in the onset of SCC for similarly stressed tubing.

SCC Test of Bulged Hydraulic Expansion (2)

Test were performed on Alloy 600 TT tube specimens hydraulically expanded in carbon steel collars to determine the corrosion performance when the hydraulic expansions were "exaggerated" to produce bulged conditions. Bulges of 0.011 inch to 0.125 inch greater than the nominal hydraulic expansion of approximately 0.020 inch were tested. Testing was performed in a doped steam environment.

In these tests, summarized on Figure 10-17, throughwall circumferential cracking was observed only in the specimens with the Δd greater than [

]. [a,b]

These tests demonstrated that for Alloy 600 TT tubing, hydraulic tube expansions to a diameter significantly in excess of the normal expected hydraulic expansions are not an issue. The bulge sizes for circumferential cracking exceeded the [ ] [a,c] maximum expansion diameter for the TSP tube expansion process.

Operating experience for plants with hydraulic expansion support this conclusion, as tube plugging due to PWSCC or ODSCC has not been required at these plants. (An exception is a plant with severe denting at the top of the tubesheet that required plugging of approximately 120 tubes). In Plant FC, which has hydraulically expanded tubesheet joints, approximately 74% of the tubes are Alloy 600 MA. No plugging has been required due to ODSCC or PWSCC in the expansion region over approximately 10 years of operation. Thus, it is concluded that for at least the expected hydraulic expansion Δd, short term cracking is also not an issue for Alloy 600 MA tubes.

<u>Stress Indexing Tests</u> (3)

Polythionic acid stress indexing tests have been performed to evaluate the relative performance of different tube expansion techniques, and to evaluate the relative performance of a range of tube Δd's for a single expansion technique. The basis of these tests is a calibration of time to crack initiation in an accelerated corrosive environment using specimens with known stress states (typically C-rings). Tests in the same environment of a specimen with unknown stress state yield a time to crack initiation, which, from the stress/time calibration and the direction and location of the crack, implies the highest stress and its location (ID or OD) and direction.

Generally, hydraulic tube expansion was found to have the longest crack initiation times of the tube expansion methods tested (including mechanical expansions), and this is substantiated by the field experience. Figure 10-18 shows the results of the polythionic acid stress indexing tests for ID and OD residual stress implied by the test results for various size bulge diameters. Bulge diameter is defined as the total Δd in excess of the normal tube diameter. For ID exposure, no significant change in crack initiation time was found for Δd of approximately [

]. [a,c]

Based on these tests, it is concluded that diametral tube expansion of [ ]^{a,c} in. maximum is not expected to exceed the stress corrosion cracking potential for hydraulic tubesheet expansions. An [ ]^{a,c} in. hydraulic expansion yields approximately the same residual stresses as the lower boundary residual stresses resulting from mechanical tube expansion. Further, since OD cracking was found to be insensitive to tube expansions in a range from less than 0.010 inch to greater than 0.050 inch, it is concluded that, for tube expansions, ODSCC is a lesser concern than PWSCC.

10.6.3 Operating Experience for Steam Generator Repairs Utilizing Tube Expansions

<u>Pre-Heater Repair</u>

In the Model D-4, e.g., Braidwood 1 and Byron 1, steam generators, approximately 132 tubes near the feedwater inlet nozzle in the cold leg were hydraulically expanded at each of two tube support plates to reduce/eliminate the support plate tube gaps. The tube expansions resulted in Δd's up to 0.041 inch. These repairs were made to provide additional tube support to eliminate a potential tube vibration issue. The expanded tubes were returned to service.

The operating temperatures of the tubes that were expanded is in the range of 558°F to 538°F, depending upon the T_{hot} of the plant.

Over approximately 7 years operation, the tubes have been inspected as a part of the normal in-service inspections. No evidence of corrosion has been detected in these tubes.

<u>Plant G-1 U-bend Repair</u>

At Plant G-1, a U-bend tube ruptured due to fatigue at approximately the top of the uppermost tube support plate. The ruptured section was bridged by an internal device that was expanded in the tube on both sides of the rupture plane. The expansion of the tube was approximately a 90 mils bulge. The tube was plugged, and the plant was restarted and operated for approximately 7 years prior to S/G replacement. No external evidence exists that would suggest short term corrosion in the expanded sections.

10.6.4 Summary/Conclusions

Although circumferential cracking has been found in operating plants, the incidence of these cracks is relatively infrequent. OD and ID circumferential cracks have been observed principally in plants with explosive TS expansions and, to a lesser extent, in plants with mechanical expansions. No circumferential cracking has been observed in operating plants with hydraulic tubesheet expansions. These plants include a significant number of Alloy 600 MA tubes.

The operating temperature of expanded and plugged tubes is between 522°F and 540°F, determined by the secondary coolant temperature. Operating experience and laboratory tests have demonstrated that the potential for SCC is significantly reduced at reduced temperatures. No circumferential cracks have been found on the cold leg of operating steam generators. Tubesheet ODSCC was essentially stopped when the T_{hot} in an operating plant was reduced to approximately 557°F. Test data show that PWSCC is reduced by a factor of about 2 when the temperature is reduced by 10°C (18°F). Therefore, a reduction of temperature from the normal operating temperature to secondary coolant conditions will reduce the potential for SCC by a factor of approximately 16.

Stress index testing has shown that ODSCC and PWSCC crack initiation for hydraulic tube expansion of Δd up to[ ]^{a,c} inch does not exceed that of the normal hydraulic tubesheet expansion of Δd of approximately 0.020 inch. OD cracking was found to be insensitive to the range of Δd from less than [ ]^{a,c}.

Doped steam testing of Alloy 600 TT has shown that hydraulic expansion bulges with Δd of approximately [ ]^{a,c} inch exhibit only axial cracks which do not progress to throughwall condition in a time equivalent to approximately 28 EFPY.

Cold leg tube repairs made by implementing hydraulic expansions in Alloy 600 MA tubing with Δd of up to 0.041 inch have not shown evidence of corrosion cracking after approximately 7 years of operation for conditions similar to plugged tube conditions.

Since the tube expansions are between [ ],^{a,c} and the operating temperature of the expanded tubes will be the secondary coolant temperature, these data suggest that the potential for circumferential cracking should be a factor of at least 16 less than IDSCC in mechanically expanded tubes on the hot leg of a steam generator. The minimum operating time to reported ID circumferential cracking has been 4 years (Table 10-6). Consequently, circumferential cracking of the expanded tubes would not be expected in the operating lifetime of the steam generator.

10.7 Requirements on Limiting Tube Denting for TSP Integrity

In severely dented S/Gs, tube support plates have been observed to be cracked, and this raises a potential concern regarding the ability of the TSP to support the axial loads applied by the tube expansion process and by postulated SLB loading. Implementation of APCs and tube expansion would not be considered for very heavily dented tube support plates, but would be appropriate for TSPs with light to moderate denting. This section develops a threshold of denting for which TSP cracking would not be expected to occur and considers the axial load carrying capacity of dented TSPs with expanded tubes to limit motion of the TSP during a postulated SLB.

10.7.1 Maximum Dent Size for TSP Cracking

The finite element analysis, discussed in Section 10.3, to determine the effect of tube expansion on the tube support plates (TSP's), both with and without denting of the tubes adjacent to the expanded tube was extended to determine the maximum dent size allowable to maintain TSP integrity. In this analysis, the maximum dent size that could be supported by the TSP without exceeding the yield strength at operating temperatures was obtained by increasing the thermal expansion of the dented tubes until the maximum stress intensity in the TSP reached 23.35 ksi.

The effective stiffness of the dented tubes was recalculated to account for the greater deformation of the dented tube in this case. The next P/R data set from the inelastic tube deformation analysis (see Section 10.3) was used to determine P/R (This was for deformations between 8 and 12 mils, well below the dent size). The resulting equivalent elastic modulus was:

$$E_{equiv} = 342{,}814 \text{ psi}$$

Of the four denting combinations considered in the analysis, the case with four adjacent tubes in the diagonal direction yields the maximum stress intensity in the TSP for large dents. Figure 10-19 shows the stress intensity contours for the case with a 0.065 inch diametral dent. The maximum stress intensity in the TSP occurs in ligament 4 and has a value of 23.33 ksi, which is slightly below the yield strength at 550 F. Thus, the maximum dent that can occur without exceeding yield in the TSP is 65 mils.

This predicted threshold dent for TSP integrity can be utilized as an indicator of adequate TSP integrity. In effect, an EC probe can be used as a Go-No-Go gauge, based on the diameter of the probe. In addition to the allowable 65 mil dent, an allowance of about 20 mils for probe centering devices must be subtracted from the tube ID to obtain an acceptable probe diameter to pass through the dent. Thus, if a probe of 0.590 in. dia. fails to pass through the tube, but a probe of 0.570 in. dia. passes through the tube, the TSP intersection is considered to have adequate integrity vis a vis denting.

10.7.2 Field Experience for Dented TSP Load Carrying Capacity

The load carrying capacity of the TSP around an expanded tube is determined by the four "cells" surrounding the expanded tube (see Figure 10-20). Complete loss of load carrying capacity would require loss of at least two contiguous cells of the four, and this would, in turn, require cracking in the six boundary ligaments and in the ligament joining the two cells, removal of the two cells from the tube support plate and bending of the expanded tube away from the remaining two cells. Cracking without loss of the cells will not significantly reduce the load carrying capacity of the TSP as noted below. Further, the presence of denting in the TSP reduces the axial load requirements on the expanded tube due to load sharing among the dented intersections.

Denting does not generally occur in isolated tubes; rather, the conditions leading to denting are bulk conditions that affect larger numbers of tubes in the same area. Denting generates in-plane compressive loads in the TSP that, despite possible distortion in the tubes and in the flow holes, will retain the TSP cells surrounding the dented intersections. This is based on the observation that the fracture surfaces on plates with heavily dented tubes are "interlocked" (that is, not a smooth plane), and on observed pull loads in tube pulls at heavily dented plants which ranged from 1000 to 9000 pounds. These high pulling forces indicate that, for heavily dented TSPs, where cracked TSP ligaments are most likely to occur, the TSP segments remain in place and provide significant axial resistance (load capacity).

The only evidence of TSP segments becoming dislodged has been found in very heavily dented plants. In one heavily dented plant (early Model 51 S/Gs, which have been replaced), a metal segment was found on the upper surface of the TSP during examination of the top TSP, that from its shape, was interpreted to be a TSP segment. This was an isolated occurrence.

At another plant (Model 44 S/Gs, which have been replaced) with reported heavy denting, a segment of the top TSP was removed after the S/Gs were retired and stored in a mausoleum. After removal of the TSP segment, the TSP segment fractured and a part of the removed segment separated from the remainder in a plane that intersected the interstitial flow holes between the three-tube segment removed. (It should be noted that the TSP segment was intact until the TSP had been cut and removed; thus, it is not known if there were cracks in the opposite side ligaments of the segment.) All three tubes in the segment removed had been reported as dented; the tube with the largest voltage was determined to have a 0.015 inch radial dent. The location of the TSP segment removed coincides with the area of most dent-related tube plugging (near the beginning or end columns of the largest radius U-bends) in heavily dented S/Gs. This suggests a buildup of forces in these areas that lead to severe tube denting and elevated stress in the TSPs. In general, denting results in compressive stresses in the TSP. The location of this TSP crack was adjacent to the edge of a TSP wedge where the stress can become tensile. There are no other known instances of TSP segments fracturing and dislocating in this area.

10.7.3 Summary

Analysis of the TSP shows that a dent of 65 mils will not generate a stress intensity in the plate greater than the minimum yield strength of the plate material. Thus, cracking due to dent loading alone would not be expected to occur. Denting of this magnitude can be detected using the EC probe as a go/no-go gauge, and severely dented TSP locations can be excluded from consideration for tube expansion.

Field experience shows that, while cracks may occur in the TSPs due to denting, the TSP segments remain in place with only very rare exceptions in severely dented TSPs that are not candidates for implementation of tube expansion. No TSP segments have become dislodged during tube pulls in dented S/Gs, thus indicating that the compressive forces in a dented TSP are sufficient to retain the segments even when the local forces have been relieved due to removal of the tube. High tube pull forces, at a minimum comparable to the axial force capacity for expanded tubes, have been required in tube pulls for dented TSPs. Load sharing among the dented tubes and the expanded tubes would be expected in dented TSPs. Thus, moderately dented TSP are expected to provide sufficient axial load capability for implementation of tube expansion and maintaining limited TSP displacements with no loss of TSP integrity.

10.8 Conclusions

The hydraulic tube expansion process developed for 3/4 inch diameter tubing satisfies the design requirements to obtain limited TSP displacements with an expansion diametral increase of [.][a,b,c] The peak stress intensity in the TSP caused by the tube expansion is well below the yield strength of the TSP even for the minimum ligament size as shown by both analysis and test. A sleeve expanded with the tube provides for tube stabilization under the assumption of a severed tube and increases the stiffness of the expansion to permit satisfaction of design requirements for smaller expansion diameters than would be obtained without the sleeve. [

.][a,b,c]

Bobbin profilometry, utilizing a prototypic expansion for calibration, provides acceptable accuracy for confirmation of the expansion diameter.

For the hydraulic expansion process and the expansion diameters required for acceptable tube stiffness, the low temperatures at the plugged tube condition for the expansions result in a negligible potential for circumferential cracking of the expansion. This conclusion is supported by plant operating experience from hydraulic expansions and tube repairs as well as laboratory tests for bulged hydraulic expansions. A reduction in temperature from the normal operating temperature to the plugged tube, secondary coolant conditions results in a factor of about 16 in the time for crack initiation. Since field experience has shown a minimum time for circumferential cracking to be identified of ≥ 4 years, the time to initiate circumferential cracking in the expanded tubes would exceed the expected operating period for the plant.

S/Gs implementing the alternate repair criteria for ODSCC at TSP intersections would have none to moderate denting since the repair criteria are not applicable at dents > 5 volts. This essentially assures TSP integrity since heavily dented TSPs are necessary for potential cracking of the TSPs as shown by field experience and analysis. Analyses show that a tube dent of 65 mils is necessary for the ligament stress to reach the yield strength of the TSP, which can be applied as an indicator of the potential for cracking of the TSP. Failure to pass a bobbin probe of 0.570 inch diameter is recommended as a measure requiring further assessment of TSP integrity. For Braidwood-1 and Byron-1, with no corrosion induced dents found at TSP intersections, there is no known existing mechanism for cracking of the TSPs and TSP integrity can be assured without more detailed assessments.

Table 10-1
Tube Expansion Maximum Stress Intensities in the TSP

Denting Condition	Maximum Stress Intensity (ksi)			
	Ligament 1	Ligament 2	Ligament 3	Ligament 4
None	19.41	13.70	3.35	2.32
8 Tubes	18.94	13.76	5.23	8.30
4 Tubes (Pitch)	18.21	13.01	5.71	1.51
4 Tubes (Diagonal)	2.12	14.44	2.80	9.67
2 Tubes (Pitch)	18.81	14.11	4.95	1.64

Table 10-2
Comparison of Actual I.D. Measurements to Those Calculated
for 7/8" Tube Samples*

Sample	Meas. I.D. 1	Meas. I.D. 2	Calc. I.D 1	Calc. I.D. 2
D	0.7680"	0.7646"	0.7684"	0.7659"
E	0.7796"	0.7802"	0.7796"	0.7822"
F	0.7776"	0.7826"	0.7793"	0.7837"
G	0.7776"	0.7792"	0.7781"	0.7792"
H	0.8058"	N/A	0.8060"	N/A
I	0.7862"	N/A	0.7870"	N/A

* I.D. 1 for all supports was on the outboard (tube end) side, I.D. 2 was on the inboard side of the expansion (between supports).

Table 10-3
Expansion Sample Profilometry Results for 7/8" Tube Samples.

Sample (Run)	E/C I.D. 1	E/C I.D. 2	Calc. I.D 1	Calc. I.D. 2
D (1)	0.7722"	*0.7659"	0.7684"	0.7659"
D (2)	0.7720"	0.7666"	---	---
D (3)	0.7719"	0.7663"	---	---
E (1)	0.7831"	0.7835"	0.7796"	0.7822"
E (2)	0.7824"	0.7836"	---	---
E (3)	0.7827"	0.7839"	---	---
F (1)	0.7821"	0.7843"	0.7793"	0.7837"
F (2)	0.7818"	0.7843"	---	---
F (3)	0.7821"	0.7842"	---	---
G (1)	0.7805"	0.7819"	0.7781"	0.7792"
G (2)	0.7803"	0.7824"	---	---
G (3)	0.7814"	0.7821"	---	---
H (1)	**0.8060"	0.7959"	0.806"	N/A
H (2)	0.8060"	0.7961"	---	---
H (3)	0.8061"	0.7963"	---	---
I (1)	0.7880"	0.7872"	0.787"	N/A
I (2)	0.7890"	0.7872"	---	---
I (3)	0.7890"	0.7873"	---	---

* I.D 1 for all supports was on the outboard (tube end) side, I.D. 2 was on the inboard side of the expansion (between supports). The ** indicates the expansion and run used to set up the calibration for profiling the expansion.

Table 10-4
Expansion Sample Profilometry Results for 3/4" Tube Samples.

Sample (Run)	E/C I.D. 1	E/C I.D. 2	Calc. I.D 1	Calc. I.D. 2
HE003 (1)	0.6977"	0.6942"	0.6976"	0.6943"
HE003 (2)	0.6988"	0.6944"	---	---
HE003 (3)	0.6981"	0.6951"	---	---
HE008 (1)	0.6969"	0.6939"	0.6960"	0.6938"
HE008 (2)	0.6966"	0.6933"	---	---
HE008 (3)	0.6970"	0.6936"	---	---
HE010 (1)	0.6884"	0.6851"	0.6861"	0.6872"
HE010 (2)	0.6884"	0.6863"	---	---
HE010 (3)	0.6864"	0.6898"	---	---
HE011 (1)	0.6549"	0.6496"	0.6566"	0.6533"
HE011 (2)	0.6552"	0.6502"	---	---
HE011 (3)	0.6515"	**0.6533"	---	---
HE017 (1)	0.6711"	0.6670"	0.6701"	0.6668"
HE017 (2)	0.6709"	0.6666"	---	---
HE017 (2)	0.6714"	0.6685"	---	---
HE018 (1)	0.6552"	0.6548"	0.6575"	0.6575"
HE018 (2)	0.6551"	0.6554"	---	---
HE018 (3)	0.6548"	0.6580"	---	---
HE022 (1)	0.7039"	0.6994"	0.7069"	0.7025"
HE022 (2)	0.7039"	0.6996"	---	---
HE022 (3)	**0.7069"	0.7023"	---	---

* I.D 1 for all supports was on the outboard (short end) side, I.D. 2 was on the inboard side of the expansion (long end). The ** indicates the expansion and run used to set up the calibration for profiling the expansion.

Table 10-5
Circumferential Cracking Observed in Operating Plants

Plant	Tube Expansion Process	Year Crack Detected	Crack Origin	Years Operation When Cracks Observed
Tubesheet Cracks				
AA	Explosive	1990	IDSCC	18
AB	Explosive	1993	ODSCC	7
AC	Explosive	1987	ODSCC	12
AD	Explosive	1992	ODSCC	12
N	Explosive	1994		18
S	Mech	1988	IDSCC	4
V-4	Mech	19[illegible]	IDSCC	5
I-	Mech	198[illegible]	IDSCC	NA
B-2	Mech	1989	ODSCC	3
C-2	Mech	1990	ODSCC	7
C-1	Mech	1989	ODSCC	8
Q	Mech	1990	ODSCC	10
B-1	Mech	1989	ODSCC/IDSCC	5
AJ	Mech + Stress Relief	1994	ODSCC	9
V-3	Mech&DAM	1989	IDSCC	8
AF-1	Mech&DAM	1989	IDSCC	NA
AF-2	Mech&DAM	1986	IDSCC	NA
V-2	Partial	1983	ODSCC	8
AE	Partial	1979	ODSCC/IGA	11
W-2	WEXTEX	1990	IDSCC	8
G-1	WEXTEX	1987	IDSCC	9
G-2	WEXTEX	1989	IDSCC	9
W-1	WEXTEX	1990	IDSCC	9
L	WEXTEX	1989	IDSCC	13
A-1	WEXTEX	1991	IDSCC	14
AG	WEXTEX	1991	IDSCC	14
AF-3	WEXTEX	1980	IDSCC	
AH	WEXTEX	1994	Indeterminate	8
A-2	WEXTEX	1990	ODSCC	9
Support Plate Cracks				
G-1	(N/A)	1987	Fatigue	9
AK	(N/A)	1988	Fatigue	12
AL	(N/A)	Mid 70s	Fatigue	2-3
AK	(N/A)	1989	Fatigue @ TSP	13
I-2	(N/A)	1991	Fatigue @ TSP	19
L	(N/A)	1991	IDSCC?/U-Bend	15
G-1	(N/A)	1991	ODSCC @ TSP	13

Table 10-6

Temperature Based Time Factor for Circumferential Cracking of Plugged Tubes

Plant	Tube Dia.	Ex. Process	Operating Time When Circ.Crack Reported IDSCC (years)	ODSCC (years)	T_{hot} (F)	T_{sat} (F)	Time Factor (note 1)	Expected Time to Crack Plugged Tube (years)
B-2	0.75	Mech.	-	3	619.9	542.6	16	48
S	0.75	Mech.	4	-	618.8	541	16	64
V-2	0.875	Mech.	-	8	610.9	517	32	128
W-2	0.875	WEXTEX (note 2)	8	-	609.7	524.7	16	128

Note 1: Time factor based on Arrhenius equation

Note 2: No mechanicai expanded tube data are available

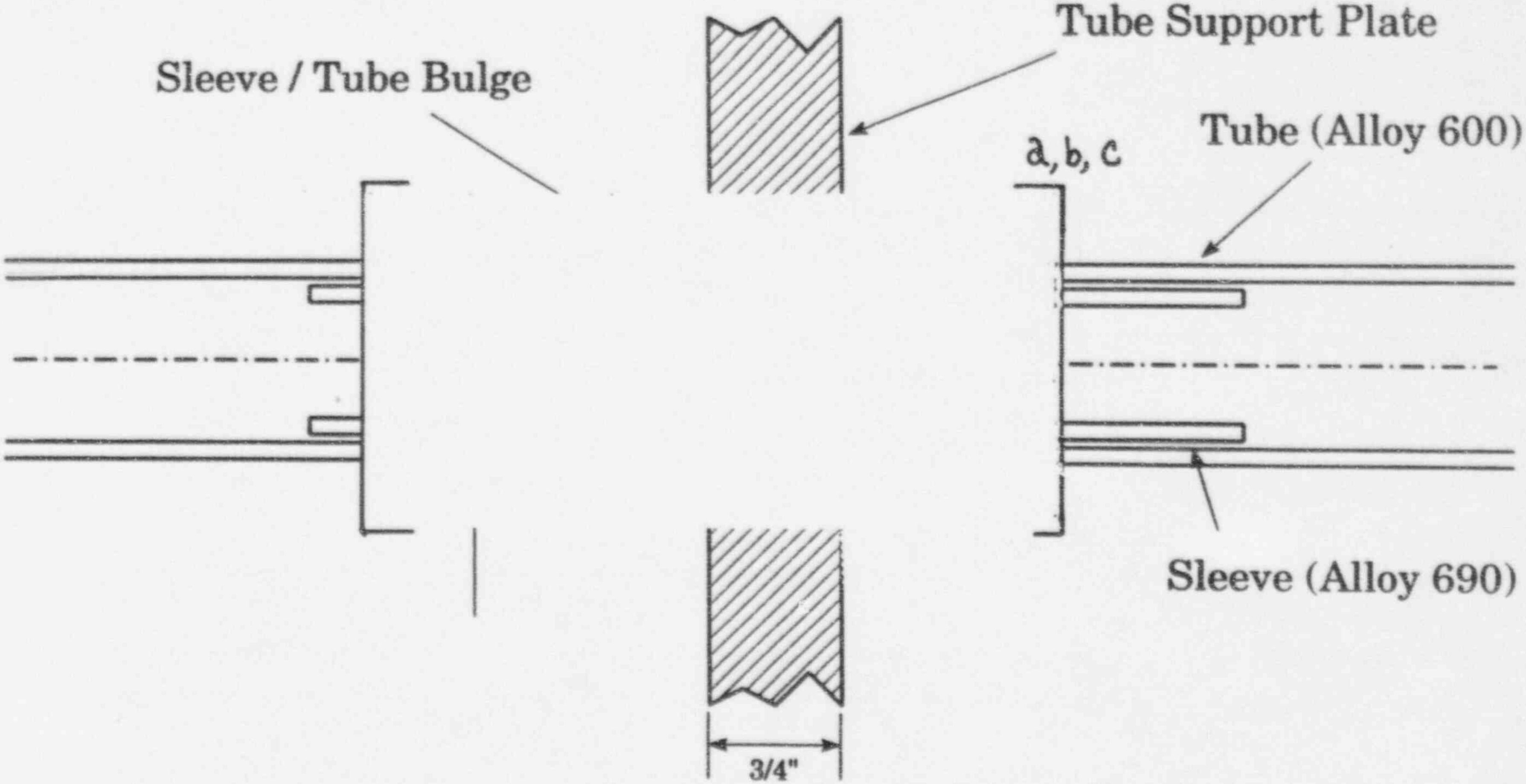

Figure 10-1: Capture of TSP by Tube/Sleeve Combination

Figure 10-2
Tube/Sleeve Expansion Profile

a,b,c

a,b,c

Figure 10-3
Pull Force vs. Tube Bulge Size

Figure 10-4
Pull Force vs. Tube OD Bulge Size for tubing heats used

HT 2004: 52 Ksi yield, 80.5 Ksi flow stress
HT 1991: 56 Ksi yield, 78 Ksi flow stress
HT 1458: 73 Ksi yield, 92.5 Ksi flow stress

a,b,c

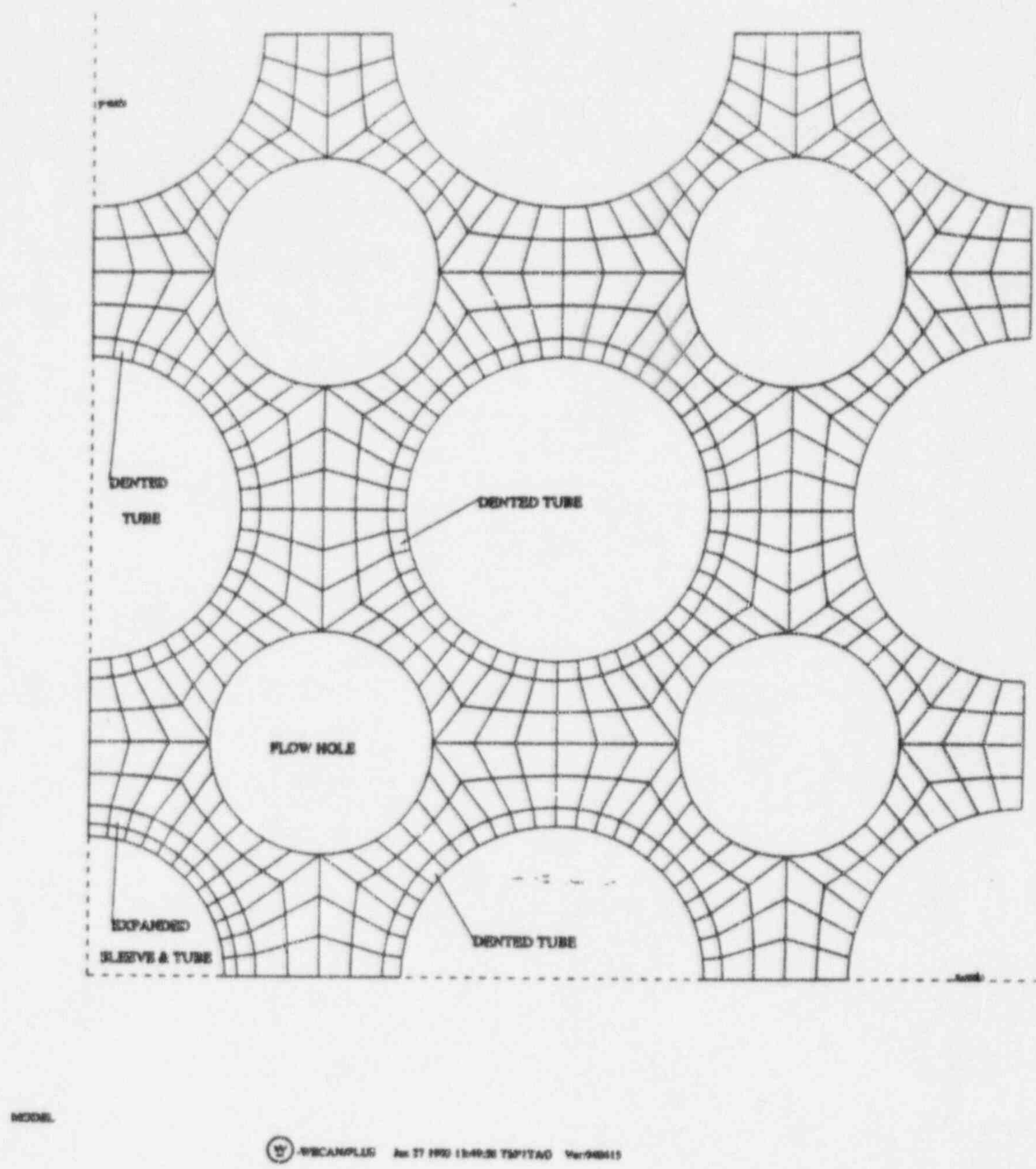

Figure 10-5. Finite Element Model of TSP With Expanded and Dented Tubes

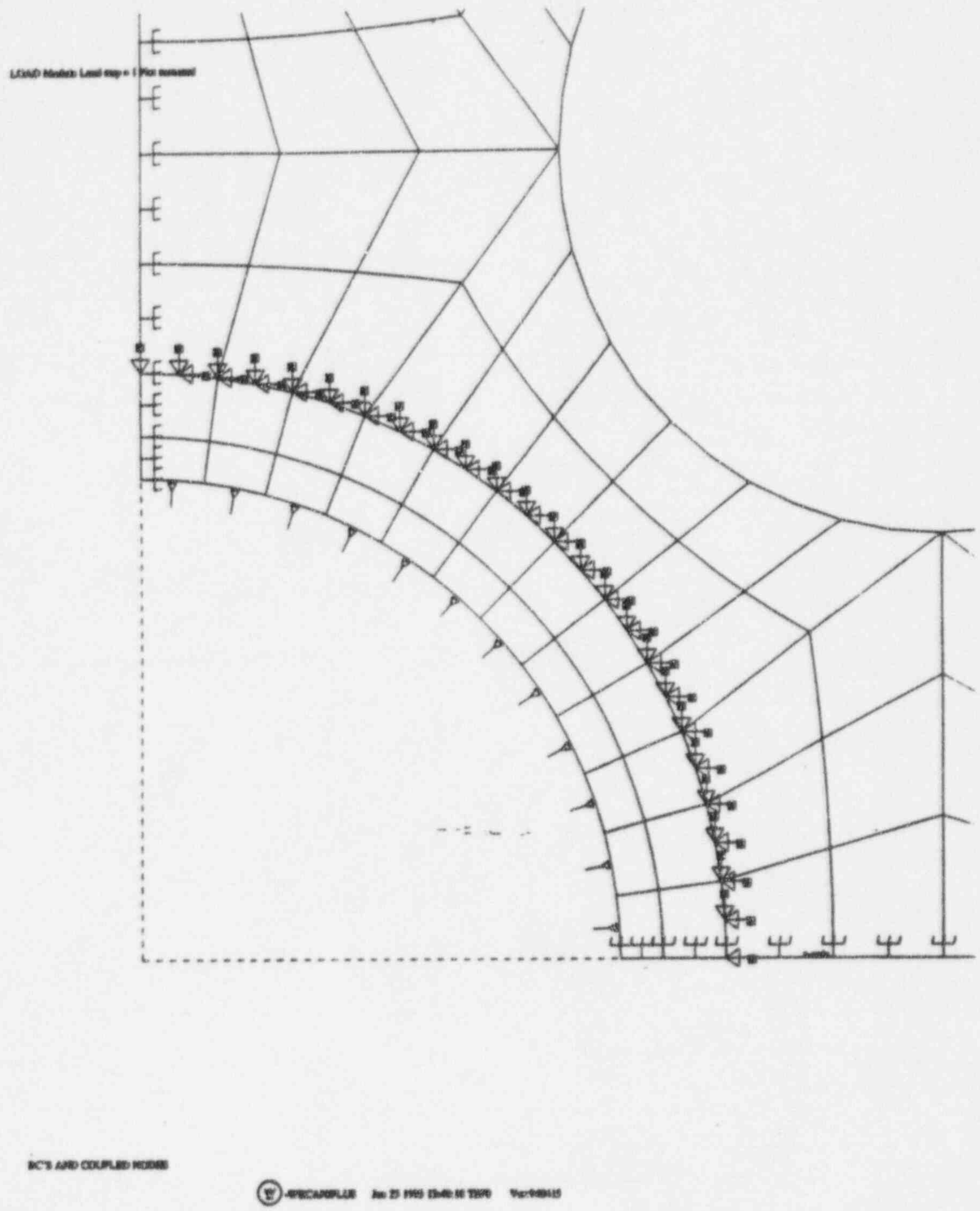

Figure 10-6. Enlargement Showing Details of Coupled Nodes

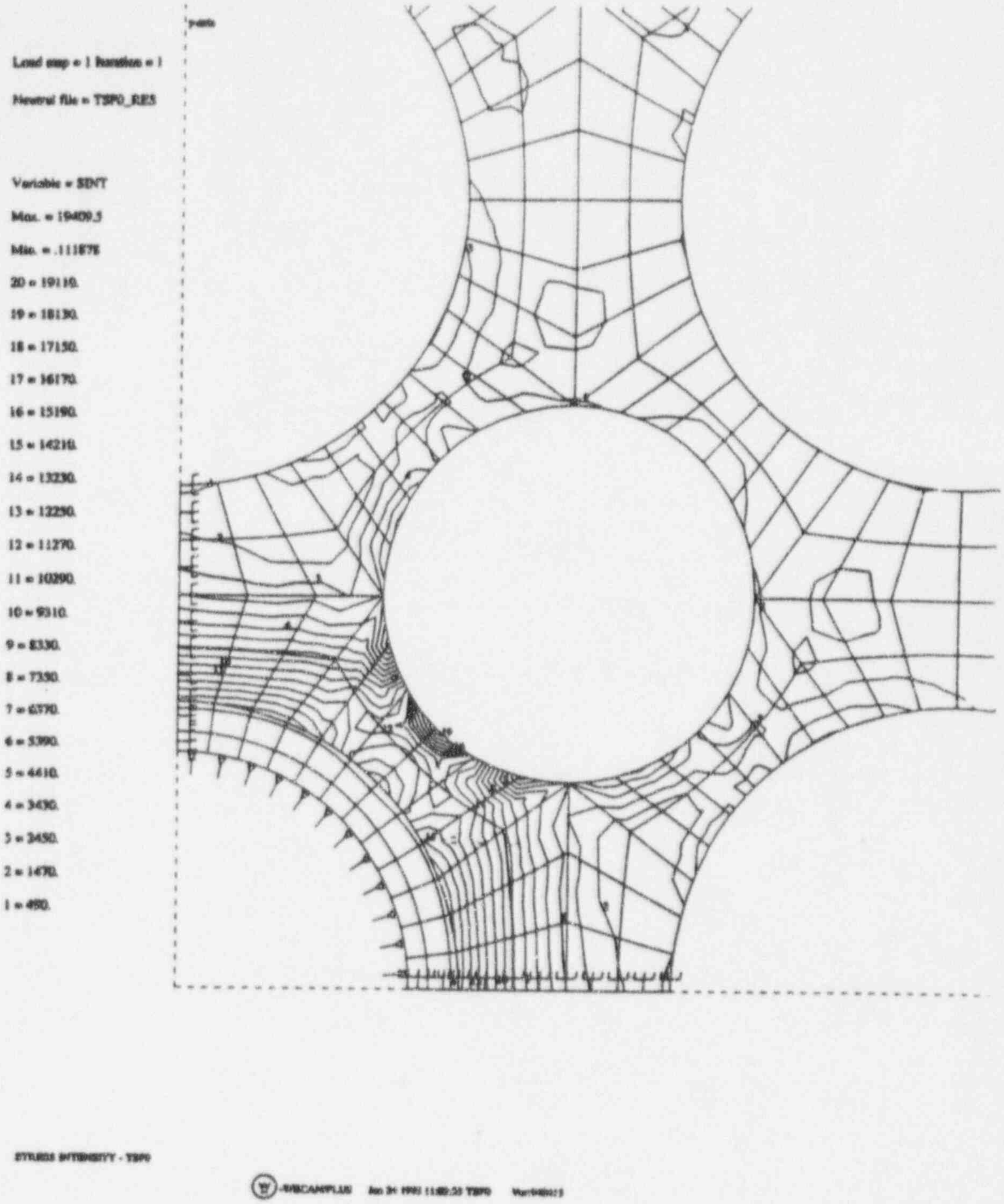

Figure 10-7. Stress Intensity Contours Near Expanded Tube

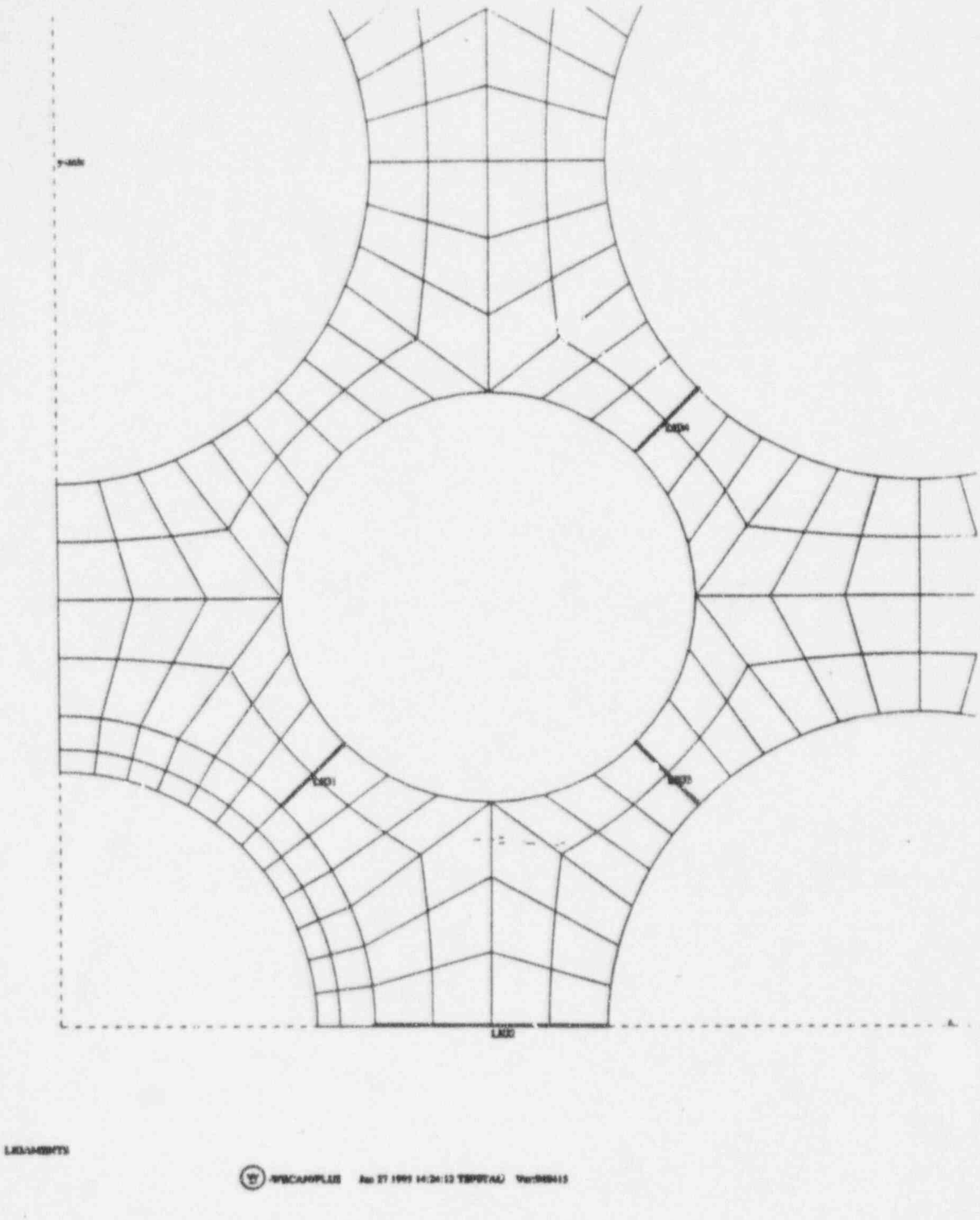

Figure 10-8. Identification of Ligament Locations

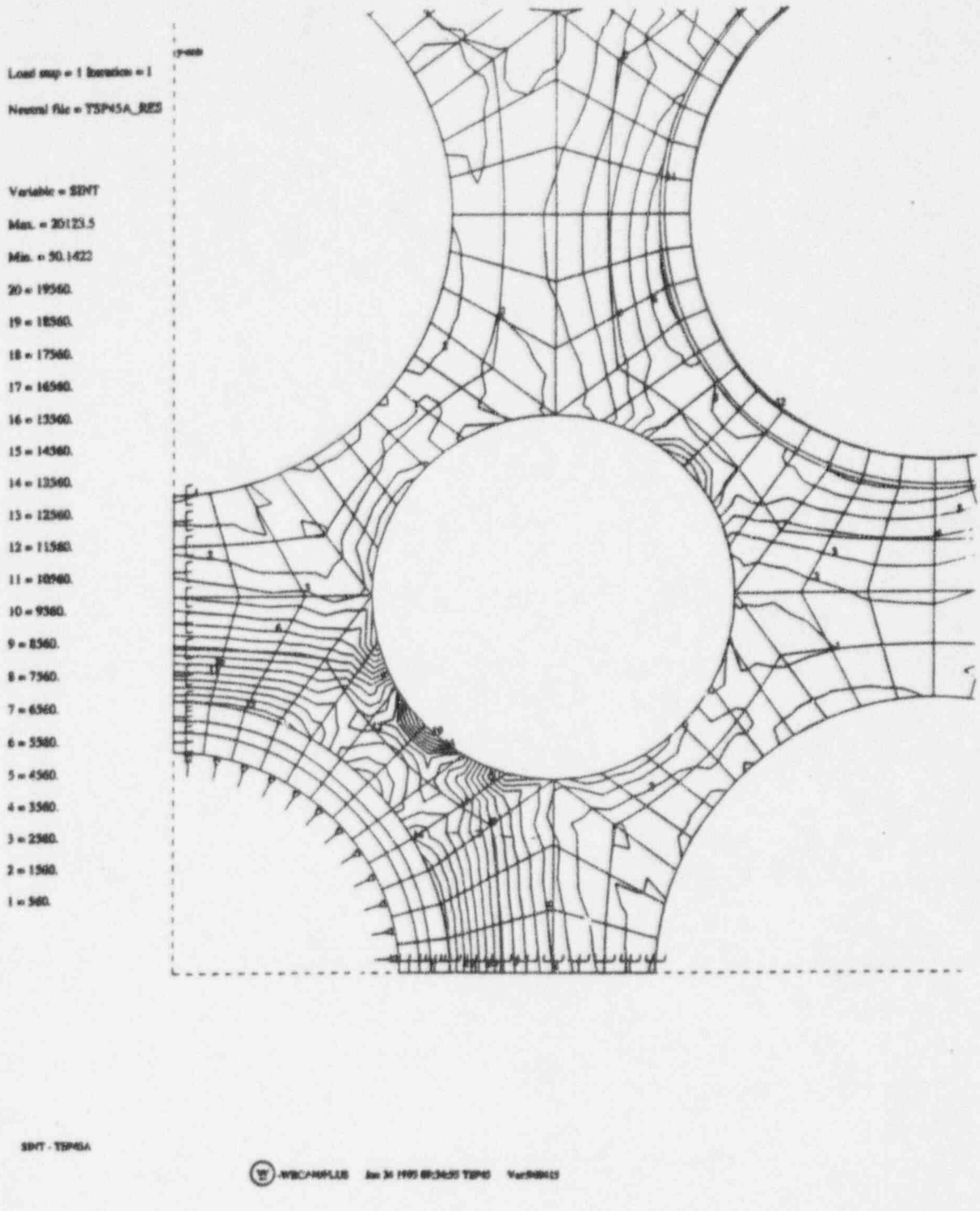

Figure 10-9. Stress Intensity Contours Produced by Tube Expansion With Four Dented Tubes in the Diagonal Direction

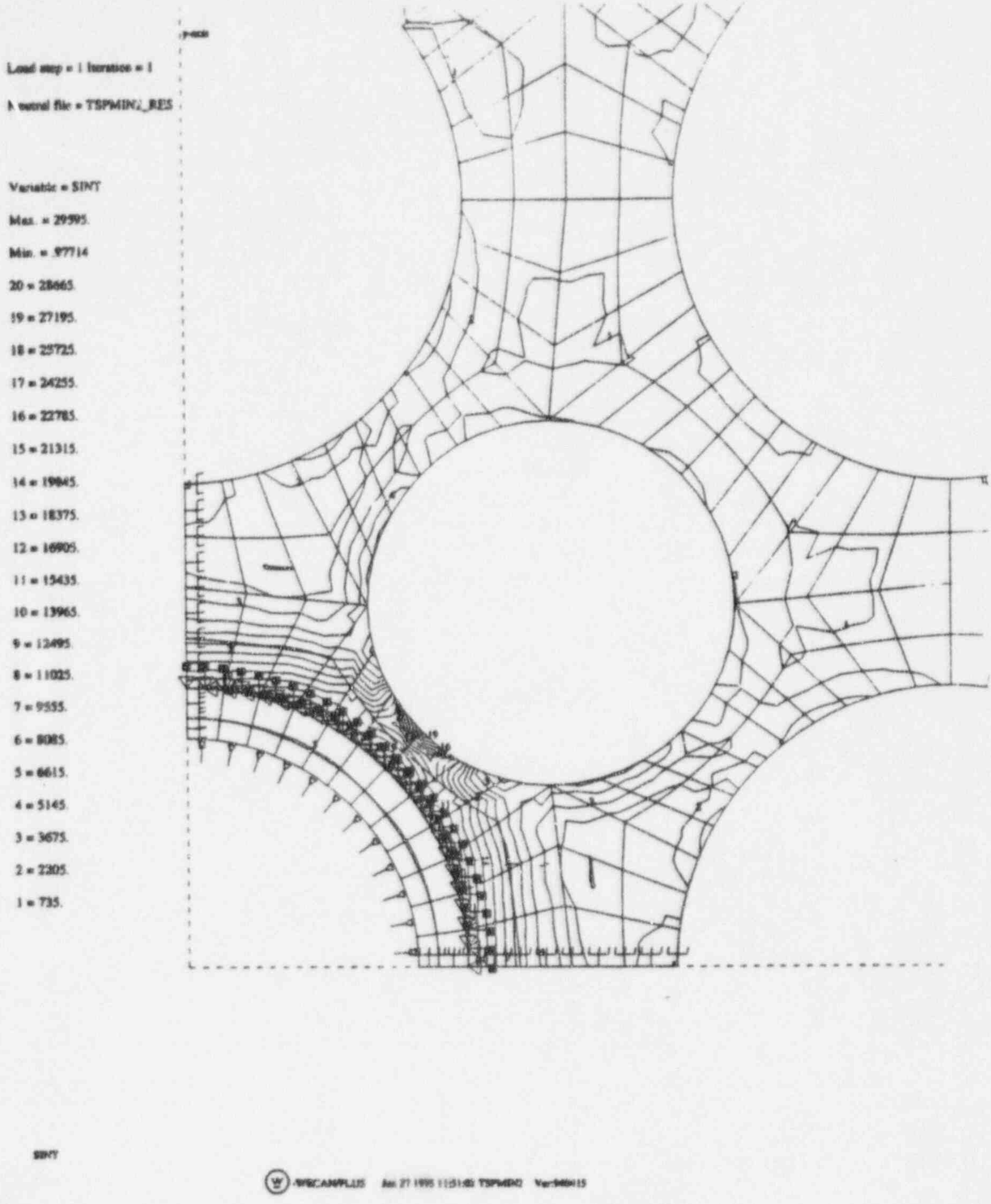

Figure 10-10. Stress Intensity Contours for Minimum Ligament

Figure 10-11. Typical Sleeve Expansion Standard

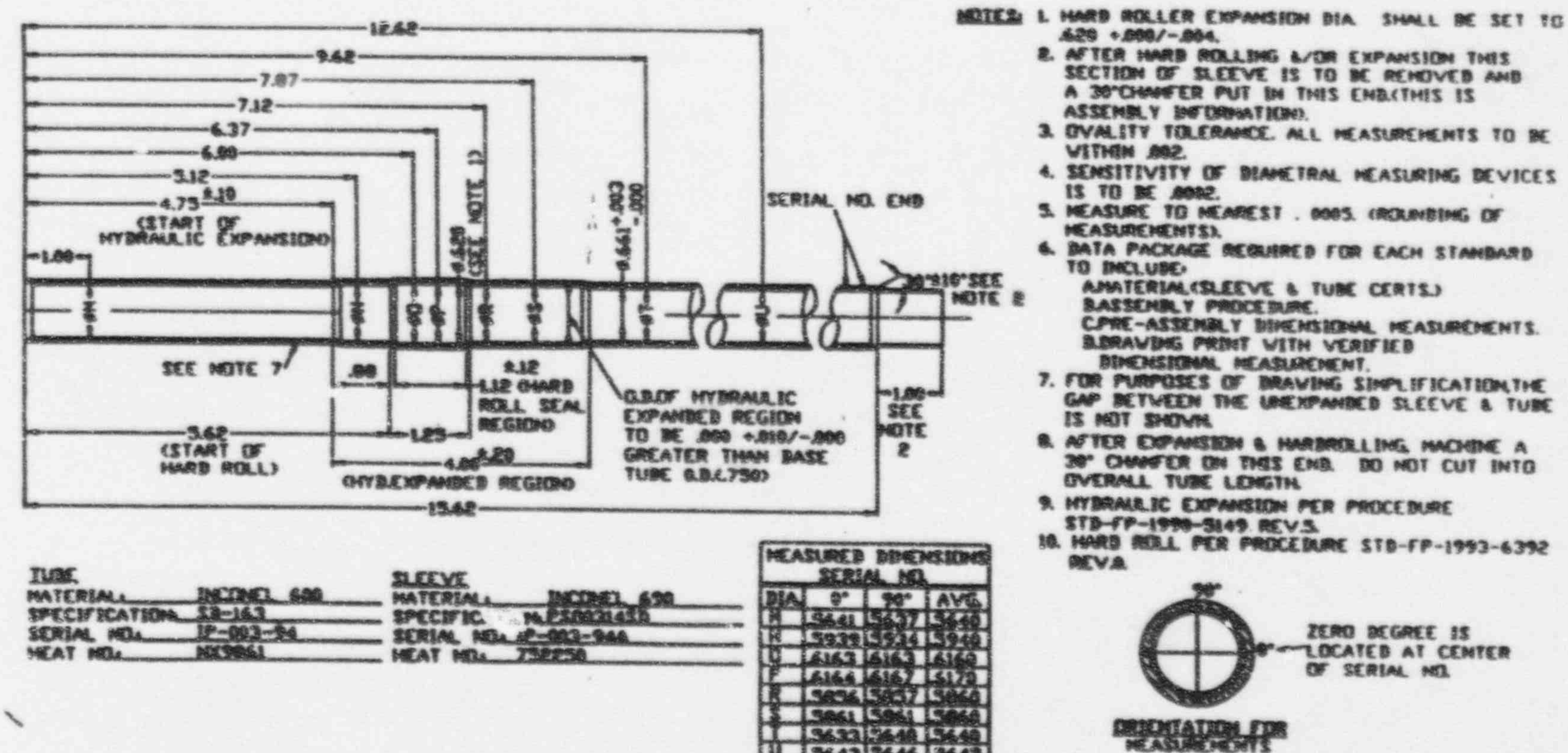

MEASURED DIMENSIONS SERIAL NO.			
DIA.	0°	90°	AVG.
H	.5641	.5637	.5640
K	.5939	.5934	.5940
Q	.6163	.6163	.6160
F	.6164	.6167	[illegible]
R	.5856	.5857	.5860
S	.5861	.5861	.5860
T	.5633	.5648	.5640
U	.5643	.5646	.5643

a,b,c

Figure 10-12. Sample with two sleeves expanded at TSP locations. The measured I.D. for the expansion indicated in 0.806 inch. Note: 7/8 inch tube OD

Figure 10-13 a. Bobbin Data for TSP with No Crack

Figure 10-13b. Bobbin Data for TSP with 50% Deep Cracks in Two Ligaments

Figure 10-13a. Bobbin Data for TSP with No Crack

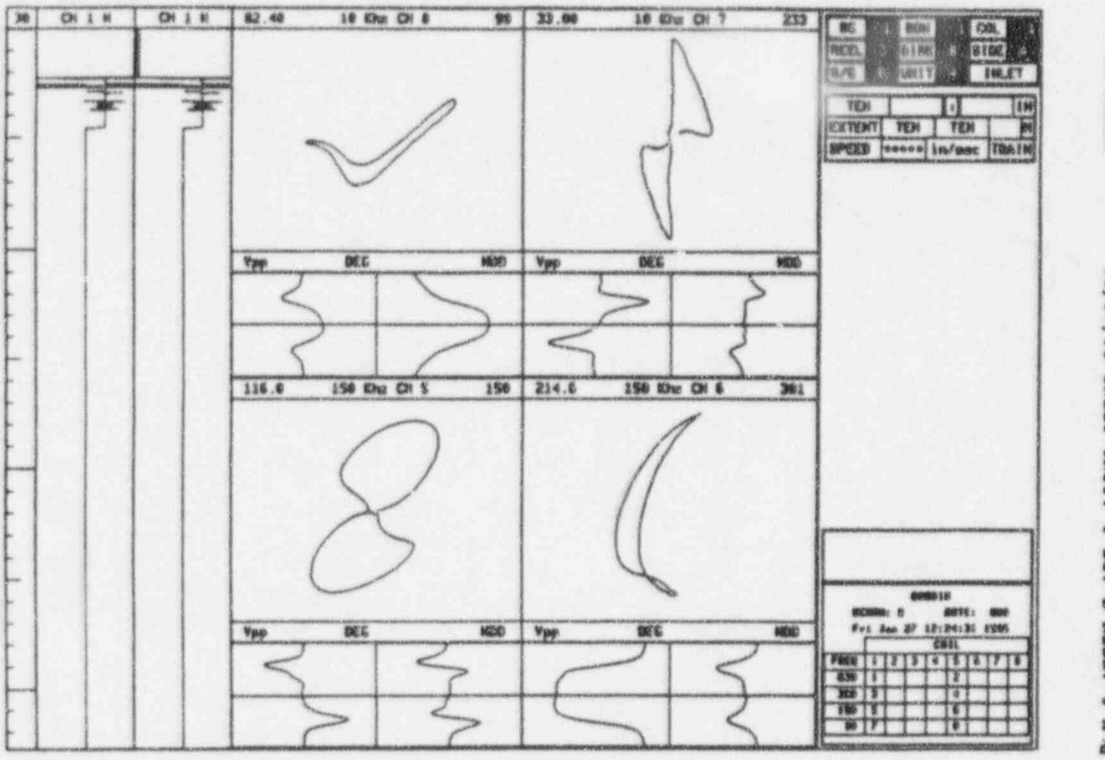

Figure 10-13b. Bobbin Data for TSP with 50% Deep Cracks in Two Ligaments

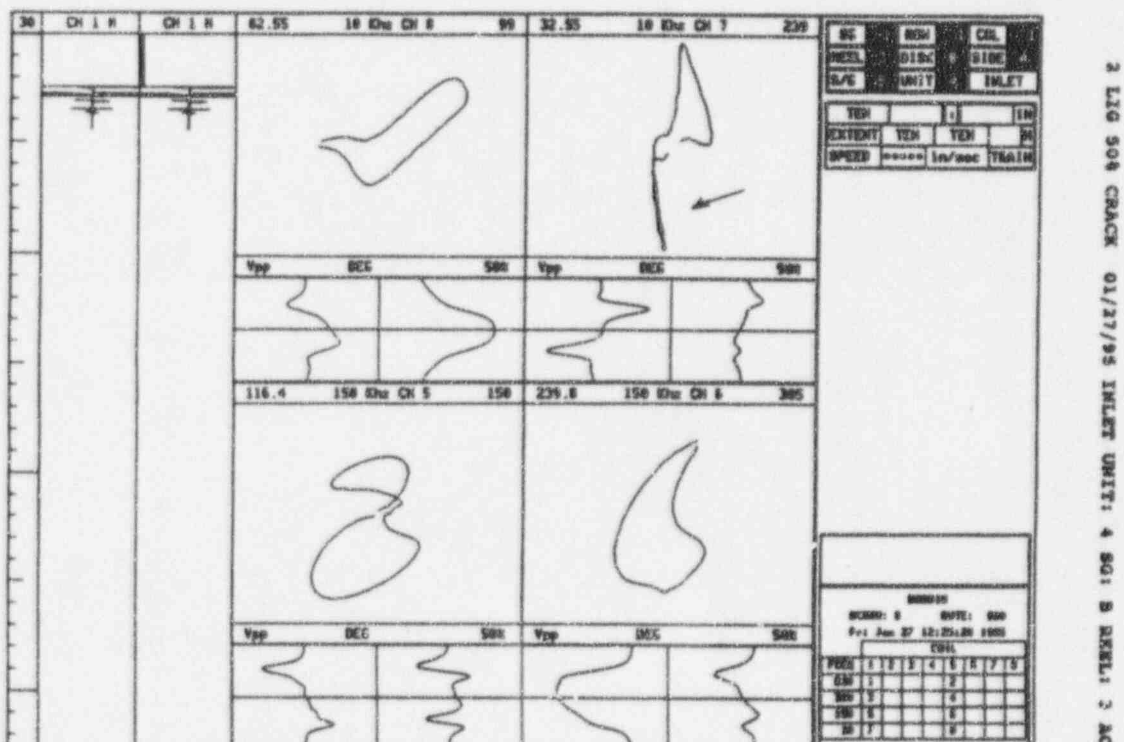

Figure 10-14a. Bobbin Data for TSP with 100% Deep Crack in One Ligament

Figure 10-14b. Bobbin Data for TSP on ASME Standard

Figure 10-14a. Bobbin Data for TSP with 100% Deep Crack in One Ligament

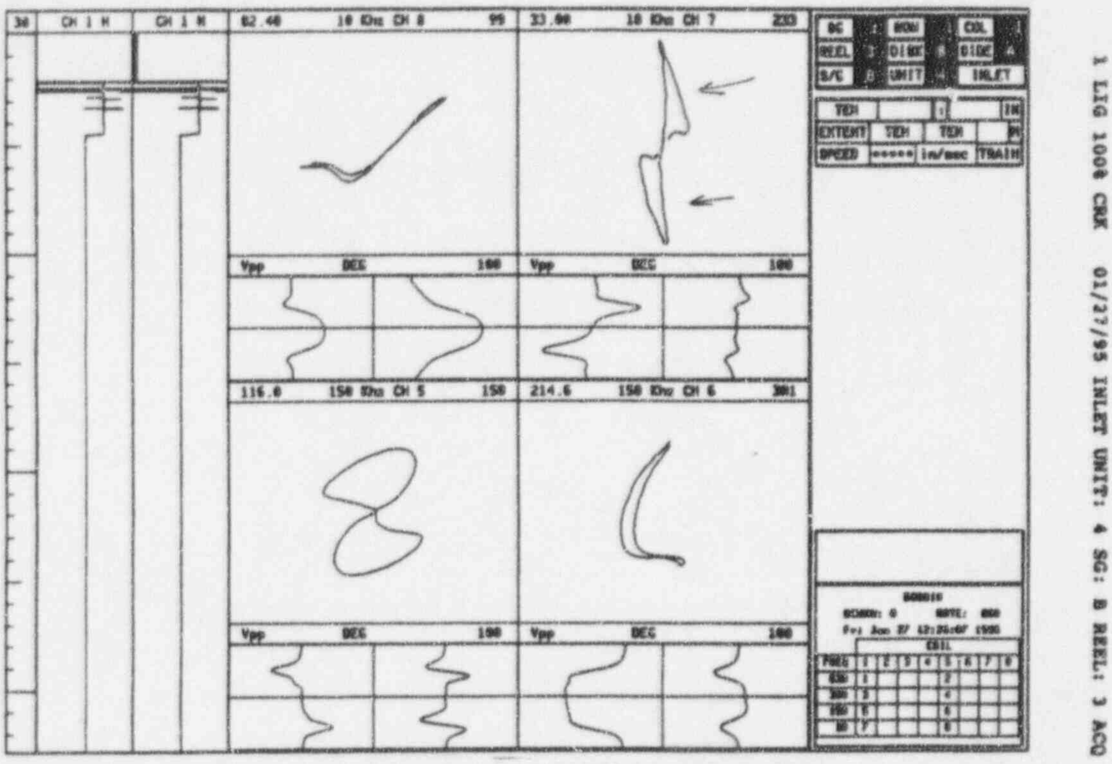

Figure 10-14b. Bobbin Data for Field TSP Expansion Candidate

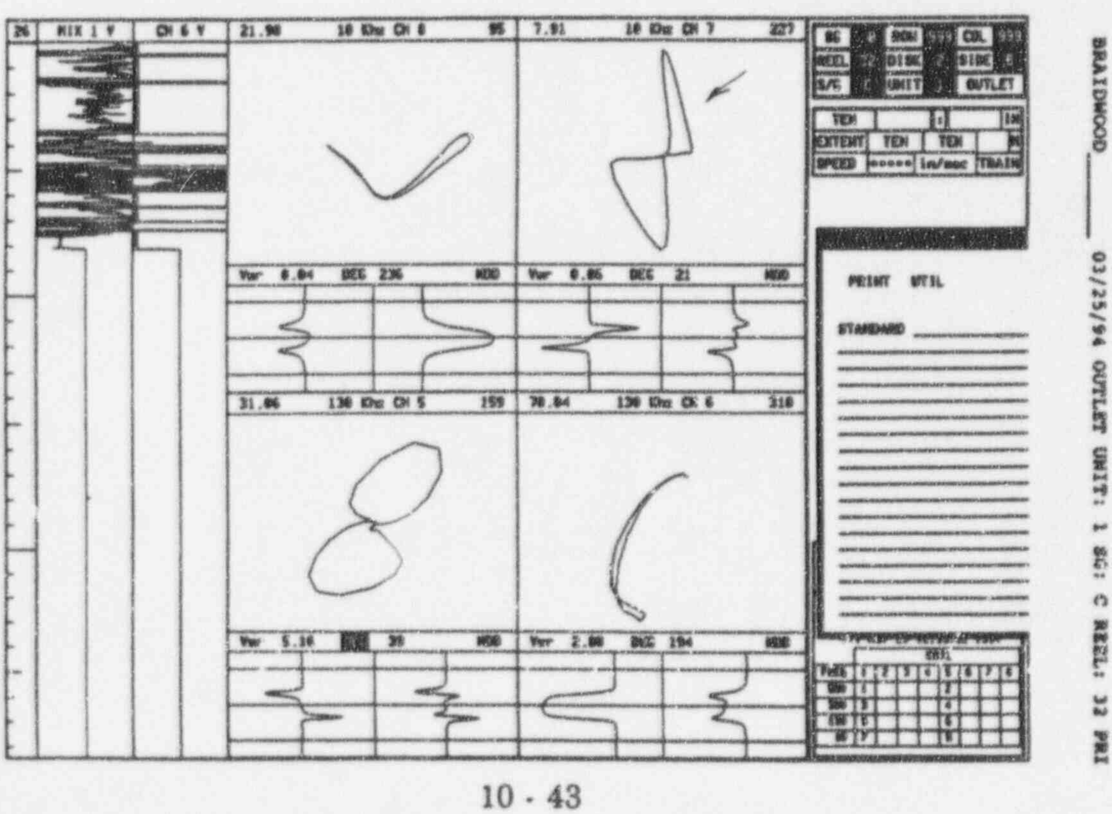

Figure 10-15 Bobbin Data for Typical Field TSP Intersection

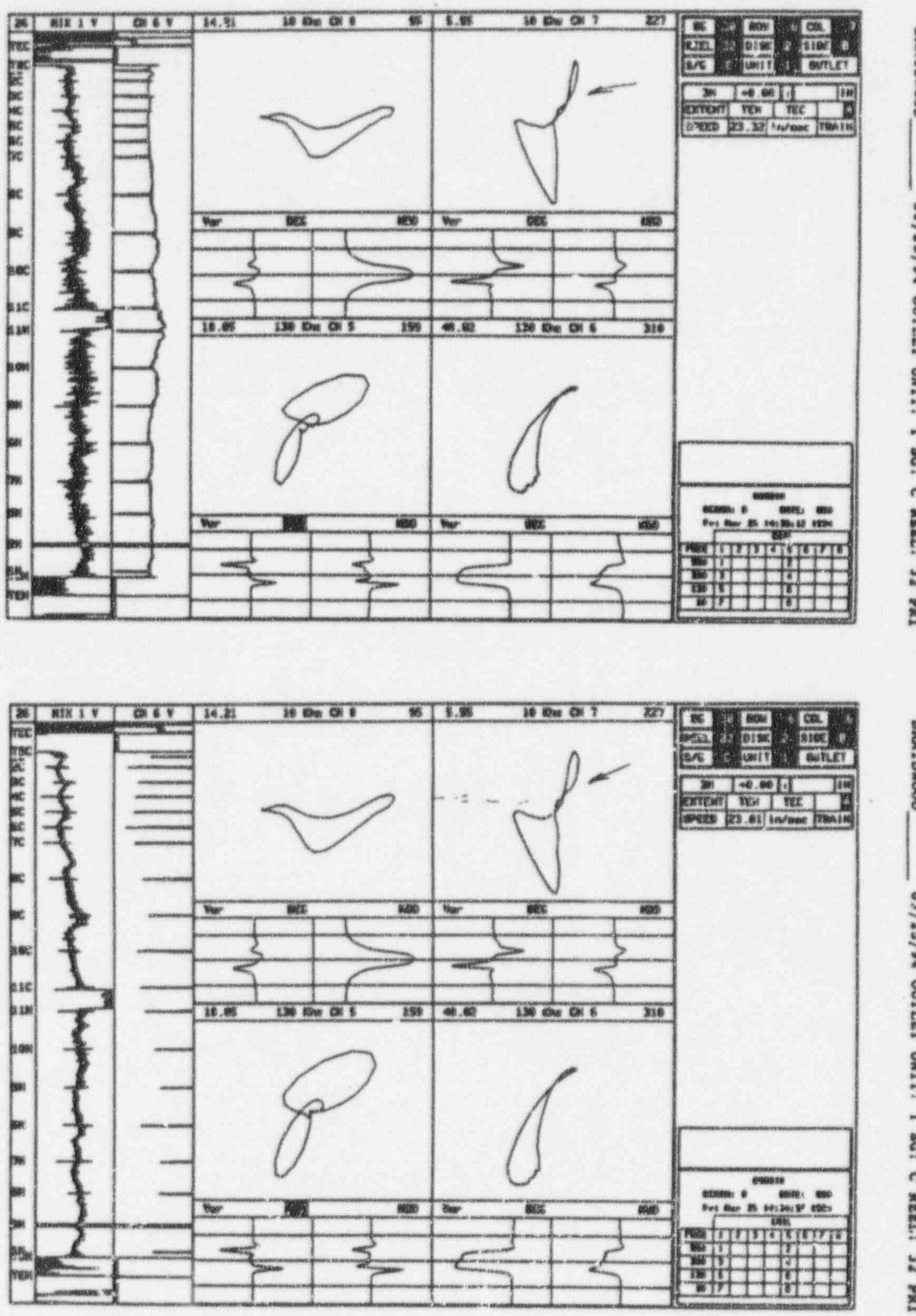

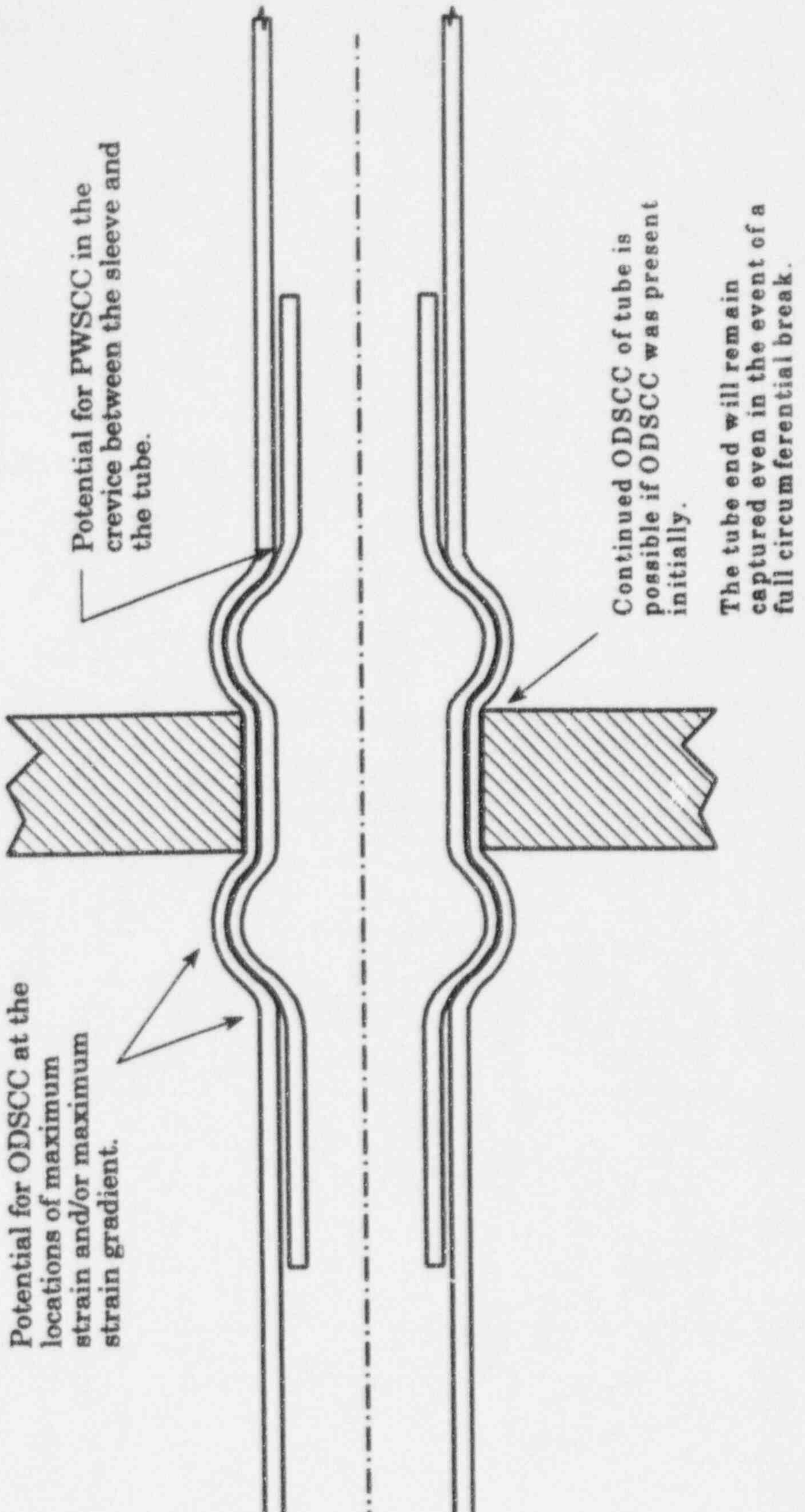

Figure 10-16. Potential PWSCC and/or ODSCC Locations

Figure 10-17. PWSCC Test Results for Bulged Hydraulic Expansions in Alloy 600 TT

a,b,c

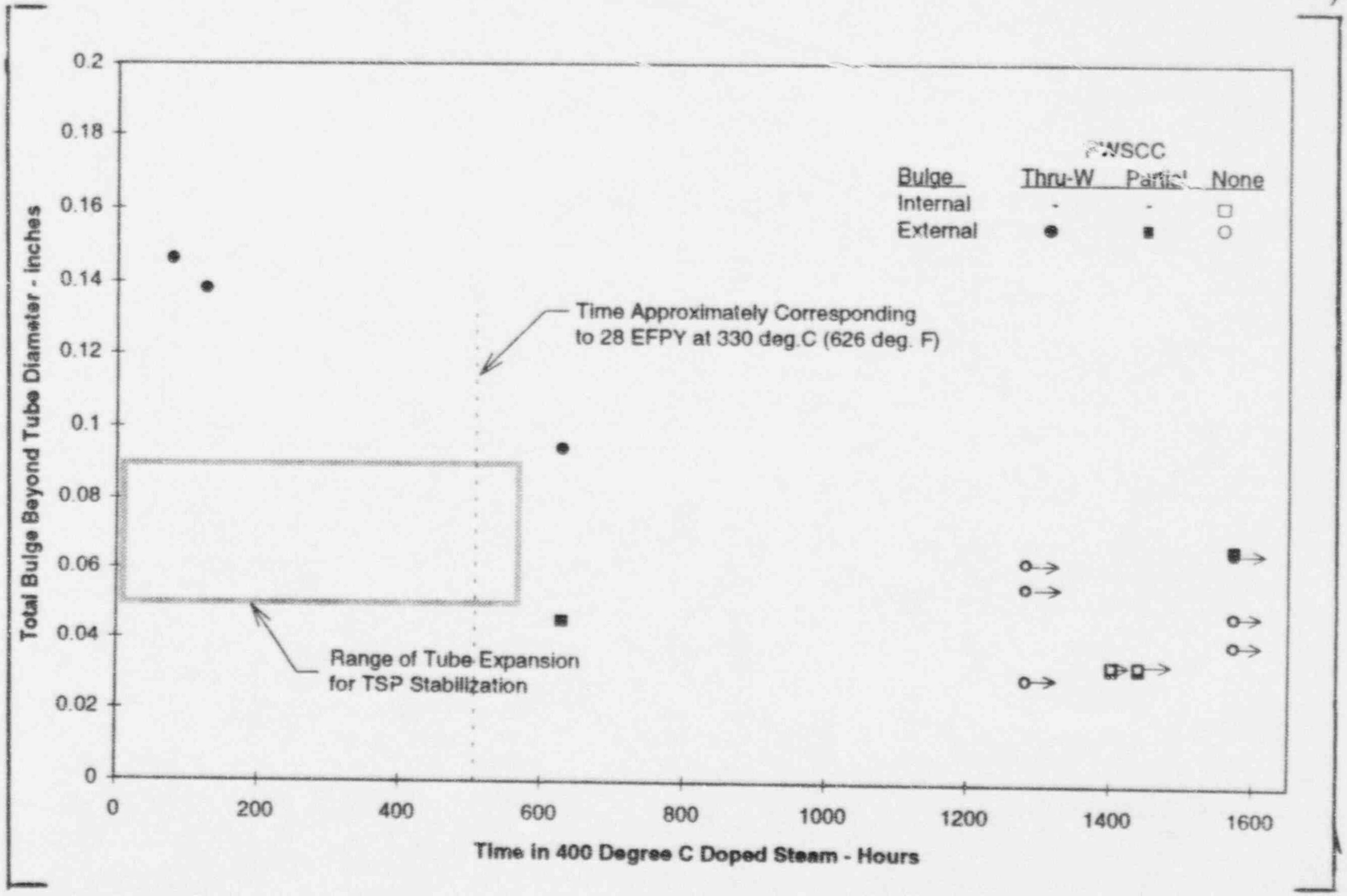

10 - 46

Westinghouse Proprietary Class 2

BULGETST.XLS

Figure 10-18 Polythionic Stress Index Testing Results for Hydraulically Expanded Tube Specimens

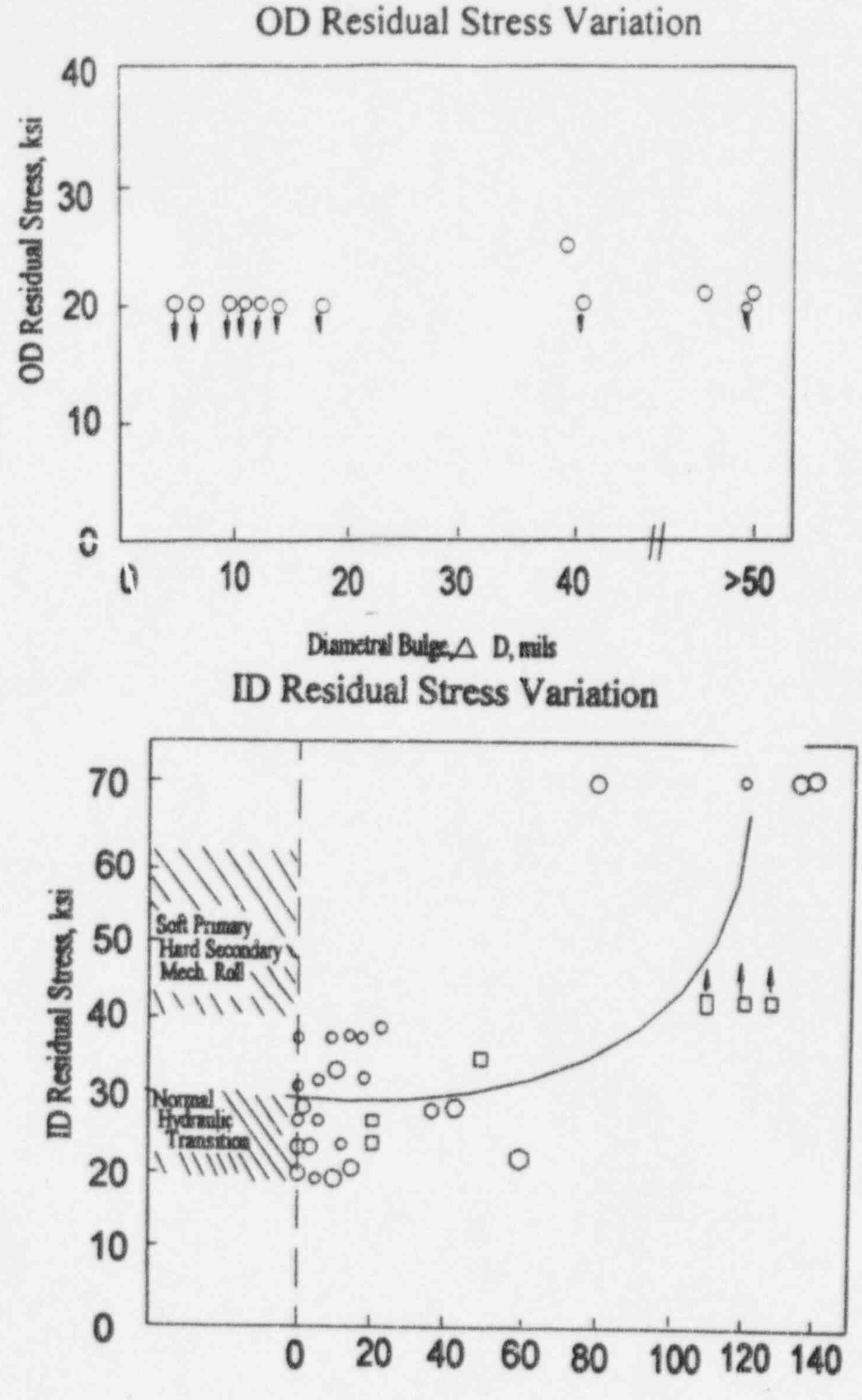

Figure 10-19 Stress Intensity Contours for 0.065 inch dented intersection

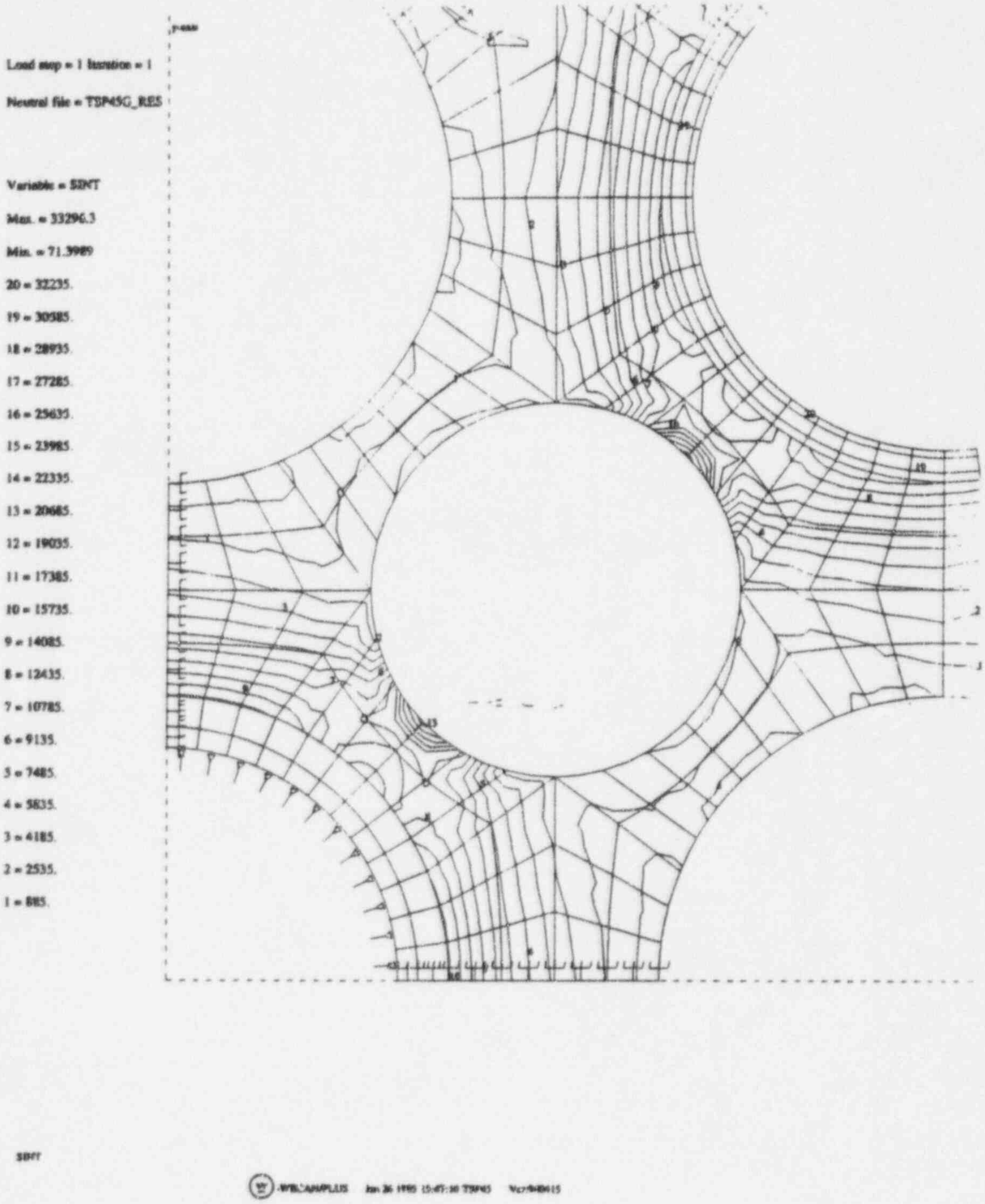

Figure 10-20. Tube Support Plate Ligament Cells

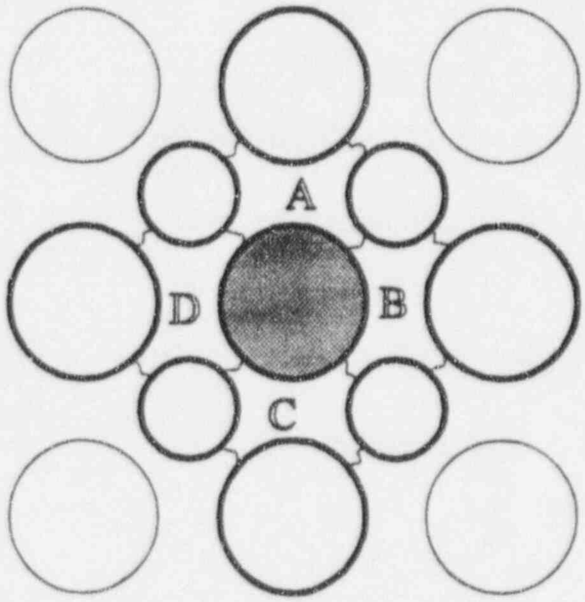

11.0 TSP DISPLACEMENT AND TUBE BURST PROBABILITY REQUIREMENTS WITH TUBE EXPANSION AT TSPs

11.1 General Approach to Tube Burst Probability

In Section 9.3, it is shown that the burst pressure of a throughwall indication extending outside the TSP has a burst pressure equal to the burst pressure for a free span crack at the length extending outside the TSP. Thus, the length of crack remaining within the TSP does not affect the burst pressure. Similarly, the burst probability for limited TSP displacements with postulated throughwall cracks can be calculated as that associated with a crack length equal to the TSP displacement. This assumes that the throughwall part of a crack is located at the edge of the plate rather than, as more commonly found in pulled tubes, near the center of the TSP. Alternately, it can be postulated that there is a throughwall crack equal to the TSP thickness and the burst probability for this indication is the same as the crack length exposed by the TSP displacement.

The most conservative possible assumption to define requirements for limited TSP displacement is to assume that all intersections at all hot leg TSPs (excluding the FDB which does not have expanded tubes) have throughwall crack lengths at least equal to the TSP displacements. This assumption is applied to develop the allowable limits on TSP displacements with tube expansion so that the design is generic and envelopes any possible tube degradation.

Even under the above bounding assumption on postulated tube degradation, it is desirable that the associated tube burst probability be small compared to acceptable levels for application of steam generator degradation specific management (SGDSM). Then, if multiple APCs are applied as part of SGDSM, the hot leg indications at TSPs will have a negligible contribution to the tube burst probability. The most conservative guideline for an acceptable SGDSM burst probability is the value of 10^{-2} given in the NRC draft generic letter. If this value is exceeded, the generic letter requires that the higher burst probability be reported to the NRC and that an assessment be performed of the significance of the result. If the burst probability for tube expansion is then $< 10^{-3}$, the TSP indications would contribute < 10% to the NRC reporting level. This 10^{-3} value is the starting point for developing a tube expansion burst probability requirement based on sensitivity analyses given in the following sections.

11.2 Allowable TSP Displacements for Acceptable Tube Burst Probability

By applying the tube burst probability as a function of throughwall crack length, as developed in Section 9.3, and the bounding assumption of throughwall cracks at all hot leg TSP intersections, tube burst probabilities can be developed as a function of TSP displacements. The tube burst probabilities are developed in Table 11-1 for the postulated 32,046 indications for the 7 hot leg TSPs with 4,578 tube intersections at each plate. Burst probabilities are given in Table 11-1 for the conservative assumption of uniform TSP displacements at all tube intersections and for a few of the unlimited number of cases with non-uniform displacements. For simplicity, the burst probabilities are calculated as the number of TSP intersections times the single tube burst probability for a throughwall crack equal to the displacement.

Although uniform TSP displacements are not realistic due to the varying locations of TSP supports, this assumption leads to a minimum allowable TSP displacement. For burst probabilities of 10^{-3}, 10^{-4} and 10^{-5}, the acceptable SLB TSP displacements are 0.36, 0.33 and 0.31 inch, respectively. As seen in Table 11-1, displacements at a limited number of TSP intersections can be significantly higher when the more realistic non-uniform displacements are considered. The intent of the tube expansion design is to generically limit TSP displacements to acceptable levels. Since multiple combinations for non-uniform TSP displacements are difficult to include in a generic assessment, the uniform TSP displacement assumption is applied to develop the design requirements for tube expansion.

11.3 TSP Displacement and Tube Burst Probability Requirements and Goals for Tube Expansion

The difference between 0.36 and 0.31 inch TSP displacement is small compared to the capabilities with tube expansion. Since a 0.31 inch TSP displacement requirement results in a factor of 100 reduction in burst probability (10^{-3} to 10^{-5} per Table 11-1) compared to 0.36 inch displacement, the 0.31 inch allowable limit for TSP displacements is established as the design requirement for tube expansion with a resulting tube burst probability of 10^{-5}. At this very low probability for a single tube rupture, the probability for multiple tube ruptures would be significantly smaller such that the rupture probabilities for both single and multiple ruptures are negligibly small for the 0.31 inch allowable TSP displacement. Thus the hot leg TSPs with tube expansion would contribute only 0.1% to the 10^{-2} guideline value of the NRC generic letter.

Although the 0.31 inch TSP displacement requirement is conservative for limiting tube burst, a goal for tube expansion is to permit in situ leak testing to demonstrate acceptable leakage if the allowable plant specific SLB leakage limits are exceeded based on leakage calculated as free span leakage per the EPRI methodology and the generic letter guidance. Since in situ leakage measurements would be performed at refueling conditions with the indications confirmed to be within the confines of the TSPs, small SLB displacements are necessary for the in situ leak tests to be a valid measurement for SLB conditions. A TSP displacement of 0.1 inch would expose negligible crack length for leakage considerations compared to the crack totally confined within the TSP as for the in situ leakage measurements. In addition, the 0.1 inch TSP displacement would not likely expose a throughwall length since the maximum throughwall crack length at up to about 30 volt indications would be less than about 0.5 inch and would most likely be nearly centered with the TSP. Thus, a maximum SLB TSP displacement of 0.1

inch is considered acceptable for application of in situ leak rate measurements to the SLB condition.

As discussed in Section 8, three redundant expanded tubes have been added to the required tube expansions to conservatively accommodate a postulated severed tube at the most limiting expansion locations relative to potential TSP displacements. Two additional expanded tubes have been included for structural considerations to limit bending stresses in the top TSP along the tubelane. As a minimum, the design goal of 0.1 inch maximum TSP displacement is to be satisfied with no postulated severed expansions. With all redundant expansions or any two non-redundant expansions postulated to be severed, the design requirement of 0.31 inch maximum TSP displacement is to be satisfied. The actual performance for the tube expansion matrix exceeds these requirements for redundancy.

The goals and requirements for the Model D4 S/G SLB TSP displacements and tube burst probabilities are summarized in Table 11-2. With the design goal TSP displacement of 0.1 inch, the tube burst probability for throughwall indications postulated at all 32,046 hot leg TSP intersections is $\leq 10^{-10}$. The design requirement of $\leq$ 0.31 inch displacement with a burst probability of $\leq 10^{-5}$ is to be satisfied for any two or three expansions postulated to be severed with the exception of the reference expansion plus it's direct redundant expansion. The postulated severing of both the reference and redundant expansions is considered to be too low a likelihood for consideration in assessing design goals and requirements.

11.4 Conclusions

The tube expansion design goal for SLB TSP displacements is established as $\leq$ 0.1 inch to permit in situ leakage measurements while the design requirement that must be satisfied by the expansion design is $\leq$ 0.31 inch to limit the tube burst probability to $\leq 10^{-5}$. Achievement of the design goal TSP displacement of 0.1 inch results in a tube burst probability of $\leq 10^{-10}$. The design requirement of $\leq$ 0.31 inch maximum TSP displacement is to be satisfied assuming that all redundant tube expansion locations are severed and that any two non-redundant expansions are severed. The performance of the tube expansion design for limiting TSP displacements for comparisons with these requirements has been developed in Section 8 and the tube expansion performance is compared to the goals and requirements in Section 12 of this report.

Table 11-1 Allowable Model D4 SLB TSP Displacements for Acceptable SLB Tube Burst Probability[1]			
No. Hot Leg TSP Intersections	**Acceptable SLB TSP Displacement**	**Burst Probability Per Indication**	**Total SLB Tube Burst Probability**
Uniform TSP Displacements at All TSPs and Tube Locations			
32,046	0.36"	3.1×10^{-8}	1.0×10^{-3}
32,046	0.33"	3.1×10^{-9}	1.0×10^{-4}
32,046	0.31"	3.1×10^{-10}	1.0×10^{-5}
Non-Uniform TSP Displacements			
45 32041 32046	0.434" 0.311"	2.2×10^{-5} 3.1×10^{-10}	0.99×10^{-3} 0.01×10^{-3} 1.0×10^{-3}
150 31896 32046	0.388" 0.315"	5.7×10^{-7} 4.7×10^{-10}	0.85×10^{-4} 0.15×10^{-4} 1.0×10^{-4}
10 32036 32046	0.424" 0.282"	1.0×10^{-5} 1.3×10^{-11}	1.00×10^{-4} 0.004×10^{-4} 1.0×10^{-4}

Notes:

1. Burst probability estimates very conservatively postulate that all hot leg TSP intersections have a throughwall crack length at least equal to the SLB TSP displacement

Table 11-2
Objectives for Model D4 SLB TSP Displacements and SLB Tube Burst Probabilities with Tube Expansion[1]

No. Postulated Severed Expansions	SLB TSP Displacement Objective	No. TSP Intersections Displaced	Single Indication SLB Burst Probability	Total SLB Tube Burst Probability
0	≤ 0.10"	32,046	$\leq 10^{-15}$	$\leq 10^{-10}$
1, 2 or 3 at redundant tube locations	≤ 0.31"	32,046	$\leq 3.1 \times 10^{-10}$	$\leq 10^{-5}$
Any 2 except reference plus its redundant location	≤ 0.31"	32,046	$\leq 3.1 \times 10^{-10}$	$\leq 10^{-5}$

Notes:
1. Burst probability estimates very conservatively postulate that all hot leg TSP intersections have a throughwall crack length at least equal to the SLB TSP displacement

12.0 ALTERNATE PLUGGING CRITERIA FOR BRAIDWOOD-1 AND BYRON-1 WITH TUBE EXPANSION AT TSPs

The general approach, design requirements and performance summary for tube expansion provided in this section are generic for Model D4 S/Gs with tube expansion. However, the voltage repair limits defined in this report are specific to the Braidwood-1 and Byron-1 S/Gs. This section integrates the results of the prior sections of this report to develop the alternate plugging criteria with tube expansion at TSP intersections. Since tube expansion is not applied at the FDB and cold leg TSP intersections, the tube repair limits for these intersections are based on the EPRI methodology and requirements of the NRC draft generic letter (Reference 13.2) and NRC resolution of public comments on the draft generic letter (Reference 13.3).

12.1 General Approach to Tube Plugging Criteria

The approach applied to developing the functional/design requirements for tube expansion and the associated tube repair criteria is based on developing the minimum requirements, establishing design objectives more limiting than the minimum requirements, and evaluating the overall performance based on supporting analyses for the tube expansion process. The general approach can be described as follows:

- Define acceptable TSP displacement to reduce the tube burst probability to negligible levels
  - The tube burst probability with tube expansion should be negligible compared to the NRC generic letter reporting guideline of 10^{-2} even with the bounding assumption that all hot leg TSP intersections have throughwall indications equal to the limited TSP displacement resulting from tube expansion
  - A cumulative tube burst probability requirement of 10^{-5} provides a negligible contribution with tube expansion
  - A TSP displacement of 0.31 inch (Table 11-2) is acceptable to obtain a tube burst probability of 10^{-5} conservatively assuming that all TSP intersections are equally displaced

- Conservatively apply a factor of two margin on the TRANFLO TSP hydraulic loads
  - A factor of two applied to the TRANFLO loads envelopes collective uncertainties in TRANFLO analyses (Section 6) and envelopes independent analysis results from the MULTIFLEX code (Section 5)

- Although the potential for circumferential cracking in the expanded and plugged tubes is very low (Section 10.6), implementation of tube expansion should include provisions for stabilization of a postulated severed expansion and the number of expanded tubes shall include redundant expansions to satisfy the acceptable TSP displacements assuming one or two expansions are severed

- Stabilization of the postulated severed expansions is obtained by expanding a sleeve together with the tube at the TSP intersections. The small (essentially zero) tube to sleeve clearance at the tube expansion prevents the severed tube from contacting adjacent tubes and thus stabilizes the severed tube
- Additional (redundant) tubes are expanded at critical TSP locations subject to displacements approaching the 0.31 inch acceptance limit under the assumption that one of the expansions is severed

- Demonstrate, by structural TSP displacement analyses, that implementation of tube expansion results in TSP displacements less than the 0.31 inch acceptance limit
  - It is shown in Section 8 that the design goal of < 0.1 inch TSP displacement is satisfied even with the postulate that the redundant expanded tubes sever at the expansion and the acceptance limit of < 0.31 inch displacement is satisfied even if two-thirds of the expansions are postulated to sever

This general approach to tube plugging criteria with tube expansion is further developed into overall functional requirements in Section 12.2, which also includes a comparison of the requirements with the performance as given in the prior sections of this report. Sections 12.3 to 12.5 develop the tube repair limits, the inspection requirements and the SLB analysis requirements. A summary of the tube repair criteria with tube expansion is given in Section 12.6.

12.2 Overall Functional Requirements and Summary Performance with Tube Expansion

The general approach described above has led to the overall functional requirements given in Table 12-1 and the tube expansion process requirements given in Table 12-2. The bases for each requirement are also given in the tables. The tube burst probability analyses supporting the 0.31 inch TSP displacement requirement are given in Section 11. While limiting TSP displacements to 0.31 inch is adequate to achieve a negligible tube burst probability of 10^{-5}, the design goal is to obtain a maximum TSP displacement of 0.1 inch for the expected condition of no severed tube expansions. This design goal is established primarily to permit in situ leak testing. The small 0.1 inch TSP displacement in a SLB event is not expected to significantly affect leakage compared to the in situ measurements even for the very unusual, high voltage indications for which the throughwall part of the crack might extend to the edge of the TSP. Of 16 throughwall indications on pulled tubes with 1 to 16 volt indications for which sufficient data are available to obtain the location of the edge of the throughwall length relative to the edge of the TSP, only 1 throughwall length was within 0.1 inch of the edge of the TSP and 12 were > 0.2 inch from the edge of the TSP. Thus, in situ measurements can be expected to be representative of leak rates with TSP displacements < 0.1 inch.

The expanded tube [ ]^{a,c,e} for TSP displacement represents the value used in the TSP displacement analyses. It is shown in Section 10 that the expansion process test results exceed this requirement by establishing a minimum diameter increase of [ ]^{a,c,e} for the expansion. An additional pull force requirement on the expanded joint is that a force of [ ]^{a,c,e} shall be required to displace the TSP > [ ]^{a,c,e} The maximum TSP load on the expanded joint calculated in the TSP displacement analyses is [ ]^{a,c,e} lbs for the design loads based on twice the TRANFLO calculated loads. The [ ]^{a,c,e} lb pull force requirement for the joint provides further assurance that even if the TRANFLO loads were increased by another factor of about two, the TSP displacements would not be expected to exceed the acceptable 0.31 inch limit.

Supporting data and analyses for application of tube expansion have been developed in Sections 8 to 11. Results from these report sections can be used to compare the demonstrated performance with the design requirements of Tables 12-1 and 12-2. This comparison is given in Table 12-3. The generic tube expansion matrix is given in Section 8.9 and requires 21 tubes to be expanded with a total of 72 expansions summed over the 21 tubes. The 21 tubes to be expanded includes 16 reference tubes to limit TSP displacements, 3 redundant tubes at critical locations for limiting TSP displacements and 2 tubes for structural considerations to limit TSP stresses. It is seen that all design requirements are satisfied with significant margin and the more conservative design goals are also satisfied. The design goal for TSP displacements of ≤ 0.1 inch is satisfied even for the postulated case of 16 of the 21 expanded tubes functional (3 redundant and 2 structural expanded tubes not functional). The design requirement of ≤ 0.31 inch TSP displacement is satisfied even for the extremely conservative factor of 4 increase in the TRANFLO hydraulic loads and even if only 7 (redundant and paired or duplicate expansions) of the 21 expanded tubes are functional. Overall, it is concluded that the tube expansion design provides acceptable TSP displacements to effectively reduce tube burst probabilities to negligible levels even when extremely conservative (factor of 4 on TRANFLO loads) loads are applied or when two thirds of the expanded tubes are assumed to be severed.

At this time, no indications at TSP intersections have been identified by NDE to extend outside the TSP and only a few pulled tube indications have been found to have shallow indications outside the TSP edges, which may be due to deposits at the top or bottom of the plate. This has resulted even though differential thermal expansion between the tube and TSP supports would lead to the expectation that the indications at the cold inspection conditions could extend outside the TSP. It is expected that the contact pressure between the tubes and TSP, as a result of packed crevices, results in the plate moving with the tube. With high contact pressures such as tubes with incipient denting, the active tubes would continue to determine the TSP elevations even with tube expansion, tube expansion is not required to limit SLB TSP displacements and the expanded tubes are equivalent to another plugged tube. With low tube to TSP contact pressures, tube expansion may result in a small change in the hot condition TSP elevation relative to the elevation prior to expansion. This can result as the plugged, expanded tubes may determine the hot TSP elevation, while before expansion, the tube contact pressure influenced the hot TSP elevation. As a result, there is an increased likelihood that indications formed within the TSPs at hot conditions may be found to extend outside the TSP at cold inspection conditions. Also, indications formed near the upper edge of the TSP prior to expansion may extend slightly outside the TSP at hot conditions, a new indication may form within the TSP and the new indication could have a total length greater than the TSP thickness. These before and after tube expansion effects on the relative tube to TSP positions at hot conditions can be expected to be insignificant for modest voltage repair limits prior to expansion such as about less than 5 volt repair limits. For these voltage levels, pre-existing crack lengths either do not extend to the plate edges or are shallow at the edges of the plate and the significant post-expansion length would remain less than the TSP thickness. For these considerations, it is generally desirable to implement tube expansion before the pre-expansion repair limits are raised to the order of about 5 volts, such as might occur with 7/8 inch diameter tube but would be less likely for 3/4 inch tubing. For Braidwood-1 and Byron-1, the pre-expansion repair limit of 1.0 volt is sufficiently low that the changes in hot TSP elevations with tube expansion would have a negligible effect on pre-existing indications. It should also be emphasized that the expanded tubes are equivalent to adding additional stay rods to support the TSPs. The interaction effects described above between expanded tubes and TSPs with varying tube to TSP contact pressures have been present near stay rod locations with no determinable influence on tube degradation.

As shown above, considerable conservatism has been included in the tube expansion design for loads, redundant expansions, expansion stiffness, etc. Table 12-4 summarizes the conservatisms included in the design process.

12.3 Tube Repair Limits for Braidwood-1 and Byron-1

Tube repair limits are required for ODSCC indications at the hot leg TSPs with expanded tubes, at the FDB which does not have expanded tube locations and at the cold leg TSPs. At the time of this report, no indications in Model D4 S/Gs have been reported at the FDB intersections or at cold leg TSP intersections. For the very large tube to plate hole clearances at FDB intersections, large expansion diameters would be required to limit TSP displacements. In addition, the large FDB crevices reduce the effectiveness of the plate constraint against tube burst and only modest increases above free span burst pressures would be expected for indications at FDB intersections. Tube expansions at cold leg TSP intersections are entirely feasible. However, cold leg expansions would essentially double the hot leg expansion effort and result in considerable exposure, field time and cost. With no reported indications at cold leg intersections, tube expansion in the cold leg is not justified and is not evaluated in this report.

Since displacements are not actively limited for the cold leg TSPs and for the FDB, it is adequate and conservative to apply the EPRI ARC for ODSCC at TSPs, which are based on the assumption of free span indications at SLB conditions. The EPRI ARC are the recommended repair criteria for ODSCC indications at the FDB and cold leg TSP intersections. For the cold leg TSP indications, the appropriate structural limit would be $1.43\Delta P_{SLB}$ since the R.G. 1.121 margin of $3\Delta P_{NO}$ is satisfied at normal operating conditions due to the constraint provided by the TSPs. The NRC resolution (Reference 13.3) of public comments on the draft generic letter requires that the full APC repair limits be updated on an outage basis to the latest database, correlations and growth information. Full APC repair limits are developed here based on available data including the Braidwood-1 and Byron-1 pulled tube results to demonstrate the methodology and to define typical repair limits with the recognition that these repair limits may require an update at the time of an outage inspection. Based on current data, the structural limit at $1.43\Delta P_{SLB}$ = 3660 psi would be about 4.75 volts. The average voltage growth at Braidwood-1 for the last operating cycle was 53 % as given in Reference 13.19. A voltage growth allowance of 55% is applied to develop the full APC repair limit. With allowances of 55% for voltage growth and 20% for NDE uncertainties, the full APC repair limit for the cold leg indications would be 2.7 volts. Due to the large tube to FDB clearances, constraint against burst cannot be confidently assured and the $3\Delta P_{NO}$ structural margin requirement is appropriate for indications at the FDB intersections. For the Braidwood-1 full power steam pressure of 910 psi, the structural limit at $3\Delta P_{NO}$ = 4020 psi would be about 3.38 volts and the full APC repair limit would be 1.9 volts. In the NRC draft generic letter (Ref. 13.2) for ODSCC at TSPs, the full APC repair limit is given as 2.7 volts. Pulled tube data obtained from the Model D4 S/Gs at Braidwood-1 and Byron-1 have increased the structural limit from 4.6 to 4.75 volts since the draft generic letter was prepared. However, the full APC repair limit for Braidwood-1 with the $1.43\Delta P_{SLB}$ = 3660 psi structural limit remains at 2.7 volts due to the larger growth allowance included for Braidwood-1 than applied in the draft generic letter.

Pending completion of the NRC review of the EPRI ARC, interim plugging criteria (IPC) have been approved for implementation by the NRC. The NRC draft generic letter and the January 18, 1995 NRC/industry meeting (Reference 13.3) to resolve public comments provide a 1.0 volt IPC repair limit for plants with 3/4 inch diameter tubing, which includes the FDB based on the January meeting. Braidwood-1 and Byron-1 have not had prior indications at the FDB intersections which would support low growth rates if indications are found in the future. In addition, these S/Gs have not operated with copper in the secondary system. Since accelerated corrosion assisted by significant copper species acting as an oxidizing agent contributed to the few cases of high growth rates at FDBs in other plants, this mode of accelerated corrosion would not be expected at Braidwood-1 or Byron-1. The 1.0 volt repair limit is recommended for ODSCC indications at the

Braidwood-1 and Byron-1 FDB and cold leg TSP intersections. Bobbin indications > 1.0 volt and below the full APC repair limits that are not confirmed by RPC inspection may be left in service. The Braidwood-1 full APC repair limits are 1.9 volts at FDB intersections and 2.7 volts at cold leg TSP intersections and bobbin flaw indications above these limits must be repaired independent of RPC confirmation.

For free span indications, tube repair limits are based on the R.G. 1.121 guidelines for structural margins against tube burst as discussed above for indications at cold leg TSPs and at FDBs. Since tube expansion reduces the tube burst probability to negligible levels ($< 10^{-5}$) independent of the degree of ODSCC at the hot leg TSP intersections (all hot leg TSP intersections are assumed to have throughwall indications), tube repair limits for axial tube burst are not required and tube repair is primarily required only as necessary to maintain SLB leakage within acceptable limits. The structural limit for the hot leg TSP intersections and the full APC repair limit with tube expansion is addressed below. Allowable SLB leakage limits are given in the Braidwood-1 and Byron-1 Technical Specifications and are not developed in this report. As developed in Section 9.8, a structural limit for axial tensile tearing of cellular and IGA indications applies for expanded tube constraint at very high voltages. Although data is currently limited, this structural limit appears to be in excess of 35 volts. Even if a factor of two reduction is applied is applied for growth and NDE allowances (factor of about 1.75 is typical as described above for the cold leg and FDB indications), the full APC repair limit would be about 17 volts. For conservatism in defining the full APC repair limit with tube expansion while additional data is obtained to further enhance confidence in the structural limit, a tube repair limit of ≥ 3.0 volts with a ≥ 10 volt full APC repair limit is conservatively applied for hot leg TSP indications with tube expansion at the Braidwood-1 and Byron-1 S/Gs. Bobbin indications ≥ 3.0 volts are repaired if confirmed as flaws by RPC inspection and indications ≥ 10.0 volts are repaired independent of RPC confirmation.

The technical data of this report support a high degree of conservatism in the 3.0 volt repair limit for ODSCC at hot leg TSP intersections.

12.4 Inspection Requirements

The requirements applied to date for IPC/APC inspections also apply to implementation of tube expansion. However, the inspection threshold for RPC confirmation of bobbin indications should be adjusted for increasing repair limits. RPC inspection of bobbin indications greater than the 3.0 volt repair limit with a sample inspection of a minimum of 100 intersections below the 3.0 volt repair limit is recommended at hot leg TSP intersections and a 1.0 volt RPC threshold is recommended for the 1.0 volt repair limit at FDB and cold leg TSP intersections.

As a part of the tube expansion process requirements, a post-expansion inspection of the expanded tube intersections is required to verify that acceptable expansion diameters and locations relative to the TSP have been obtained. This inspection is performed with bobbin coil profilometry to verify that an expansion diameter increase of [ ]^{a,c,e} has been obtained above and below the TSP intersection.

In addition to the inspection requirements for ODSCC at TSP intersections, additional inspection requirements are needed for implementation of tube expansion. The additional inspection requirements include: a review of overall inspection results for large corrosion induced dents which could limit application of the tube expansion based repair limits to assure integrity of the TSPs, an analysis of bobbin data for TSP intersections to be expanded prior to application of the expansion process to exclude tube expansion at intersections with corrosion induced dents > 5.0 volts and for periodic inspections of the expanded tube intersections for circumferential cracks at the expansions. These additional requirements are discussed below.

In S/Gs with extensive tube denting at TSP intersections, cracking of TSP ligaments has been identified. For the extensive denting associated with TSP cracks, the alternate repair criteria of this report would not be applicable since the criteria are only applicable to dents < 5 volts. Conceptually, however, it is possible to have locally large dents, which could challenge the integrity of ligaments at the TSP tube or flow holes. Operating experience has indicated that plants with corrosion induced denting large enough to challenge TSP integrity have generally uniform denting at all or nearly all TSP intersections. A quantity that can be used to evaluate denting for TSP integrity is the reduced tube diameter at the dented intersection as measured by the ability to pass a minimum bobbin probe diameter through the TSP intersection. In Section 10.7, an acceptable limit for tube denting is developed. A reduction in the tube diameter of 65 mils is required to develop stress levels above yield in the TSP ligaments at the dented intersection. Thus, for 3/4 inch diameter tubing with a nominal 0.664 inch tube ID and a clearance allowance for probe centering devices of about 20 mils for probe passage past the dented intersection, a bobbin probe of ≤ 570 mils must be able to pass through the TSP intersections. The nominal probe diameter for IPC/APC inspections is a 610 mil probe. If a 570 mil probe does not pass through a dented intersection, all surrounding tube locations must be repaired to the free span repair criteria applied to the cold leg TSPs rather than the hot leg TSP repair criteria. In addition, all TSP intersections selected for tube expansion and all adjacent intersections must not have corrosion induced dents > 5 volts to conservatively support TSP integrity at the expanded intersections. Corrosion induced denting has essentially been arrested at all Westinghouse plants being considered for IPC/APC applications. Therefore, this evaluation for dented TSP intersections can be based on prior inspection data and should be performed as a part of the licensing submittal for implementation of the expansion based repair criteria. If necessary, exclusion areas for repair limits should be a part of the license amendment request. Braidwood-1 and Byron-1 have not identified corrosion induced dents (reported dents are mechanically induced "dings" generally traceable to preservice conditions. Therefore, no exclusion areas are required and all TSP intersections are acceptable candidates for tube expansion.

In Section 10.6, it is shown that the potential for circumferential cracking at the expanded tube locations in plugged tubes is very low. Utilization of hydraulic expansions and limited expanded tube diameters minimize residual stresses at the expansions and crack initiation and growth at the ≤ 550 °F plugged tube temperature is not expected. However, it is prudent to periodically inspect a small sample of the expansions for circumferential cracks. Since the expanded tubes are plugged, the hot leg plugs must be removed for inspection. An inspection of three expanded tubes at all expanded TSP intersections is recommended at every third planned inspection (frequency of every 3 cycles). The expanded tubes inspected should be alternated between the periodic inspections. If a circumferential crack is identified at an expansion, the inspection should be extended to other expanded tubes in the S/G with the inspection scope extension dependent on the severity of the indications found in the base inspection. Following identification of circumferential cracks, the adequacy of the tube expansion matrix for limiting TSP displacements should be evaluated under the assumption that the circumferential crack further develops to a severing of the tube at the expansion location. The TSP displacement analyses of Section 8 can be used for this assessment and supplemented by further sensitivity analyses if required. This assessment should evaluate the adequacy of the existing redundancy in the expansion matrix to meet the acceptable TSP displacement limits of this report and determine if additional tube expansions are required.

12.5 SLB Analysis Requirements

Per the draft generic letter and NRC resolution of industry comments as presented at the January 28, 1995 NRC/industry meeting, SLB leak rate and tube burst probability analyses are required prior to returning to power and are to be included in a report to the NRC within 90 days of restart. SLB leak rates and burst probabilities obtained for the actual voltage distribution measured at the inspection are required prior to restart and the projected next EOC values are required in the 90 day report. If allowable limits on leak rates and burst probability are exceeded for either the actual EOC distribution found in the outage inspection or the distribution projected to the end of the next operating cycle, the results are to be reported to the NRC and an assessment of the significance of the results is to be performed. With the Model D4 S/G tube expansion, SLB leak rates are to be calculated for the hot leg TSP indications and both leak rates and tube burst probability are to be calculated for the FDB and cold leg TSP indications. The required SLB analyses are discussed below.

The SLB leak rates for hot leg TSP indications are to be calculated as free span leakage using the leak rate methods described in Section 9.5 with an additional component for the potentially overpressurized indications. Free span leak rate methods must be applied for the FDB and cold leg TSP indications. The free span leak rates are based on the EPRI methodology for correlating probability of leakage and SLB leak rates with bobbin voltage.

In addition to the free span leak rates, the leak rate analyses for hot leg TSP indications are to include the potential leakage from overpressurized indications within the TSP. There is a finite probability that a crack might open up significantly more than the crack opening that occurred in the SLB leak rate measurements. The probability that a crack will open up to the limits of the tube to TSP gap is equivalent to the probability of free span burst. The analysis methods for the overpressurized condition are given in Section 9.7. The overpressurized condition leak rates are obtained from the probability of free span burst and a bounding leak rate for the overpressurized condition.

The SLB leak rate analysis can be symbolically represented as:

$$LR_{SLB} = [(1\text{-}POB)^*POL^*LR_c + POB^*LR_b]_{\text{Hot Leg TSPs}} + [POL^*LR_c]_{\text{FDB+Cold Leg TSPs}}$$

where:

LR_{SLB} = Total SLB leak rate
POL = Probability of leakage based on POL versus voltage correlation
LR_c = Leak rate based on leak rate versus voltage correlation
POB = Probability of burst at SLB conditions for hot leg TSP indications based on free span burst pressure versus voltage correlation
LR_b = Bounding leak rate for overpressurized indications as developed in Section 9.6

The free span tube burst probability must be calculated for the FDB and cold leg TSP indications per the requirements of the draft generic letter. Analysis methods are described in Section 9.5. Per the generic letter, the burst probability limit for the FDB and cold leg TSP indications for reporting results to the NRC is $> 10^{-2}$.

12.6 Summary of Braidwood-1 and Byron-1 APC with Tube Expansion at TSPs

This section provides a summary of the alternate tube plugging criteria (APC), as developed above, to be applied at Braidwood-1 and Byron-1 with implementation of tube expansion at selected TSP intersections. This summary includes the tube repair limits, general inspection requirements, supplemental inspection requirements for tube expansion implementation and SLB leak rate and tube burst probability analysis requirements. SLB analysis methodology is summarized in Section 12.5 and described in detail in Section 9. The generic matrix of the 21 tube locations and TSP elevations requiring tube expansion is given in Section 8. As described in Section 8, the plant specific selection of tubes for expansion can differ from the generic matrix by selecting alternate tubes in close proximity to the generic tube locations.

Braidwood-1 and Byron-1 Tube Repair Limits

- For hot leg TSP indications, bobbin flaw indications > 3.0 volts and confirmed by RPC inspection shall be repaired. Bobbin flaw indications > 10.0 volts shall be repaired independent of RPC confirmation.

- For indications at the FDB and cold leg TSP intersections, bobbin flaw indications > 1.0 volt and confirmed by RPC inspection shall be repaired. Bobbin flaw indications greater than the full APC repair limits of 1.9 and 2.7 volts for Braidwood-1 indications at FDBs and hot leg TSP intersections, respectively, shall be repaired independent of RPC confirmation. The full APC repair limits for the FDB and cold leg TSP intersections shall be updated at each inspection based on the latest database, correlations and plant specific growth rate information. If growth rate data for the latest cycle are available from the current inspection results, this latest growth rate should be used to establish the full APC repair limits. Unless the inspection results indicate a substantial increase (> 20%) in the average voltage growth rates, the larger of the prior two cycle growth rates may be used to develop the full APC repair limits in order to expedite tube repairs while the growth rate data are being developed.

- All indications found to extend outside of the TSP and all circumferential crack indications shall be repaired and the NRC shall be notified of these indications prior to returning the S/Gs to service.

- All flaw indications found in the RPC sampling plan for dented TSP intersections and bobbin mixed residuals potentially masking flaw indications shall be repaired.

- For Model D4 S/Gs, some intersections near TSP wedge supports are excluded from application of APC repair limits due to potential deformation of these tube locations under combined LOCA + SSE loads. The tube locations for exclusion from APC application shall be defined for Braidwood-1 and Byron-1 in a separate report.

General Inspection Requirements

- The bobbin coil inspection shall include 100% of all hot leg FDB and TSP intersections and cold leg TSP intersections down to the lowest cold leg TSP with ODSCC indications. The lowest cold leg TSP with ODSCC indications shall be determined from an inspection of at least 20% of the cold leg TSP intersections.

- All bobbin flaw indications exceeding 3.0 volts for hot leg TSP intersections and 1.0 volt for FDB and cold leg TSP intersections shall be RPC inspected. In addition, a minimum of 100 hot leg TSP intersections with bobbin voltages less that 3.0 volts shall be RPC inspected. The RPC dat shall be evaluated to confirm responses typical of ODSCC within the confines of the TSP.

- A RPC inspection shall be performed for intersections with dent signals > 5.0 volts and with bobbin mixed residual signals, if identified in the inspection, that could potentially mask flaw responses near or above the voltage repair limits. The RPC inspection sample shall include a minimum of 100 intersections.

Supplemental Inspection Requirements for Tube Expansion Implementation

- Braidwood-1 and Byron-1 have no known corrosion induced dents at the TSP intersections. Mechanical dings, typically present prior to initial operation, are present at a modest number of TSP intersections. Without corrosion induced denting, there is no concern for TSP integrity and there is no need to identify exclusion areas for application of the APC repair limits or for tube expansion candidates.

- Prior or current cycle bobbin data for candidate tubes for expansion and surrounding tubes shall be evaluated for corrosion induced denting. The tubes selected for expansion and the surrounding tubes shall not have corrosion induced dents > 5.0 volts. Since Braidwood-1 and Byron-1 have no corrosion induced denting, there are no restrictions on selection of tubes for expansion.

- Following application of tube expansion, the expanded TSP intersections shall be inspected with a bobbin probe for process verification. This inspection applies bobbin profilometry to verify that acceptable expansion diameters ([ ][a,c,e]) have been achieved and that the expansions are properly located relative to the TSP.

- At every third planned inspection following tube expansion, a minimum of three expanded tubes shall be deplugged and inspected for circumferential crack indications at the expanded TSP intersections. If a circumferential crack is found at an expanded intersection, the inspection should be extended to other expanded tubes in the S/G with the inspection scope extension dependent on the severity of the indications found in the base inspection. Following identification of circumferential cracks, the adequacy of the tube expansion matrix for limiting TSP displacements should be evaluated under the assumption that a circumferential crack further develops to a severing of the tube at the expansion location.

SLB Leak Rate and Tube Burst Probability Analyses

- SLB leak rates and tube burst probabilities shall be evaluated for the actual voltage distribution found by inspection and for the projected next EOC distribution.

- Based on the voltage distribution obtained at the inspection, the SLB leak rate shall be compared to the Braidwood-1 or Byron-1 allowable limits as given in the Technical Specifications and potentially modified by administrative controls, the SLB tube burst probability for FDB and cold leg TSP intersections shall be compared to the reporting value of 10^{-2} and the NRC shall be notified prior to returning the S/Gs to service if the allowable limits are exceeded. If the allowable limits are exceeded for the projected EOC distribution, the NRC shall be notified and an assessment of the significance of the results shall be performed. A report shall be prepared that includes inspection results and the SLB analyses within 90 days following return to power.

Table 12-1. Overall Requirements for Tube Expansion Application

TSP Displacements and Tube Expansion Process Design Loads Shall be Based on Factor of Two Margin on TRANFLO Hydraulic Loads

- Provides margin against load uncertainties based on TRANFLO uncertainty study and independent analyses with the MULTIFLEX code

Maximum SLB TSP Displacements Shall Be Less Than 0.31" Even if It is Postulated That an Expanded Tube Severs

- Provides redundant tube expansions against a postulated circumferential crack in an expanded tube
- Results in a tube burst probability < 10^{-5} even under extremely conservative assumption of throughwall cracks at all hot leg TSP intersections

As a Design Goal, the Maximum SLB TSP Displacements Shall Be Less Than 0.1" With No Severed Expanded Tubes

- Permits application of in situ leak rate measurements if required to limit leakage to acceptable levels (applied if predicted free span leakage using EPRI correlation exceeds allowable leak rate)
- Expanded tube stiffness shall be sufficient to satisfy this requirement
- Provides tube burst probability < 10^{-10} even under extremely conservative assumption of throughwall cracks at all hot leg TSP intersections

The Tube Expansion Process Shall Provide Adequate Tube Stiffness to Limit TSP Displacements to Acceptable Levels and Shall Provide Tube Stabilization Capability for a Postulated Severed Expansion

- This requirement is further developed into process functional requirements in Table 12-2

Table 12-2. Tube Expansion Process Requirements

Tube Expansion Shall Be Performed with a Hydraulic Expansion Process

- Limits residual stresses compared to alternate expansion processes

Tubes Shall be Expanded Above and Below the TSP

- Provides for uncertainty in the direction of the hydraulic TSP loads

The Expanded Tube Shall Have a TSP Pull Force Capability of [

]^{a,b,c}

- Provides adequate tube stiffness to limit TSP displacements to < 0.1" at design hydraulic loads (twice expected) and to < 0.31" at twice the design loads. The tube stiffness requirement is used in TSP displacement analyses.

A Sleeve Stabilizer Shall be Installed by Hydraulic Expansion at the Expanded Parent Tube TSP Intersections

- Prevents damage to adjacent tubes for a postulated severed tube at the tube expansion

The Maximum Expanded Tube Diameter Increase Shall be [ ]^{a,b,c}

- Limits residual stresses for hydraulic expansions to less than that typical of a tubesheet hardroll expansion. This is a process development goal and not a basis for rejection of field expansions.

Table 12-3. Comparison of Tube Expansion Design Requirements and Demonstrated Performance				
Parameter	**Requirement**	**Design Goal**	**Demonstrated Performance**	
			Result	**Report Section**
Design Requirements				
Maximum TSP Displacement • All 21 tube expansions functional • 16 tube expansions functional (Excludes redundant exp.)	 ≤ 0.31" ≤ 0.31"	 ≤ 0.10" ≤ 0.31"	 0.094" 0.094"	 8.5 8.6
Expanded tube stiffness				a,b,c
Expanded tube TSP pull force at 3/8" displacement				
Sensitivity Analysis Results				
Maximum TSP displacement with factor of 4 on TRANFLO loads (design basis is factor of 2)	None	≤ 0.31"	0.189"	8.6
Maximum TSP displacement assuming severed expansions for 6 of 8 expanded tubes (excluding redundant locations) at TSPs 3, 5 and 7 (lower 3 TSPs above FDB)	≤ 0.31"	≤ 0.31"	0.097 Note 1	8.6
Maximum TSP displacement assuming severed expansions for 12 of 17 expanded tubes (excluding duplicate nearby locations) at TSPs 8 to 11 (top 4 TSPs)	≤ 0.31"	≤ 0.31"	0.200	8.6
Maximum TSP displacement with only 7 of the 21 expanded tubes functional (duplicate expansions functional)	≤ 0.31"	≤ 0.31"	0.199	8.6

Note 1. The sleeved expansion is fail safe against severed parent tubes at the lower 3 TSPs for which the hydraulic loads act in the downward direction toward the tubesheet.

Table 12-4. Summary of Conservatisms in Application of Tube Expansion for Limited TSP Displacement

Hydraulic Loads for TSP Displacements and Tube Expansion Requirements

- For design and analysis loads, TRANFLO hydraulic loads on TSPs increased by a factor of two to envelope TRANFLO uncertainties and independent analyses with the MULTIFLEX code
- Sensitivity analyses show that acceptable TSP displacements to limit burst probabilities can be obtained with a factor of four on the TRANFLO hydraulic loads

Number of Expansions

- Redundant tube expansions are included at regions of largest TSP displacements without expansion to limit tube burst probabilities even if the reference (excluding redundant expansions) expanded tubes are postulated to sever
- Sensitivity analyses show that acceptable TSP displacements to limit burst probabilities can be obtained with only two expanded tubes limiting displacements

TSP Displacements

- TSP displacements are limited to 0.10" compared to the acceptable 0.31" to limit tube burst probability
- TSP displacement analyses are based on an expanded tube [ ][a,b,c] which is exceeded by all acceptable expansions [ ][a,c,e] based on process qualification tests
- TSP displacements are essentially independent of a severed expansion at lower three TSPs (3, 5, 7) due to downward loads on the TSPs and lateral restraint to tube motion provided by the sleeve stabilizer

Burst Probability Estimates

- All hot leg TSP intersections postulated to have a throughwall indication at least equal to the TSP displacement at each tube location

SLB Leakage

- SLB leakage initially calculated as free span leakage as long as the conservative results remain within acceptable limits

13.0 REFERENCES

13.1 WCAP-14222, "Braidwood Unit 1 and Byron Unit 1 Model D4 Steam Generator Limited Tube Support Plate Displacement Analysis in Support of Interim Plugging Criteria," November 1994.

13.2 Draft Generic Letter 94-XX, Voltage-Based Repair Criteria for the Repair of Westinghouse Steam Generator Tubes Affected by Outside Diameter Stress Corrosion Cracking," United States Nuclear Regulatory Commission, Federal Register, Vol. 59, No. 155, August 12, 1994, pp. 41520-41529.

13.3 USNRC/Industry Meeting, "Resolution of Public Comments, NRC Draft GL 94-XX," January 18, 1995.

13.4 TR-100407, Revision 1 (Draft), "PWR Steam Generator Tube Repair Limits - Technical Support Document for Outside Diameter Stress Corrosion Crack at Tube Support Plates," Electric Power Research Institute, August 1993.

13.5 NP-7480-L, Volume 2, "Steam Generator Tubing Outside Diameter Stress Corrosion Cracking at Tube Support Plates - Database for Alternate Repair Limits, Volume 2: 3/4 Inch Diameter Tubing," Electric Power Research Institute, October, 1993.

13.6 EPRI Letter, "Exclusion of Data from Alternate Repair Criteria (ARC) Databases Associated with 3/4 inch Tubing Exhibiting ODSCC," D. A. Steininger (EPRI) to Mehdi Sarram (NEI), June 6, 1994 [to become Appendix C of Reference 13.5].

13.7 Regulatory Guide 1.121 (Draft), "Bases for Plugging Degraded PWR Steam Generator Tubes," United States Nuclear Regulatory Commission, issued for comment in August, 1976.

13.8 NUREG-1477 (Draft), "Voltage-Based Interim Plugging Criteria for Steam Generator Tubes - Task Group Report," United States Nuclear Regulatory Commission (NRC), June 1, 1993.

13.9 [United States Nuclear Regulatory Commission] Meeting with EPRI, NUMARC, "Resolution of Public Comments on Draft NUREG-1477," United States Nuclear Regulatory Commission, February 8, 1994.

13.10 WCAP-8821, "TRANFLO Steam Generator Code Description," Westinghouse Nuclear Energy Systems (Land, R. E.), September, 1976.

13.11 Memo from C. O. Thomas to E. P. Rahe, "Proprietary Content Review of SER on WCAP-8821 and WCAP-8822," October 14, 1982.

13.12 P. W. Bird and P. J. Prabhu, "Review of Primary Separator Loss Coefficient," WTD-TH-80-010, July, 1980.

13.13 John F. Stolz, "Evaluation of Westinghouse Topical Reports (WCAP-8708(P) and WCAP-8709(NP)," United States Nuclear Regulatory Commission, June 17, 1977.

13.14 K. Takeuchi, et al., "MULTIFLEX, A FORTRAN-IV Computer Program for Analyzing Thermal-Hydraulic-Structure Dynamics," WCAP-8708-PA-V1, Westinghouse PWR Systems, September, 1977.

13.15 Docket STM-50-456, "Safety Evaluation by the Office of Nuclear Reactor Regulation Related to Amendment No. ? to Facility Operating License No. NPF-72 Commonwealth Edison Company Braidwood Station, Unit No. 1," United States Nuclear Regulatory Commission, May, 1994.

13.16 Economy, G., and F. W. Pement, "Temperature Effects on Alloy 600 PWSCC," NACE Symposium on Corrosion of Materials in Nuclear Power Systems, 1989.

13.17 SG-92-01-025, "Simulated Primary Water Stress Corrosion Cracking Tests of Bulged Hydraulic Expansion Mockups," R. E. Gold, et al, Westinghouse Electric Corporation, January 1992.

13.18 WCAP-14046, Revision 1, "Braidwood Unit 1 Technical Support for Cycle 5, Steam Generator Interim Plugging Criteria," August 1994.

13.19 WCAP-14277, "SLB Leak Rate and Tube Burst Probability Analysis Methods for ODSCC at TSP Intersections," Westinghouse Electric Corporation, January 1995.